Antibody responses after SARS-CoV-2 infection

By

Maya F. Amjadi

A dissertation submitted in partial fulfillment of

the requirements for the degree of

Doctor of Philosophy

(Cellular and Molecular Biology)

at the

UNIVERSITY OF WISCONSIN-MADISON

2023

Date of final oral examination: May 1, 2023

The dissertation is approved by the following members of the Final Oral Committee:

Miriam A. Shelef, Associate Professor, Cellular and Molecular Biology, Cellular and Molecular Pathology
Ajay K. Sethi, Professor, Epidemiology, Population Health
Yun Liang, Assistant Professor, Microbiology, Molecular and Cellular Pharmacology, Endocrinology and Reproductive Physiology, Cellular and Molecular Biology, Cellular and Molecular Pathology, Molecular and Environmental Toxicology
David H. O'Connor, Professor, Microbiology, Cellular and Molecular Pathology, Cellular and Molecular Biology
Anna Huttenlocher, Professor, Microbiology, Cellular and Molecular Biology, Cellular and Molecular Pathology, Molecular and Cellular Pharmacology, Cancer Biology, Toxicology, Pathobiological Sciences

Table of Contents

Acknowledgements

Fantastic teachers inspire, promote, listen, advocate, and empower. I am extremely fortunate to have been taught by many of these outstanding teachers who selflessly dedicated themselves to higher education, created exceptional learning opportunities, fostered environments where exploration and creativity were encouraged, and allowed my love for learning to flourish.

To my teachers at Cedar Falls High School, especially Mr. Brian Winkel, Mrs. Judy Timmons, Mrs. Lynn Griffin, Mr. Chad Van Cleve, and Mr. Nicholas Chizek, thank you for your encouragement and support.

To my professors at the University of Iowa, especially Dr. Bob Kirby, Lindsay Marshall, and Dr. Lori Adams, thank you for supporting my interests in research and teaching.

To my research mentors at the University of Iowa, Dr. Bill Nauseef and Dr. Mallary Greenlee-Wacker, thank you for being rigorous scientists, thoughtful teachers, and exemplary colleagues.

To the University of Wisconsin Medical Scientist Training Program (MSTP), thank you for supporting me throughout my graduate training. Especially former and current MSTP directors, Dr. Anna Huttenlocher and Dr. Mark Burkard, thank you for believing in me.

To my thesis advisor, Dr. Miriam Shelef, thank you for guiding scientific discovery. To my thesis committee, Dr. Miriam Shelef, Dr. Ajay Sethi, Dr. Yun Liang, Dr. David O'Connor, and Dr. Anna Huttenlocher, thank you for providing guidance and advice throughout my graduate research.

And lastly, my sincerest thanks to my earliest teacher, my mother, Dr. Michelle Buchan. I dedicate this doctoral thesis to you. Thank you for your unwavering support and unending love.

Abstract

Antibodies develop shortly after exposure to an antigen as part of the adaptive immune response. In the acute phase of infection, antibodies respond by neutralization, opsonization of antigens, and stimulation of other immune system components. In the convalescent phase, antibodies persist despite antigen clearance, thanks to plasma cells. Upon antigen re-exposure, activated memory cells rapidly differentiate into plasma cells and contribute high affinity antibodies. In January of 2020, Severe Acute Respiratory Syndrome Coronavirus Two (SARS-CoV-2), a novel coronavirus, was identified, and a pandemic was declared a couple of months later. Severity of coronavirus disease 2019 (COVID-19) ranged from asymptomatic disease to respiratory failure leading to hospitalization, intubation, and death. Little was known about the immune response to SARS-CoV-2, given its recent emergence in humans and rapid spread. Here I investigate antibody responses after SARS-CoV-2 infection, specifically investigating anti-viral antibody responses in the early and late convalescent periods. I find that in the early convalescent period, anti-viral antibodies are elevated, including neutralizing antibodies. And higher anti-viral antibody levels are associated with more severe COVID-19, older age, male sex, higher body mass index, and symptoms, including fever and low appetite. In the late convalescent period, I find that some anti-viral antibodies persist for a year while others decline. I determine that anti-membrane antibodies in combination with anti-spike antibodies can be used to differentiate past SARS-CoV-2 infection and vaccination, and that both anti-membrane and anti-spike antibodies persist for at least one year, in contrast to the anti-nucleocapsid antibodies that decline over several months. I also investigate autoantibodies detected after SARS-CoV-2 infection. Little was known about rheumatoid factors, antibodies that bind to the Fc region of IgG, after recent infection. I find that rheumatoid factors after COVID-19 bind to unique, novel linear epitopes in the CH2 and CH3 regions of IgG Fc and bind viral antigens, including the SARS-CoV-2 spike protein. Taken together, these findings contribute to our knowledge of the antibody response following SARS-CoV-2 infection and highlight the potential

contributions of antibodies that recognize foreign and self-antigens, linking infectious disease and autoimmunity.

Chapter 1: Introduction

ANTIBODIES

Antibody Structure

Antibodies are comprised of two heavy chains and two light chains, held together by disulfide bonds [1]. Antibodies have a constant region that interacts with effector cells and a variable region that binds antigen [2]. Proteases can cleave antibodies into Fc and Fab fragments [2]. The Fc fragment corresponds to heavy chain constant domains CH_2 and CH_3 [2]. The Fab fragment is a mixed light-heavy chain dimer (V_L, C_L, V_H, CH_1) responsible for recognizing diverse antigens through somatic recombination (VDJ for heavy chain and VJ for light chain) [3]. The Fab and Fc fragments are connected by the flexible hinge region [2]. The class, or isotype, of an antibody is determined by its heavy chain structure of which there are five: μ, γ, α, ε, and δ. These correspond to the major classes of antibodies: IgM, IgG, IgA, IgE, and IgD [2]. IgM (half-life ~5-6 days) is a pentamer with up to 10 antigen binding sites [1, 4]. The multivalency of IgM allows it to bind pathogens and aggregate infectious material to facilitate clearance by macrophages, thereby preventing pathogens from infecting target cells [1]. IgM also fixes complement efficiently [5]. IgG is the most abundant isotype in human serum, has the longest half-life (~21 days), and has four subclasses: IgG1, IgG2, IgG3, and IgG4 [1]. The subclasses of IgG are different with respect to binding antigen, forming immune complexes, activating complement, and triggering effector cells. The IgG1 and IgG3 subclasses are better at binding protein antigens and activating complement than IgG2 and IgG4 [6, 7]. IgA (half-life ~6 days) is mostly found in secretions and protects mucosal surfaces by cross-linking pathogens and facilitating their removal by ciliated epithelium [1].

Antibody Development

Adaptive antibodies are secreted from plasma cells [8]. Initially in the bone marrow, a pro-B cell undergoes heavy chain rearrangement, becomes a pre-B cell, and undergoes light chain

rearrangement to form functional membrane IgM, which can cross-link upon antigen binding [9]. The bone marrow contains many self-antigens. At this stage it is important to determine if immature B cells are autoreactive because they may undergo apoptosis (called clonal deletion), become anergic, or unresponsive to the antigen, thereby preventing injury to the host [10]. Not all autoreactive B cells are eliminated in healthy individuals [11]. Some autoreactive B cells proceed to maturity and perform functions that are beneficial to the host [11]. For example, autoreactive B1 cells can produce natural antibodies involved in tissue homeostasis, and autoreactive follicular B cells can participate in germinal center reactions [11]. Immature B cells expressing IgD and IgM travel from the bone marrow to secondary lymphoid organs, such as the lymph nodes or spleen, looking for their cognate antigens [12]. A majority of immature B cells do not identify their cognate antigens within a week, and the absence of stimulatory signals leads to cell death [13]. In order for B cells to class switch and produce IgG, IgA, or IgE, they need help from activated CD4+ T cells [14]. After T cell stimulation, B cells divide to produce thousands of daughter cells [12]. B cells undergo somatic hypermutation in germinal centers of the lymph nodes or spleen, which involves mutating their antigen binding sites, and cells with the highest affinity for antigens survive [15]. B cells in lymphoid follicles respond to antigens presented by follicular dendritic cells and differentiate or enter germinal center reactions [16]. In the germinal centers, B cells face activated T cells presenting peptides, undergo somatic hypermutation and affinity maturation, and differentiate into high affinity B cells involved in memory [17]. B cell progeny become memory cells, plasma cells, and long-lived plasma cells that can produce antibodies at an accelerated rate and survive for many years [18, 19]. Peripheral tolerance, such as inducing B Cell Receptor anergy and desensitization, inhibits self-reactivity [20].

During an initial response to an antigen, the primary immune response (low-affinity IgM) is detected within 5-7 days [1, 21]. The IgG response follows two to three weeks after the

exposure [22]. On re-exposure to the same antigen, memory B cells allow for faster antibody production (within 1-2 days) that are mainly IgG and are higher affinity because they have gone through the germinal center reaction and somatic hypermutation [23].

Natural antibodies are produced before exposure to foreign antigens [24]. They are mainly IgM, low affinity, polyreactive (to self and exogenous antigens), and can have many functions [24, 25]. For example, they can recognize antigenic determinants that arise during apoptosis or oxidation and can accelerate clearance of damaged or dying cells [24]. Natural antibodies also can activate complement, opsonize antigen, and are involved in phagocytosis [25]. Natural antibodies perform homeostatic roles when reacting with self-antigens and act as an initial defense when reacting with microbial antigens [25].

Antibody Epitopes

The parts of antigens recognized by antibodies are epitopes [26]. Antigen surfaces can have many different overlapping epitopes, with epitopes being about 15 amino acids [27]. Approximately five of these 15 amino acids in the given epitope strongly influence binding [28], whereas other amino acids have less influence on binding and still others have no detectable effect. An antibody binding site is a paratope, which binds the epitope on the antigen [26]. About 50 amino acids constitute the binding area of antibodies but only around 15 of these are contact residues that define the structural epitope [29]. Similarly to epitopes, five amino acids in the paratope have the strongest influences on binding [29]. Mutations in the binding sites can alter the strength of the binding reaction by changing the conformation of the region [30].

Epitope Identification

Antibodies' variable regions promote the diversity of our immune system to recognize a vast repertoire of different antigens [31]. When an antibody recognizes an associated antigen, it can bind, and the six to 12 amino acids of the antigen that fit in the antigen-binding cleft of the antibody are called the epitope [1]. Epitopes can be linear or conformational [32]. Linear epitopes are made of continuous amino acids, whereas conformational epitopes recognize protein segments that are brought together by protein folding [33]. Epitope mapping, or the identification of epitopes that antibodies bind on antigens, is important for novel therapeutics, vaccine design, and diagnostic testing [34, 35]. Historically, x-ray crystallography was used to visualize the antibody-antigen interaction for epitope identification [36]. However, this method is time-consuming, expensive, and technically challenging. Epitopes have also been identified using site-directed mutagenesis and exon exchange [37]. A more high-throughput technology, a peptide array, can assess the binding of antibodies to overlapping peptides comprising entire proteomes [38]. With this technique, epitope mapping efficiency has increased [39].

Epitope Spreading

Epitope spreading occurs when there is an immune response to distinct epitopes that are not cross-reactive with the epitope of origin [40]. In infectious disease, diversifying the targets of a pathogen has advantages [40]. However, epitope spreading has been implicated in autoimmune diseases in which autoantibodies bind additional self-targets [40]. For example, anti-citrullinated protein antibodies (ACPAs) are present in pre-clinical rheumatoid arthritis and bind many different citrullinated antigens (i.e. histones, fibrinogen, and biglycan), forming immune complexes that stimulate macrophages and propagate subclinical inflammation and rising cytokine levels [41]. Somatic hypermutations in B cells during affinity maturation change

antibody paratopes, leading to epitope spreading and polyreactivity of ACPAs in rheumatoid arthritis [42].

SEVERE ACUTE RESPIRATORY SYNDROME CORONAVIRUS TWO (SARS-COV-2)

Human Coronaviruses

Coronaviruses are enveloped, positive sense, single stranded RNA viruses [43]. Coronaviruses HKU1, OC43, NL63, and 229E are responsible for causing mild respiratory symptoms in humans [44]. Other coronaviruses have caused epidemics, infecting thousands of people and killing hundreds [45]. Severe acute respiratory syndrome associated coronavirus (SARS-CoV) in 2002 and Middle East respiratory syndrome coronavirus (MERS-CoV) in 2012 emerged and spread internationally [45]. SARS-CoV-2 in 2020 was the first coronavirus to cause a pandemic [46]. SARS-CoV-2 causes coronavirus disease 2019 (COVID-19), which can cause asymptomatic disease, mild to moderate symptoms, severe symptoms with hospitalization, intubation, and even death [47, 48]. There have been over 762 million cases worldwide and over 6.8 million deaths [49].

SARS-CoV-2 has four structural proteins (spike, nucleocapsid, membrane, and envelope) along with non-structural and accessory proteins [50]. The structural proteins are responsible for viral production, replication, attachment, entry, and proliferation [50]. The receptor binding domain in the S1 subunit of spike binds to the host angiotensin converting enzyme two (ACE2) receptor, which mediates entry of SARS-CoV-2 into human cells [50].

SARS-CoV-2 Variants of Concern

SARS-CoV-2 evolves as genetic mutations and viral recombination occur [51]. Variants arise when mutations differentiate viruses from a common ancestor [51]. Variants of concern have

increased transmissibility, higher severity of disease, lower neutralization by antibodies, or increased difficulty in treatment [52]. Variants of concern emerged that had higher infectivity rates than the original ancestral strain of SARS-CoV-2 [52]. In December of 2020, alpha, beta, and gamma variants were classified as variants of concern, and in September of 2021 they were redesignated as variants being monitored (due to their low threat to public health because of low circulatory levels) [53]. Epsilon was a variant of concern from March 2021 to September 2021, and Delta was a variant of concern from June 2021 to April 2022 [53]. Omicron continues to be a variant of concern from November 2021 to the time of this writing [53]. It features many spike protein substitutions that have allowed for increased transmissibility and reduced neutralization by antibodies (post-vaccine or monoclonal antibody treatment) [54].

SARS-CoV-2 Vaccine

The first COVID-19 vaccines were deployed in December 2020. To date, over 13 billion doses have been administered, resulting in ~70% of the world population receiving at least one dose [55]. The messenger ribonucleic acid (mRNA) vaccines were the first to receive emergency use authorization in December 2020. These vaccines (BNT162b2 by Pfizer BioNTech and mRNA-1273 by Moderna) contain the mRNA of the spike protein of SARS-CoV-2 in a lipid nanoparticle, which gets injected intramuscularly, endocytosed by muscle cells or antigen presenting cells, and translated by host cellular machinery in the cytoplasm [56]. Most of the spike protein gets degraded in proteosomes and presented on class I major histocompatibility complexes to T cells [56]. Some of the newly synthesized spike protein is secreted to the extracellular space, endocytosed by antigen presenting cells, and incorporated in class II major histocompatibility complexes for presenting antigen to B and T cells [56]. mRNAs are unstable and strategies were used to prevent degradation by RNases and allow for efficient and safe delivery into cells [57]. The major strategies of the mRNA vaccines were 5’-capping, nucleoside modification, codon optimization, and delivery in nanoparticles [56]. Another vaccine (Ad26.COV2.S by

Johnson & Johnson) that received emergency use authorization (in February 2021) is a viral vector vaccine [58]. However, this vaccine has limited authorization because of the risk of thrombosis [59, 60]. A protein subunit vaccine (NVX-CoV2373 by Novavax) received emergency use authorization (in October 2022) much later in the United States, despite its use in other countries previously [61]. Dosing schedule recommendations for the mRNA vaccines have included completing the primary series (2 doses separated by at least 3-8 weeks) and a booster at least two months after [62]. The viral vector vaccine only requires one dose in its primary series [62].

DETECTION OF SARS-COV-2 INFECTION

Nucleic acid amplification test

Real-time reverse transcription polymerase chain reaction (RT-PCR) is a nucleic acid amplification test and is the most common method for detecting SARS-CoV-2 [63]. SARS-CoV-2 viral RNA is detected from nasopharyngeal swabs, throat swabs, or saliva [64]. Extracted RNA is reverse transcribed to complementary deoxyribonucleic acid (cDNA), and primers bind and amplify viral DNA if present [65]. False negative results can occur due to inappropriate timing of sample collection and sampling technique [66]. Specificity of RT-PCR is near 100% since designed primers are specific to the genomic sequence of SARS-CoV-2 [64]. False positive results can still occur from testing errors and contamination [64]. RT-PCR diagnoses acute infection, detects viral RNA as early as day one of symptoms, and peaks in the first week of symptoms [64]. Detecting viral RNA does not indicate viable virus, so the PCR test may remain positive after infection is cleared if viral nucleic acid remnants are still present [67].

Antigen tests

Antigen tests are rapid but are not as reliable as nucleic acid amplification tests [68]. Antigen tests detect small viral proteins as evidence that SARS-CoV-2 is actively producing viral proteins and infecting its host [69]. Although results are quicker (minutes instead of hours), false negative test results may occur if viral protein production is low in the sample [69, 70]. Therefore, a negative test does not rule out infection. At home rapid antigen tests are lateral flow assays where SARS-CoV-2 antigens, if present in the sample, flow across a conjugate pad with anti-SARS-CoV-2 antibodies [71, 72]. SARS-CoV-2 antigens from the sample bind the anti-SARS-CoV-2 antibodies on the pad, form a complex which binds to antibodies on the test line, and result in a color change indicating a positive test result [71, 72]. Rapid detection tests that can be performed at home are important for minimizing the spread of COVID-19. Individuals can determine their infection statuses without entering clinics, hospitals, or community spaces, and instead, can follow isolation procedures [73-75].

Antibody tests

Antibody testing can be used to demonstrate a recent infection [76]. In the first year of the COVID-19 pandemic, antibody testing could detect recent past SARS-CoV-2 infections [77]. In the weeks following a SARS-CoV-2 infection, antibodies are generated and can be detected months later [78]. In addition to providing individual information about infection and risk status, antibody tests were used to estimate population wide seroprevalence rates to further inform testing and isolation efforts [79]. Commercially available antibody tests detected antibodies against the spike or nucleocapsid proteins [80]. However, after vaccinations became available and widespread, anti-spike antibody tests were no longer able to differentiate between a past infection and vaccination [81, 82]. Another limitation of antibody testing is that some individuals do not mount strong antibody responses. Therefore, some individuals had positive PCR tests

and symptoms, but their antibody tests were negative [83]. Antibody responses also wane over time, and in the early convalescent period, some individuals became seronegative for virus-specific antibodies [84].

ANTIBODY TESTING METHODOLOGIES

Enzyme-linked immunosorbent assays (ELISAs)

First described in 1971, ELISAs are analytical biochemistry assays that detect and quantify products such as antibodies, proteins, and hormones [85, 86]. ELISAs are considered the gold standard of immunoassays and have high sensitivity [87]. Assay plates are incubated with an antibody or antigen. Next a primary antibody binds the target of interest, and finally a secondary detection antibody binds the primary antibody and is enzyme conjugated, creating a color change upon substrate addition [87]. Multiplex immunoassays are a derivative of the ELISA that measure multiple analytes in a single experiment, rather than a single protein or antibody of interest [88].

Neutralization assays

Neutralization assays detect neutralizing antibodies, which are protective antibodies that neutralize a pathogen and render it unable to perform its functions of infecting host cells and replicating its genome [89]. Neutralizing antibodies are important markers of immunity and prevent against infection or re-infection [90]. Neutralization assays are labor intensive to perform because they may use live viruses, which require a biosafety level three (BSL3) laboratory environment for viruses that are potentially lethal through inhalation [91, 92]. Two common assays are the plaque reduction neutralization test (PRNT) [93] and the focus reduction neutralization test (FRNT) [94]. The PRNT is the gold standard for measuring neutralizing antibodies against SARS-CoV-2 and involves serially diluting and incubating sera with virus to

form immune complexes and incubating immune complexes with a cell monolayer [95]. Then plaques (cytopathic effects) are visualized, and neutralizing antibody titers are determined based on the maximum dilution at which serum prevents cell death [96]. FRNT can accelerate detection rates and uses an antibody conjugated to horseradish peroxidase to visualize foci of infected cells [95].

Functional assays

Functional assays, such as competition assays, can demonstrate the functionality of the antibody, rather than only indicating the presence of an antibody [97]. For example, to determine if antibodies in a sample can block binding of viral protein to a host receptor, a competition assay can be used [98]. Functional assays that quantify ACE2 receptor blocking antibodies detect functional immunity, as these antibodies block entry of SARS-CoV-2 into host cells [98].

Antibody purification

Antibody purification can be used to isolate antibodies from serum [99]. Affinity chromatography is a common method for antibody purification [100]. Briefly, it includes attaching a ligand to a solid support resin, allowing a complex mixture (such as serum) to interact with the ligand-bound resin in the mobile phase, binding of target protein (or antibody) to affinity ligand, washing away non-specific proteins and antibodies, and eluting the retained antibodies of interest off the ligand-bound resin [101]. Buffers, salt concentration, pH, incubation times, and resin can all affect antibody purification and yield [101]. Once purified, antibodies can be used in ELISA to determine isotype and reactivity.

AUTOANTIBODIES

Autoantibody development

When antibodies recognize self-antigens, they are termed autoantibodies [102]. In early B cell compartments, about half of the antibodies expressed are self-reactive and polyreactive [103]. Most of these antibodies are removed in the immature B cell stage with receptor editing and deletion, and the autoreactive B cells do not survive to maturity in the periphery [103]. Central and peripheral tolerance mechanisms exist to prevent autoreactivity [20, 104, 105]. However, a loss of tolerance due to genetic and environmental factors can contribute to autoimmune disease [106, 107]. Autoantibodies are detected in the general, healthy population [108]. It is unknown whether this represents normal physiology, and autoantibodies are present to protect cognate antigens [109]. Or, whether this represents a pre-disease state in which autoantibodies are detected first, and symptoms will follow in the coming years [110, 111].

Rheumatoid Factor

Discovered in 1939, rheumatoid factor is antibody of any isotype that binds the Fc region of IgG [37, 112]. After its initial discovery for agglutinating sheep red blood cells, it was detected in rheumatoid arthritis patients [112-114]. It is currently used in the diagnosis of rheumatoid arthritis [115]. Rheumatoid factor is also present in many other states of inflammation including autoimmune diseases (Systemic Lupus Erythematous [116], Sjogren's disease [117]), lymphoma, acute and chronic infections [118, 119], recent vaccination [120], smoking, and aging [121]. Additionally, about 4% of Caucasians in the general population have detectable rheumatoid factor, and some groups have a higher rheumatoid factor at baseline [121].

Rheumatoid factor epitopes

Rheumatoid factor has two known conformational epitopes: the Ga determinant and part of the hinge [37, 122]. The Ga determinant is comprised of loops from the CH2 and CH3 regions, and the hinge is highly flexible, connecting the CH1 and CH2 regions [37, 122]. Rheumatoid factors do not normally bind IgG in circulation because IgG requires enzymatic cleavage, binding of antigen, or other modifications, to reveal rheumatoid factor binding sites [123]. More recently, it was discovered that rheumatoid factors from rheumatoid arthritis patients bind linear IgG epitopes that have been post-translationally modified by citrullination or homocitrullination [124, 125]. Additionally, a linear peptide in the hinge was identified as an epitope for rheumatoid factors in Sjogren's disease, whereas this region was not an epitope for rheumatoid factors from other autoimmune diseases [125]. This indicates that rheumatoid factors in different disease states may have different epitopes. Rheumatoid factors can also be polyreactive [126]. In addition to binding the Fc region of IgG, they can also bind other self and foreign antigens [126].

Post-translational modifications of epitopes in rheumatoid arthritis

Citrullination is the enzymatic conversion of the amino acid arginine to citrulline [127], and homocitrullination is the enzymatic conversion of the amino acid lysine to homocitrulline [128, 129] in a protein. Post-translational modifications occur in healthy individuals, such as the citrullination of keratin K1 during terminal differentiation of normal keratinocytes, which allows keratin filaments to become compact for cornification of the epidermis [130]. However, antibodies against modified (citrullinated or homocitrullinated) proteins are detected in the serum and synovial fluid of rheumatoid arthritis patients [131]. These autoantibodies form immune complexes that can deposit in the joints, activate complement, activate immune cells, lead to chemokine and cytokine release, and contribute to chronic inflammation and bone destruction [132-134]. Therefore, anti-citrullinated protein antibodies (ACPAs) likely contribute to

rheumatoid arthritis disease pathology. ACPAs are used in rheumatoid arthritis diagnosis and have higher specificity for rheumatoid arthritis than rheumatoid factors [135]. Many proteins can be modified, including IgG [124, 125]. Citrullinated regions of IgG are bound by ACPAs and rheumatoid factors; therefore, it has been suggested that IgG may be a common antigen for rheumatoid factors and ACPAs in rheumatoid arthritis [125]. ACPAs bind to different epitopes with the same post-translational modifications, so citrullination and homocitrullination may increase the multi-reactivity of ACPAs [136].

Timing of autoantibodies to disease

Rheumatoid factors and ACPAs can develop many years before rheumatoid arthritis diagnosis, and ACPAs often developing before rheumatoid factors [137-139]. Before rheumatoid arthritis, a pre-rheumatoid arthritis phase occurs when patients may start to have symptoms (such as arthralgias), yet they do not meet all diagnostic criteria [140]. Following this prodromal phase, many patients develop rheumatoid arthritis within the coming years [141]. Patients can have seropositive (marked by detection of rheumatoid factors or ACPAs) or seronegative (absence of these autoantibodies) disease [142]. About 25% of patients develop seronegative rheumatoid arthritis, which indicates that while autoantibodies likely contribute to disease pathology, they are not the sole cause of rheumatoid arthritis [143]. Additionally, asymptomatic individuals without clinical disease can have autoantibodies with the same antigenic specificity as those with disease, which raises questions regarding autoantibody pathogenicity and disease course predictions [144].

Rheumatoid factors in infection

Rheumatoid factors can be triggered and detected after infections [121]. Rheumatoid factors are detected at an increased frequency of 10-15% after viral infections that cause common colds,

such as Coxsackie B Virus and Parvovirus [145, 146]. In chronic infections with Hepatitis B or C Viruses, rheumatoid factors persist in about 25% or 50% of patients, respectively [118, 119]. In periodontitis patients with oral bacterial diseases, rheumatoid factor is detected that is cross-reactive with bacteria and IgG [147]. In Herpes Simplex viral infection, rheumatoid factors enhance neutralization by complement *in vitro* [148], indicating a mechanism of action that may extend to other infections as well, although this has not been well investigated.

Rheumatoid factors in COVID-19

Autoantibodies in COVID-19 have been detected as early as the first week of hospitalization and as late as one-year post-COVID-19 [149, 150]. Rheumatoid factors have been reported in COVID-19 in up to 20% of patients [151, 152]. Published studies that assess rheumatoid factors in COVID-19 patients with no history of rheumatoid arthritis mostly focus on the acute period while patients are hospitalized [151-153]. One of these studies followed five patients longitudinally and found two of them continued to have high IgM rheumatoid factor after 50 days [151]. Another followed three intensive care unit patients longitudinally and two of the three showed increased reactivities to autoantigens seven and 10 months after symptom onset [153]. Although small sample sizes, these studies indicate that autoreactivity post-COVID-19 may persist. The COVID-19 pandemic, while devastating, presents a unique opportunity to study rheumatoid factors produced during a primary immune response.

KNOWLEDGE GAPS

Objectives

There have been many unpredictable facets of the COVID-19 pandemic. The scientific community did not know how long anti-SARS-CoV-2 antibodies would last or whether they would protect against re-infection. We did not know which antibody tests were optimal for

detecting SARS-CoV-2 infections or how the utility of these tests may change throughout the pandemic. Even after billions of people have recovered from acute SARS-CoV-2 illness, long term complications of COVID-19 remain unknown. In this dissertation I aim to address several of the gaps in knowledge that existed in the field. The objectives of our investigations were to: 1) define the anti-viral antibody responses and correlated clinical factors in the early convalescent period, 2) determine the anti-spike, anti-membrane, and anti-nucleocapsid antibody levels of vaccinated, naive, breakthrough infection, and convalescent individuals and evaluate the one-year longevity of these antibodies in convalescent samples, and 3) define epitopes for rheumatoid factors post-COVID-19. These studies will shed light on the primary immune responses to a novel antigen and will inform areas for future research.

REFERENCES

1. Birdsall HH, Casadevall A. Adaptive Immunity: Antibodies and Immunodeficiencies. Mandell, Douglas, and Bennett's Principles and Practice of Infectious Diseases. Ninth Edition ed: Elsevier, Inc., **2020**:35-50.
2. Janeway CAJ, Travers P, Walport M, Shlomchik MJ. The structure of a typical antibody molecule. Immunobiology: The Immune System in Health and Disease. 5th Edition ed. New York: Garland Science, **2001**.
3. Stanfield RL, Wilson IA. Antibody Structure. Microbiol Spectr **2014**; 2.
4. Antibodies. In: Flaherty DK, ed. Immunology for Pharmacy: Mosby, **2012**:70-8.
5. Garson JA, Quindlen EA, Kornblith PL. Complement fixation by IgM and IgG autoantibodies on cultured human glial cells. J Neurosurg **1981**; 55:19-26.
6. Bindon CI, Hale G, Brüggemann M, Waldmann H. Human monoclonal IgG isotypes differ in complement activating function at the level of C4 as well as C1q. J Exp Med **1988**; 168:127-42.
7. Vidarsson G, Dekkers G, Rispens T. IgG subclasses and allotypes: from structure to effector functions. Front Immunol **2014**; 5:520.
8. Allen HC, Sharma P. Histology, Plasma Cells. StatPearls. Treasure Island (FL): StatPearls Publishing, **2022**.
9. Janeway CJ, Travers P, Walport M, Shlomchik M. The rearrangement of antigen-receptor gene segments controls lymphocyte development. Immunobiology: The Immune System in Health and Disease. 5th Edition ed. New York: Garland Science, **2001**.
10. Nemazee D, Buerki K. Clonal deletion of autoreactive B lymphocytes in bone marrow chimeras. Proc Natl Acad Sci U S A **1989**; 86:8039-43.
11. Lee S, Ko Y, Kim TJ. Homeostasis and regulation of autoreactive B cells. Cell Mol Immunol **2020**; 17:561-9.
12. Cyster JG, Allen CDC. B Cell Responses: Cell Interaction Dynamics and Decisions. Cell **2019**; 177:524-40.
13. Allman DM, Ferguson SE, Lentz VM, Cancro MP. Peripheral B cell maturation. II. Heat-stable antigen(hi) splenic B cells are an immature developmental intermediate in the production of long-lived marrow-derived B cells. J Immunol **1993**; 151:4431-44.
14. Shinomiya N, Kuratsuji T, Yata J. The role of T cells in immunoglobulin class switching of specific antibody production system in vitro in humans. Cell Immunol **1989**; 118:239-49.
15. Kelsoe G. The germinal center: a crucible for lymphocyte selection. Semin Immunol **1996**; 8:179-84.
16. Kranich J, Krautler NJ. How Follicular Dendritic Cells Shape the B-Cell Antigenome. Front Immunol **2016**; 7:225.
17. LeBien TW, Tedder TF. B lymphocytes: how they develop and function. Blood **2008**; 112:1570-80.
18. Calame KL. Plasma cells: finding new light at the end of B cell development. Nat Immunol **2001**; 2:1103-8.
19. Slifka MK, Ahmed R. Long-lived plasma cells: a mechanism for maintaining persistent antibody production. Curr Opin Immunol **1998**; 10:252-8.
20. Brooks JF, Murphy PR, Barber JEM, Wells JW, Steptoe RJ. Peripheral Tolerance Checkpoints Imposed by Ubiquitous Antigen Expression Limit Antigen-Specific B Cell Responses under Strongly Immunogenic Conditions. J Immunol **2020**; 205:1239-47.
21. Sathe A, Cusick J. Biochemistry, Immunoglobulin M. StatPearls: StatPearls Publishing, **2021**.
22. Bandilla KK, McDuffie FC, Gleich GJ. Immunoglobulin classes of antibodies produced in the primary and secondary responses in man. Clin Exp Immunol **1969**; 5:627-41.
23. Palm AE, Henry C. Remembrance of Things Past: Long-Term B Cell Memory After Infection and Vaccination. Front Immunol **2019**; 10:1787.

24. Palma J, Tokarz-Deptuła B, Deptuła J, Deptuła W. Natural antibodies - facts known and unknown. Cent Eur J Immunol **2018**; 43:466-75.
25. Reyneveld GI, Savelkoul HFJ, Parmentier HK. Current Understanding of Natural Antibodies and Exploring the Possibilities of Modulation Using Veterinary Models. A Review. Front Immunol **2020**; 11:2139.
26. Sela-Culang I, Kunik V, Ofran Y. The structural basis of antibody-antigen recognition. Front Immunol **2013**; 4:302.
27. Benjamin DC, Perdue SS. Site-Directed Mutagenesis in Epitope Mapping. Methods **1996**; 9:508-15.
28. Dougan DA, Malby RL, Gruen LC, Kortt AA, Hudson PJ. Effects of substitutions in the binding surface of an antibody on antigen affinity. Protein Eng **1998**; 11:65-74.
29. Van Regenmortel MH. From absolute to exquisite specificity. Reflections on the fuzzy nature of species, specificity and antigenic sites. J Immunol Methods **1998**; 216:37-48.
30. Wedemayer GJ, Patten PA, Wang LH, Schultz PG, Stevens RC. Structural insights into the evolution of an antibody combining site. Science **1997**; 276:1665-9.
31. Alberts B, A J, Lewis J. The Generation of Antibody Diversity. Molecular Biology of the Cell. 4th Edition ed. New York: Garland Science, **2002**.
32. Sela M, Schechter B, Schechter I, Borek F. Antibodies to Sequential and Conformational Determinants. Vol. 32. Cold Spring Harbor Symposia on Quantitative Biology: Cold Spring Harbor Laboratory Press, **1967**:537-45.
33. Forsström B, Axnäs BB, Rockberg J, Danielsson H, Bohlin A, Uhlen M. Dissecting antibodies with regards to linear and conformational epitopes. PLoS One **2015**; 10:e0121673.
34. Gershoni JM, Roitburd-Berman A, Siman-Tov DD, Tarnovitski Freund N, Weiss Y. Epitope mapping: the first step in developing epitope-based vaccines. BioDrugs **2007**; 21:145-56.
35. Irving MB, Pan O, Scott JK. Random-peptide libraries and antigen-fragment libraries for epitope mapping and the development of vaccines and diagnostics. Curr Opin Chem Biol **2001**; 5:314-24.
36. Toride King M, Brooks CL. Epitope Mapping of Antibody-Antigen Interactions with X-Ray Crystallography. Methods Mol Biol **2018**; 1785:13-27.
37. Artandi SE, Calame KL, Morrison SL, Bonagura VR. Monoclonal IgM rheumatoid factors bind IgG at a discontinuous epitope comprised of amino acid loops from heavy-chain constant-region domains 2 and 3. Proc Natl Acad Sci U S A **1992**; 89:94-8.
38. Szymczak LC, Kuo HY, Mrksich M. Peptide Arrays: Development and Application. Anal Chem **2018**; 90:266-82.
39. Buus S, Rockberg J, Forsström B, Nilsson P, Uhlen M, Schafer-Nielsen C. High-resolution mapping of linear antibody epitopes using ultrahigh-density peptide microarrays. Mol Cell Proteomics **2012**; 11:1790-800.
40. Powell AM, Black MM. Epitope spreading: protection from pathogens, but propagation of autoimmunity? Clin Exp Dermatol **2001**; 26:427-33.
41. Sokolove J, Bromberg R, Deane KD, et al. Autoantibody epitope spreading in the pre-clinical phase predicts progression to rheumatoid arthritis. PLoS One **2012**; 7:e35296.
42. Kongpachith S, Lingampalli N, Ju CH, et al. Affinity Maturation of the Anti-Citrullinated Protein Antibody Paratope Drives Epitope Spreading and Polyreactivity in Rheumatoid Arthritis. Arthritis Rheumatol **2019**; 71:507-17.
43. Weiss SR. Forty years with coronaviruses. J Exp Med **2020**; 217.
44. Liu DX, Liang JQ, Fung TS. Human Coronavirus-229E, -OC43, -NL63, and -HKU1 (*Coronaviridae*): Encyclopedia of Virology, **2021**:428-40.
45. Zhu Z, Lian X, Su X, Wu W, Marraro GA, Zeng Y. From SARS and MERS to COVID-19: a brief summary and comparison of severe acute respiratory infections caused by three highly pathogenic human coronaviruses. Respir Res **2020**; 21:224.

46. WHO Director-General's opening remarks at the media briefing on COVID-19- 11 March 2020: World Health Organization, **2020**.
47. Lamba M, Mishra PR, Verma R, Bharti A, Punia V, Mittal S. The COVID-19 Clinical Spectrum and the Effect of Associated Comorbidities on Illness Severity in the North Indian Population: A Cross-Sectional Study. Cureus **2022**; 14:e28192.
48. Carrillo Hernandez-Rubio J, Sanchez-Carpintero Abad M, Yordi Leon A, et al. Outcomes of an intermediate respiratory care unit in the COVID-19 pandemic. PLoS One **2020**; 15:e0243968.
49. WHO Coronavirus Dashboard. January 23, 2023 ed. online, **2023**.
50. Satarker S, Nampoothiri M. Structural Proteins in Severe Acute Respiratory Syndrome Coronavirus-2. Arch Med Res **2020**; 51:482-91.
51. Singh D, Yi SV. On the origin and evolution of SARS-CoV-2. Exp Mol Med **2021**; 53:537-47.
52. Liu H, Wei P, Kappler JW, Marrack P, Zhang G. SARS-CoV-2 Variants of Concern and Variants of Interest Receptor Binding Domain Mutations and Virus Infectivity. Front Immunol **2022**; 13:825256.
53. SARS-CoV-2 Variant Classifications and Definitions. Centers for Disease Control and Prevention, **2022**.
54. Bálint G, Vörös-Horváth B, Széchenyi A. Omicron: increased transmissibility and decreased pathogenicity. Signal Transduct Target Ther **2022**; 7:151.
55. Mathieu E, Ritchie H, Rodés-Guirao L, et al. Coronavirus Pandemic (COVID-19). Coronavirus (COVID-19) Vaccinations: OurWorldInData.org, **2020**.
56. Park JW, Lagniton PNP, Liu Y, Xu RH. mRNA vaccines for COVID-19: what, why and how. Int J Biol Sci **2021**; 17:1446-60.
57. Zhang NN, Li XF, Deng YQ, et al. A Thermostable mRNA Vaccine against COVID-19. Cell **2020**; 182:1271-83.e16.
58. Mascellino MT, Di Timoteo F, De Angelis M, Oliva A. Overview of the Main Anti-SARS-CoV-2 Vaccines: Mechanism of Action, Efficacy and Safety. Infect Drug Resist **2021**; 14:3459-76.
59. Coronavirus (COVID-19) Update: FDA Limits Use of Janssen COVID-19 Vaccine to Certain Individuals: U.S. Food & Drug Administration, **2022**.
60. Sharifian-Dorche M, Bahmanyar M, Sharifian-Dorche A, Mohammadi P, Nomovi M, Mowla A. Vaccine-induced immune thrombotic thrombocytopenia and cerebral venous sinus thrombosis post COVID-19 vaccination; a systematic review. J Neurol Sci **2021**; 428:117607.
61. Heath PT, Galiza EP, Baxter DN, et al. Safety and Efficacy of NVX-CoV2373 Covid-19 Vaccine. N Engl J Med **2021**; 385:1172-83.
62. Stay Up to Date with COVID-19 Vaccines Including Boosters: Centers for Disease Control and Prevention, **2023**.
63. LeBlanc JJ, Gubbay JB, Li Y, et al. Real-time PCR-based SARS-CoV-2 detection in Canadian laboratories. J Clin Virol **2020**; 128:104433.
64. Sethuraman N, Jeremiah SS, Ryo A. Interpreting Diagnostic Tests for SARS-CoV-2. JAMA **2020**; 323:2249-51.
65. Nolan T, Hands RE, Bustin SA. Quantification of mRNA using real-time RT-PCR. Nat Protoc **2006**; 1:1559-82.
66. Gupta-Wright A, Macleod CK, Barrett J, et al. False-negative RT-PCR for COVID-19 and a diagnostic risk score: a retrospective cohort study among patients admitted to hospital. BMJ Open **2021**; 11:e047110.
67. Wölfel R, Corman VM, Guggemos W, et al. Virological assessment of hospitalized patients with COVID-2019. Nature **2020**; 581:465-9.
68. Fajardo Á, Perbolianachis P, Ferreiro I, Moreno P, Moratorio G. Molecular accuracy vs antigenic speed: SARS-CoV-2 testing strategies. Curr Opin Pharmacol **2022**; 62:152-8.

69. Jakobsen KK, Jensen JS, Todsen T, et al. Accuracy and cost description of rapid antigen test compared with reverse transcriptase-polymerase chain reaction for SARS-CoV-2 detection. Dan Med J **2021**; 68.
70. Yamayoshi S, Sakai-Tagawa Y, Koga M, et al. Comparison of Rapid Antigen Tests for COVID-19. Viruses **2020**; 12.
71. O'Farrell B. Evolution in Lateral Flow–Based Immunoassay Systems. Lateral Flow Immunoassay: Humana Press, **2008**:1-33.
72. Peto T, Team UC-LFO. COVID-19: Rapid antigen detection for SARS-CoV-2 by lateral flow assay: A national systematic evaluation of sensitivity and specificity for mass-testing. EClinicalMedicine **2021**; 36:100924.
73. Larremore DB, Wilder B, Lester E, et al. Test sensitivity is secondary to frequency and turnaround time for COVID-19 screening. Sci Adv **2021**; 7.
74. Love J, Wimmer MT, Toth DJA, et al. Comparison of antigen- and RT-PCR-based testing strategies for detection of SARS-CoV-2 in two high-exposure settings. PLoS One **2021**; 16:e0253407.
75. Ricks S, Kendall EA, Dowdy DW, Sacks JA, Schumacher SG, Arinaminpathy N. Quantifying the potential value of antigen-detection rapid diagnostic tests for COVID-19: a modelling analysis. BMC Med **2021**; 19:75.
76. Dimech W. The Standardization and Control of Serology and Nucleic Acid Testing for Infectious Diseases. Clin Microbiol Rev **2021**; 34:e0003521.
77. Liu C, Yu X, Gao C, et al. Characterization of antibody responses to SARS-CoV-2 in convalescent COVID-19 patients. J Med Virol **2021**; 93:2227-33.
78. Xiao K, Yang H, Liu B, et al. Antibodies Can Last for More Than 1 Year After SARS-CoV-2 Infection: A Follow-Up Study From Survivors of COVID-19. Front Med (Lausanne) **2021**; 8:684864.
79. Wiegand RE, Deng Y, Deng X, et al. Estimated SARS-CoV-2 antibody seroprevalence trends and relationship to reported case prevalence from a repeated, cross-sectional study in the 50 states and the District of Columbia, United States-October 25, 2020-February 26, 2022. Lancet Reg Health Am **2023**; 18:100403.
80. EUA Authorized Serology Test Performance. fda.gov, **2021**.
81. Macdonald PJ, Schaub JM, Ruan Q, Williams CL, Prostko JC, Tetin SY. Affinity of anti-spike antibodies to three major SARS-CoV-2 variants in recipients of three major vaccines. Commun Med (Lond) **2022**; 2:109.
82. Shrotri M, Fragaszy E, Nguyen V, et al. Spike-antibody responses to COVID-19 vaccination by demographic and clinical factors in a prospective community cohort study. Nat Commun **2022**; 13:5780.
83. Long QX, Tang XJ, Shi QL, et al. Clinical and immunological assessment of asymptomatic SARS-CoV-2 infections. Nat Med **2020**; 26:1200-4.
84. Long QX, Tang XJ, Shi QL, et al. Clinical and immunological assessment of asymptomatic SARS-CoV-2 infections. Nat Med **2020**.
85. Engvall E, Perlmann P. Enzyme-linked immunosorbent assay (ELISA). Quantitative assay of immunoglobulin G. Immunochemistry **1971**; 8:871-4.
86. Engvall E, Jonsson K, Perlmann P. Enzyme-linked immunosorbent assay. II. Quantitative assay of protein antigen, immunoglobulin G, by means of enzyme-labelled antigen and antibody-coated tubes. Biochim Biophys Acta **1971**; 251:427-34.
87. StatPearls, **2022**.
88. Vostrý M. Multiplex Immunoassays: Chips and Beads. EJIFCC **2010**; 20:162-5.
89. Morales-Núñez JJ, Muñoz-Valle JF, Torres-Hernández PC, Hernández-Bello J. Overview of Neutralizing Antibodies and Their Potential in COVID-19. Vaccines (Basel) **2021**; 9.
90. Khoury DS, Cromer D, Reynaldi A, et al. Neutralizing antibody levels are highly predictive of immune protection from symptomatic SARS-CoV-2 infection. Nat Med **2021**; 27:1205-11.

91. Perera RA, Mok CK, Tsang OT, et al. Serological assays for severe acute respiratory syndrome coronavirus 2 (SARS-CoV-2), March 2020. Euro Surveill **2020**; 25.
92. Okba NMA, Müller MA, Li W, et al. Severe Acute Respiratory Syndrome Coronavirus 2-Specific Antibody Responses in Coronavirus Disease Patients. Emerg Infect Dis **2020**; 26:1478-88.
93. Mendoza EJ, Manguiat K, Wood H, Drebot M. Two Detailed Plaque Assay Protocols for the Quantification of Infectious SARS-CoV-2. Curr Protoc Microbiol **2020**; 57:ecpmc105.
94. Vanderheiden A, Edara VV, Floyd K, et al. Development of a Rapid Focus Reduction Neutralization Test Assay for Measuring SARS-CoV-2 Neutralizing Antibodies. Curr Protoc Immunol **2020**; 131:e116.
95. Liu KT, Han YJ, Wu GH, Huang KA, Huang PN. Overview of Neutralization Assays and International Standard for Detecting SARS-CoV-2 Neutralizing Antibody. Viruses **2022**; 14.
96. Wang S, Sakhatskyy P, Chou TH, Lu S. Assays for the assessment of neutralizing antibody activities against Severe Acute Respiratory Syndrome (SARS) associated coronavirus (SCV). J Immunol Methods **2005**; 301:21-30.
97. Wouters E, Verbrugghe C, Devloo R, et al. A novel competition ELISA for the rapid quantification of SARS-CoV-2 neutralizing antibodies in convalescent plasma. Transfusion **2021**; 61:2981-90.
98. Walker SN, Chokkalingam N, Reuschel EL, et al. SARS-CoV-2 Assays To Detect Functional Antibody Responses That Block ACE2 Recognition in Vaccinated Animals and Infected Patients. J Clin Microbiol **2020**; 58.
99. Bergmann-Leitner ES, Mease RM, Duncan EH, Khan F, Waitumbi J, Angov E. Evaluation of immunoglobulin purification methods and their impact on quality and yield of antigen-specific antibodies. Malar J **2008**; 7:129.
100. Ayyar BV, Arora S, Murphy C, O'Kennedy R. Affinity chromatography as a tool for antibody purification. Methods **2012**; 56:116-29.
101. Arora S, Saxena V, Ayyar BV. Affinity chromatography: A versatile technique for antibody purification. Methods **2017**; 116:84-94.
102. Janeway CAJ, Travers P, Walport M, Shlomchik MJ. Autoimmune responses are directed against self antigens. Immunobiology: The Immune System in Health and Disease. 5th Edition ed. New York: Garland Science, **2001**.
103. Wardemann H, Yurasov S, Schaefer A, Young JW, Meffre E, Nussenzweig MC. Predominant autoantibody production by early human B cell precursors. Science **2003**; 301:1374-7.
104. Nemazee D. Mechanisms of central tolerance for B cells. Nat Rev Immunol **2017**; 17:281-94.
105. Cashman KS, Jenks SA, Woodruff MC, et al. Understanding and measuring human B-cell tolerance and its breakdown in autoimmune disease. Immunol Rev **2019**; 292:76-89.
106. Menard L, Saadoun D, Isnardi I, et al. The PTPN22 allele encoding an R620W variant interferes with the removal of developing autoreactive B cells in humans. J Clin Invest **2011**; 121:3635-44.
107. Khan MF, Wang G. Environmental Agents, Oxidative Stress and Autoimmunity. Curr Opin Toxicol **2018**; 7:22-7.
108. Bowen RA, Bertholf RL, Holmquist B. Maximizing the value of laboratory tests. Handbook of Diagnostic Endocrinology. 3rd Edition ed, **2021**.
109. Nicolò A, Amendt T, El Ayoubi O, et al. Rheumatoid factor IgM autoantibodies control IgG homeostasis. Front Immunol **2022**; 13:1016263.
110. Burbelo PD, Gordon SM, Waldman M, et al. Autoantibodies are present before the clinical diagnosis of systemic sclerosis. PLoS One **2019**; 14:e0214202.
111. Arbuckle MR, McClain MT, Rubertone MV, et al. Development of autoantibodies before the clinical onset of systemic lupus erythematosus. N Engl J Med **2003**; 349:1526-33.

112. Waaler E. On the occurrence of a factor in human serum activating the specific agglutintion of sheep blood corpuscles. 1939. APMIS **2007**; 115:422-38; discussion 39.
113. ROSE HM, RAGAN C. Differential agglutination of normal and sensitized sheep erythrocytes by sera of patients with rheumatoid arthritis. Proc Soc Exp Biol Med **1948**; 68:1-6.
114. PIKE RM, SULKIN SE, COGGESHALL HC. Serological reactions in rheumatoid arthritis; factors affecting the agglutination of sensitized sheep erythrocytes in rheumatid-arthritis serum. J Immunol **1949**; 63:441-6.
115. Aletaha D, Neogi T, Silman AJ, et al. 2010 Rheumatoid arthritis classification criteria: an American College of Rheumatology/European League Against Rheumatism collaborative initiative. Arthritis Rheum **2010**; 62:2569-81.
116. Witte T, Hartung K, Sachse C, et al. Rheumatoid factors in systemic lupus erythematosus: association with clinical and laboratory parameters. SLE study group. Rheumatol Int **2000**; 19:107-11.
117. Markusse HM, Otten HG, Vroom TM, Smeets TJ, Fokkens N, Breedveld FC. Rheumatoid factor isotypes in serum and salivary fluid of patients with primary Sjögren's syndrome. Clin Immunol Immunopathol **1993**; 66:26-32.
118. Philémon EA, Tume C, Okomo Assoumou MC, et al. A Cross Sectional Study of the Impact of Human Immunodeficiency Virus, Hepatitis B Virus and Hepatitis C Virus on Rheumatoid Factor Production. Arch Rheumatol **2018**; 33:402-7.
119. Lin KM, Chen WM, Tung SY, et al. Prevalence and predictive value of high-positive rheumatoid factor and anti-citrullinated protein antibody levels in nonarthritic patients with chronic hepatitis C infection. Int J Rheum Dis **2019**; 22:116-20.
120. Welch MJ, Fong S, Vaughan J, Carson D. Increased frequency of rheumatoid factor precursor B lymphocytes after immunization of normal adults with tetanus toxoid. Clin Exp Immunol **1983**; 51:299-304.
121. Ingegnoli F, Castelli R, Gualtierotti R. Rheumatoid factors: clinical applications. Dis Markers **2013**; 35:727-34.
122. Terness P, Kohl I, Hübener G, et al. The natural human IgG anti-F(ab')2 antibody recognizes a conformational IgG1 hinge epitope. J Immunol **1995**; 154:6446-52.
123. Maibom-Thomsen SL, Trier NH, Holm BE, et al. Immunoglobulin G structure and rheumatoid factor epitopes. PLoS One **2019**; 14:e0217624.
124. Zheng Z, Mergaert AM, Fahmy LM, et al. Disordered Antigens and Epitope Overlap Between Anti-Citrullinated Protein Antibodies and Rheumatoid Factor in Rheumatoid Arthritis. Arthritis Rheumatol **2020**; 72:262-72.
125. Mergaert AM, Zheng Z, Denny MF, et al. Rheumatoid Factor and Anti-Modified Protein Antibody Reactivities Converge on IgG Epitopes. Arthritis Rheumatol **2022**; 74:984-91.
126. Nakamura M, Burastero SE, Notkins AL, Casal P. Human monoclonal rheumatoid factor-like antibodies from CD5 (Leu-1)+ B cells are polyreactive. J Immunol **1988**; 140:4180-6.
127. Khandpur R, Carmona-Rivera C, Vivekanandan-Giri A, et al. NETs are a source of citrullinated autoantigens and stimulate inflammatory responses in rheumatoid arthritis. Sci Transl Med **2013**; 5:178ra40.
128. Pruijn GJ. Citrullination and carbamylation in the pathophysiology of rheumatoid arthritis. Front Immunol **2015**; 6:192.
129. van Delft MAM, Huizinga TWJ. An overview of autoantibodies in rheumatoid arthritis. J Autoimmun **2020**; 110:102392.
130. Vossenaar ER, Zendman AJ, van Venrooij WJ, Pruijn GJ. PAD, a growing family of citrullinating enzymes: genes, features and involvement in disease. Bioessays **2003**; 25:1106-18.
131. Trouw LA, Rispens T, Toes REM. Beyond citrullination: other post-translational protein modifications in rheumatoid arthritis. Nat Rev Rheumatol **2017**; 13:331-9.

132. Daha NA, Banda NK, Roos A, et al. Complement activation by (auto-) antibodies. Mol Immunol **2011**; 48:1656-65.
133. Trouw LA, Haisma EM, Levarht EW, et al. Anti-cyclic citrullinated peptide antibodies from rheumatoid arthritis patients activate complement via both the classical and alternative pathways. Arthritis Rheum **2009**; 60:1923-31.
134. Chang MH, Nigrovic PA. Antibody-dependent and -independent mechanisms of inflammatory arthritis. JCI Insight **2019**; 4.
135. Nishimura K, Sugiyama D, Kogata Y, et al. Meta-analysis: diagnostic accuracy of anti-cyclic citrullinated peptide antibody and rheumatoid factor for rheumatoid arthritis. Ann Intern Med **2007**; 146:797-808.
136. Steen J, Forsström B, Sahlström P, et al. Recognition of Amino Acid Motifs, Rather Than Specific Proteins, by Human Plasma Cell-Derived Monoclonal Antibodies to Posttranslationally Modified Proteins in Rheumatoid Arthritis. Arthritis Rheumatol **2019**; 71:196-209.
137. Nielsen SF, Bojesen SE, Schnohr P, Nordestgaard BG. Elevated rheumatoid factor and long term risk of rheumatoid arthritis: a prospective cohort study. BMJ **2012**; 345:e5244.
138. Rantapää-Dahlqvist S. What happens before the onset of rheumatoid arthritis? Curr Opin Rheumatol **2009**; 21:272-8.
139. Kelmenson LB, Wagner BD, McNair BK, et al. Timing of Elevations of Autoantibody Isotypes Prior to Diagnosis of Rheumatoid Arthritis. Arthritis Rheumatol **2020**; 72:251-61.
140. Greenblatt HK, Kim HA, Bettner LF, Deane KD. Preclinical rheumatoid arthritis and rheumatoid arthritis prevention. Curr Opin Rheumatol **2020**; 32:289-96.
141. Paul BJ, Kandy HI, Krishnan V. Pre-rheumatoid arthritis and its prevention. Eur J Rheumatol **2017**; 4:161-5.
142. Salma K, Nessrine A, Krystel E, et al. Rheumatoid Arthritis: Seropositivity versus Seronegativity; A Comparative Cross-sectional Study Arising from Moroccan Context. Curr Rheumatol Rev **2020**; 16:143-8.
143. Coffey CM, Crowson CS, Myasoedova E, Matteson EL, Davis JM. Evidence of Diagnostic and Treatment Delay in Seronegative Rheumatoid Arthritis: Missing the Window of Opportunity. Mayo Clin Proc **2019**; 94:2241-8.
144. Reed JH. Transforming mutations in the development of pathogenic B cell clones and autoantibodies. Immunol Rev **2022**; 307:101-15.
145. Newkirk MM. Rheumatoid factors: host resistance or autoimmunity? Clin Immunol **2002**; 104:1-13.
146. Shmerling RH, Delbanco TL. The rheumatoid factor: an analysis of clinical utility. Am J Med **1991**; 91:528-34.
147. Thé J, Ebersole JL. Rheumatoid factor from periodontitis patients cross-reacts with epitopes on oral bacteria. Oral Dis **1996**; 2:253-62.
148. Ashe WK, Daniels CA, Scott GS, Notkins AL. Interaction of rheumatoid factor with infectious herpes simplex virus-antibody complexes. Science **1971**; 172:176-7.
149. Chang SE, Feng A, Meng W, et al. New-onset IgG autoantibodies in hospitalized patients with COVID-19. Nat Commun **2021**; 12:5417.
150. Son K, Jamil R, Chowdhury A, et al. Circulating anti-nuclear autoantibodies in COVID-19 survivors predict long COVID symptoms. Eur Respir J **2023**; 61.
151. Xu C, Fan J, Luo Y, et al. Prevalence and Characteristics of Rheumatoid-Associated Autoantibodies in Patients with COVID-19. J Inflamm Res **2021**; 14:3123-8.
152. Anaya JM, Monsalve DM, Rojas M, et al. Latent rheumatic, thyroid and phospholipid autoimmunity in hospitalized patients with COVID-19. J Transl Autoimmun **2021**; 4:100091.
153. Woodruff MC, Ramonell RP, Haddad NS, et al. Dysregulated naive B cells and de novo autoreactivity in severe COVID-19. Nature **2022**; 611:139-47.

Chapter 2: Specific COVID-19 Symptoms Correlate with High Antibody Levels against SARS-CoV-2

Maya F. Amjadi[1], Sarah E. O'Connell[2], Tammy Armbrust[3], Aisha M. Mergaert[1,4], Sandeep R. Narpala[2], Peter J. Halfmann[3], S. Janna Bashar[1], Christopher R. Glover[1], Anna S. Heffron[4], Alison Taylor[2], Britta Flach[2], David H. O'Connor[4], Yoshihiro Kawaoka[3], Adrian B. McDermott[2], Ajay K. Sethi[5], Miriam A. Shelef[1,6]

[1]Department of Medicine, University of Wisconsin-Madison, Madison, WI 53705 USA

[2]Vaccine Immunology Program, Vaccine Research Center, National Institutes of Allergy and Infectious Diseases, National Institutes of Health, Bethesda, MD 20892 USA

[3]Department of Pathobiological Sciences, School of Veterinary Medicine, Influenza Research Institute, University of Wisconsin–Madison, Madison, WI 53711 USA

[4]Department of Pathology and Laboratory Medicine, University of Wisconsin-Madison, Madison, WI 53705 USA

[5]Department of Population Health Sciences, University of Wisconsin-Madison, Madison, WI 53726 USA

[6]William S. Middleton Memorial Veterans Hospital, Madison, WI 53705 USA

Immunohorizons. 2021 Jun 17;5(6):466-476. doi: 10.4049/immunohorizons.2100022. PMID: 34398806; PMCID: PMC8452279.

Contributions: I contributed to analyzing the data, made the figures and tables, wrote the first draft of the manuscript, and assisted in editing the manuscript.

ABSTRACT

Lasting immunity will be critical for overcoming COVID-19. However, factors that drive the development of high titers of anti-SARS-CoV-2 antibodies and how long those antibodies persist remain unclear, due in part to study limitations necessitated by urgency. To overcome these limitations, we quantified serum anti-SARS-CoV-2 antibodies in clinically diverse COVID-19 convalescent subjects five weeks (n=113) and three months (n=79) after symptom resolution with three methods: a novel multiplex assay to quantify IgG against four SARS-CoV-2 antigens, a new SARS-CoV-2 receptor binding domain-angiotensin converting enzyme 2 inhibition assay, and a SARS-CoV-2 neutralizing assay. We then identified clinical and demographic factors, including never before assessed COVID-19 symptoms, that consistently correlate with high anti-SARS-CoV-2 antibody levels. We detected anti-SARS-CoV-2 antibodies in 98% of COVID-19 convalescent subjects five weeks after symptom resolution and antibody levels did not decline at three months. Greater disease severity, older age, male sex, higher body mass index, and higher Charlson Comorbidity Index score correlated with increased anti-SARS-CoV-2 antibody levels. Moreover, we report for the first time that COVID-19 symptoms, most consistently fever, body aches, and low appetite, correlate with higher anti-SARS-CoV-2 antibody levels. Our results provide robust and new insights into the development and persistence of anti-SARS-CoV-2 antibodies.

INTRODUCTION

Severe acute respiratory syndrome coronavirus 2 (SARS-CoV-2), isolated January 2020 [1], causes coronavirus disease 2019 (COVID-19), which ranges from no symptoms to a flu-like illness to death [2]. As of December 2020, there have been over 78 million cases worldwide and over 1.7 million deaths [3], with devastating effects on health, economies, and societies [4].

Lasting immunity, often estimated by persistent antibodies, will be critical for overcoming the COVID-19 pandemic, but our understanding of the development of persistent anti-SARS-CoV-2 antibodies is still emerging. In severe acute respiratory syndrome (SARS), caused by related SARS-CoV, antibodies typically persist at least three years [5-7]. Less is known about SARS-CoV-2, but a few reports suggest that immunity may last at least three to six months [8-11]. However, other reports suggest that anti-SARS-CoV-2 neutralizing and IgG antibodies can decline within a few months, with some patients becoming seronegative [12-21]. These discrepant findings may be due to small sample sizes, use of variable or loosely defined time points, differing disease severity (a known correlate of antibody levels and persistence [16, 21-23]), and the use of different antibody detection methods, with neutralizing titers more likely to be low [24, 25]. Also, many studies do not evaluate clinical correlates of antibody titers and none have systematically evaluated COVID-19 symptoms. A standardized approach to evaluating anti-SARS-CoV-2 antibodies with uniform time points defined by the resolution of disease, multiple antibody tests, and incorporation of clinical and demographic factors including COVID-19 symptoms would shed light on the development of antibody-based immunity in COVID-19.

Thus, we broadly evaluated the antibody response against SARS-CoV-2 in a clinically diverse COVID-19 convalescent population at five weeks and three months after symptom resolution using three different assays and then correlated antibody levels with clinical and demographic factors including COVID-19 symptoms. We found that greater disease severity, older age, male sex, higher body mass index, and higher Charlson Comorbidity Index score correlate with higher anti-SARS-CoV-2 antibody levels. We also identified fever, body aches, and low appetite as symptoms that consistently correlate with higher anti-SARS-CoV-2 antibody levels and demonstrate antibody persistence three months after symptom resolution.

MATERIALS AND METHODS

Human Subjects

Human studies were performed according to the Declaration of Helsinki and were approved by the University of Wisconsin (UW) Institutional Review Board. All subjects provided written informed consent. COVID-19 convalescent sera and data were obtained from the UW COVID-19 Convalescent Biorepository and control sera collected prior to 2019 were obtained from the UW Rheumatology Biorepository [26] and the NIH clinical protocol VRC200. For the COVID-19 Convalescent Biorepository, all individuals 18+ years old who tested positive for SARS-CoV-2 by PCR at UW Health were invited to participate until 120 subjects were recruited. Clinical and demographic data were collected by survey upon recruitment. Additional data and blood were collected 5 weeks and 3 months +/- 10 days post-symptom resolution. Age, sex, address (for area of deprivation index, ADI [27]), medications, lab values, height and weight (for body mass index, BMI), medical problems, and the date of the most recent primary care appointment were abstracted from the UW Health electronic medical record (EMR). Race, ethnicity, tobacco use, COVID-19 symptoms, and date of symptom resolution were self-reported by questionnaire. Hospitalization and intubation for COVID-19 were obtained by questionnaire and EMR abstraction. COVID-19 severity was scored as critical (4, intubated), severe (3, hospitalized but not intubated), moderate (2, fever defined as temperature >100°F, chills, productive cough, or shortness of breath, but not hospitalized), or mild (1, none of the above). Charlson Comorbidity Index Scores were calculated [28]. Subjects were excluded from this study if they received convalescent plasma, if blood was collected >14 days from the intended time point, or if they did not provide consent for all aspects of the study.

IgG binding to coronavirus antigens (multiplex assay)

Plates (96 well) printed with SARS-CoV-2 spike protein, receptor binding domain (RBD) of spike, N terminal domain (NTD) of spike, and nucleocapsid protein, as well as spike from SARS-CoV, HCoV-HKU1, HCoV-OC43, HCoV-NL63, and HCoV-229E, in addition to bovine serum albumin (BSA) were supplied by Meso Scale Discovery (MSD, Rockville, USA). Plates were blocked for 60 minutes with MSD Blocker A (5% BSA) followed by washing. Then, sera were applied to the wells at 4 dilutions (1:100, 1:800, 1:3200 and 1:12,800) and incubated with shaking for 2 hours. Plates were washed and SULFO-TAG labeled anti-IgG (MSD) was applied to the wells for 1 hour. Plates were washed, enhanced chemiluminescence (ECL) substrate (MSD) applied, and light emission (as a measure of bound IgG) read with the MSD Sector instrument. BSA readings were subtracted from CoV antigen readings. Area under the curve values for each sample were used for statistical analysis with zero values (3 samples for anti-NTD) depicted as ten in graphs for optimal visualization using the log scale.

Inhibition assay

Plates (384 well) precoated with RBD were supplied by MSD. Plates were blocked for 30 minutes with MSD Blocker A, washed, sera applied at 1:10 dilution, and incubated with shaking for 1 hour. SULFO-TAG labeled angiotensin converting enzyme (ACE)2 was applied to the wells, incubated for 1 hour, and washed. ECL substrate was applied, and light emission (a measure of RBD-ACE2 complex) was read by the MSD Sector instrument. The amount of light emitted in wells containing no sample (assay diluent only) was considered the maximal binding response. Reduction of ECL response from the maximal binding response was directly proportional to the extent of competitive binding activity.

Neutralization assay

Vero E6/TMPRSS2 cells were grown in Dulbecco's Modified Eagle Medium supplemented with 5% fetal calf serum, HEPES, amphotericin B, and gentamicin sulfate. Sera (100µl) were diluted in cell culture solution with 2-fold serial dilutions from 5x to 2560x. Virus (SARS-CoV-2/UW-001/Human/2020/Wisconsin) was diluted in cell culture solution to an adjusted titer of 100 plaque-forming units (PFU) per 60µl. Diluted sera (60µl) and diluted virus (60µl) were mixed in wells of 96-well U-bottom plates in duplicate. Plates were incubated at 37ºC for 30 minutes. Culture supernatant was aspirated from Vero E6/TMPRSS2 cells plated in 96 well dishes and replaced with the mixtures of serially diluted sera and virus (100µl/well, in duplicate) followed by incubation at 37°C with 5% CO_2 for 3 days. Crystal violet stain was added to wells to stain for living cells. Neutralization titers were determined by the maximum fold dilution at which the serum samples could completely prevent cell death as determined by eye. Some duplicates diverged by a single fold dilution in their neutralization titer. In this situation, the lower dilution was used as the neutralization titer. Sera with cell death at all dilutions were assigned a dilution value of 1 for analysis purposes.

Statistical analysis

Antibody levels were compared between COVID-19 convalescent and control sera using a t test or among subsets of COVID-19 convalescent sera by one-way ANOVA with Tukey's, Dunnett's, or Dunn's multiple comparisons tests. Welch's correction was used for unequal variance. Anti-SARS-CoV-2 antibody levels from different time points in the same subject were compared by paired t test. Correlations between antibody levels from different tests were estimated by Spearman rank correlation. The relationship between clinical and demographic factors and COVID-19 hospitalization or antibody levels were examined using the Pearson's chi-squared test for categorical variables and Kruskal-Wallis test for non-normally distributed continuous

data. Analyses were performed using GraphPad Prism software (San Diego, USA) and STATA version 16 (College Station, USA). Multiple linear regression analysis was performed in STATA to compare symptoms and antibody levels with age, BMI, Charlson Comorbidity Index Score and sex accounted for in the model. Antibody data was transformed prior to regression analysis (square root transformed for Spike, RBD and nucleocapsid and log transformed for NTD, ACE2 inhibition and viral neutralization). For all analyses, $p<0.05$ was considered significant.

RESULTS

We recruited 120 COVID-19 convalescent subjects into the UW COVID-19 Convalescent Biorepository. Seven subjects were excluded from this study due to erroneous blood collection timing (n=1), receipt of convalescent plasma (n=3), or partial consent (n=3). Two additional subjects were excluded from longitudinal evaluation due to a blood draw >14 days from the 3 month time point. Of the included subjects, blood was collected from 113 at 5 weeks (range 29-48 days, median 36 days, IQR 35-39 days) and from 79 at 3 months (range 85-102 days, median 91 days, IQR 90-93 days) post-symptom resolution. Eighty-one percent of COVID-19 convalescent subjects had a primary care appointment within two years of the first blood draw and/or a hospital admission note with past medical history and medications. Subjects ranged in age from 19-83 years and had a variety of COVID-19 manifestations (Table 1 and Supplementary Figure 1). One subject was a current smoker. As expected [22, 29], hospitalized subjects were more likely to be older and male with more comorbidities like vascular disease, but less likely to have asthma (Supplementary Table 1). Additionally, hospitalized subjects were more likely to have fever and less likely to have chest tightness, sore throat, or headache than non-hospitalized patients. We detected no correlation between race, ethnicity, ADI, BMI, cancer, immunosuppressing medications, or other COVID-19 symptoms and hospitalization, potentially due to the relative uniformity of race and ethnicity and the low number of subjects with cancer or immunosuppressing medications in our cohort.

We used a multiplex approach to evaluate IgG levels against four SARS-CoV-2 antigens (spike, RBD of spike, NTD of spike, and nucleocapsid) as well as IgG against the spike protein of SARS-CoV and four seasonal coronaviruses HCoV-OC43, HCoV-HKU1, HCoV-NL63, and HCoV-229E) in subjects five weeks post-COVID-19 symptom resolution (Figure 1A). COVID-19 convalescent subjects had higher IgG levels against all 4 SARS-CoV-2 antigens compared to naive subjects. Further, 98% of convalescent subjects had higher binding than any naive subject in at least one test. Finally, IgG levels against spike from SARS-CoV, HCoV-OC43, and HCoV-HKU1, but not HCoV-NL63 and HCoV-229E, were higher in convalescent subjects compared to controls.

We then evaluated the antibody response against SARS-CoV-2 in a more functional manner. Since the RBD of spike binds to ACE2, enabling viral entry [30], we quantified the ability of sera to inhibit RBD binding to ACE2. Compared to naive sera, five week convalescent sera demonstrated much higher inhibition of RBD-ACE2 binding (Figure 1B). Further, in a neutralizing assay using live SARS-CoV-2, COVID-19 convalescent sera had higher titers compared to naive sera, although 15% of convalescent subjects did not have neutralizing titers above controls (Figure 1C). Overall, neutralizing titers correlated well with IgG levels against SARS-CoV-2 and RBD-ACE2 binding inhibition (Figure 1D).

Next, we evaluated if antibody titers at five weeks post-symptom resolution varied with disease severity in our cohort. Hospitalized subjects had higher antibody levels than non-hospitalized subjects according to all of our tests, and, in general, antibody titers increased with COVID-19 severity (Figure 2). To determine if clinical and demographic factors apart from severe disease correlate with antibody levels, we analyzed non-hospitalized subjects alone. Older age, male sex, higher BMI and a Charlson Comorbidity Index score >2 correlated with higher antibody

titers in non-hospitalized subjects for all or most tests (Table 1). Race, ethnicity, ADI, cancer, diabetes, vascular disease, asthma, immunosuppressive medications and inhaled/intranasal steroids did not correlate with antibody levels in general (Supplementary Table 2).

We then turned our attention to the range of symptoms reported by our cohort to determine if symptoms might correlate with antibody levels. To this end, we first performed a univariate analysis to determine if any symptoms correlated with age, BMI, Charlson Comorbidity Score, or sex, characteristics shown to correlate with some antibody titers (Figure 3, Table 2). Since some symptoms correlated with hospitalization, again we evaluated only non-hospitalized patients. We found that most symptoms did not correlate with these characteristics. However, vomiting, abdominal pain, and diarrhea correlated with several. Additionally, males were more likely to report productive cough and body aches and subjects with higher comorbidity burden were more likely to report fever.

We then performed a univariate analysis to determine if antibody titers at five weeks post-symptom resolution varied with symptoms in our non-hospitalized subjects. As shown in Figure 3 and Table 3, fever, low appetite, abdominal pain, and diarrhea correlated with higher antibody levels measured by every test. Cough, body aches, headache, nausea, and vomiting correlated with some antibody tests, and chills, shortness of breath, chest tightness, sore throat, loss of taste or smell, and runny or stuffed nose correlated with no or almost no antibody tests.

Concerned that age, sex, BMI, or Charlson score, which correlate with anti-SARS-CoV-2 antibodies and some symptoms, could be confounding our univariate analysis, we performed a multiple linear regression analysis controlling for these variables (Figure 3 and Table 4). We found that fever and low appetite remained strong correlates and chills, shortness of breath, chest tightness, sore throat, and nasal symptoms remained weak correlates of anti-SARS-CoV-

2 antibody levels when accounting for these characteristics. However, gastrointestinal symptoms had little correlation with antibody levels in the multivariable analysis. Further, the strength of association between antibody levels and cough, particularly productive cough, was reduced whereas the correlation between body aches and headaches increased. Interestingly, when controlling for age, BMI, comorbidities, and sex, loss of taste or smell was strongly associated with almost all antibody tests. Finally, we also evaluated the symptoms included in severity score of 2 as well as total symptom number and found that the former correlated strongly with some antibody tests and the latter correlated with a low beta coefficient, but high level of significance, with all antibody levels.

For our last analysis, we evaluated the antibody response against SARS-CoV-2 and other coronaviruses in COVID-19 convalescent subjects three months post symptom resolution. In our cohort as a whole, anti-SARS-CoV-2 IgG, RBD-ACE2 binding inhibition, and neutralizing titers did not decline from five weeks to three months post-symptom resolution (Figure 4). However, when hospitalized and non-hospitalized subjects were analyzed separately (Figure 4), anti-spike and anti-nucleocapsid IgG rose slightly in hospitalized subjects (area under the curve: 4,525,184 +/- 796,452 versus 5,247,312 +/- 811,346 and 5,765,064 +/- 588,170 versus 7,004,295 +/- 654,857, respectively) and neutralizing titers decreased slightly in non-hospitalized subjects (titers: 49 +/- 11 versus 37 +/-10) over time. Titers against SARS-CoV and seasonal coronaviruses also did not fall, and in fact appeared to rise mildly regardless of hospitalization status (Supplementary Figure 2).

DISCUSSION

We have demonstrated that the vast majority of COVID-19 convalescent subjects generate antibodies against SARS-CoV-2 that inhibit ACE2 binding, neutralize live SARS-CoV-2, and persist at least three months post-COVID-19 symptom resolution. Further, greater disease

severity, older age, male sex, higher BMI, higher Charlson Comorbidity Index score, fever, body aches and low appetite consistently correlate with higher antibody titers.

Although we detected IgG against SARS-CoV-2 in the majority of COVID-19 convalescent subjects, there was variability among tests. IgG levels against spike and RBD, but not NTD or nucleocapsid, showed an impressive difference between COVID-19 convalescent and control sera. Similar strong results were observed for RBD-ACE2 binding inhibition. Of note, two convalescent subjects had similar values to naive subjects in all three tests. It is unknown if these subjects had false positive SARS-CoV-2 PCR tests, if they did not make antibodies, or if our tests were insufficiently sensitive.

All of the antibody tests correlated well with neutralizing titers, a gold standard for protective antibodies. This correlation is encouraging, suggesting that our antibody assays are measuring relevant antibodies without the cost, hazards, time, and expertise needed for neutralizing assays. However, similar to related studies [24, 25], more COVID-19 convalescent subjects had antibody titers no higher than naive controls using the neutralizing assay as compared to other assays. It is unknown if these subjects truly lack protective antibodies (in many cases despite the presence of anti-SARS-CoV-2 IgG) or if the neutralization assay is insufficiently sensitive.

In addition to the development of anti-SARS-CoV-2 antibodies in COVID-19 convalescent sera five weeks post-symptom resolution, we saw a small increase in antibodies against seasonal betacoronaviruses (OC43 and HKU1), but not alphacoronaviruses (NL63 and 229E), likely because SARS-CoV-2 is a betacoronavirus [30]. Moreover, antibodies that bind to seasonal coronaviruses rose slightly from five weeks to three months post-symptom resolution. This “back boost” phenomenon [31] could represent cross-reactivity of newly developed anti-SARS-CoV-2 antibodies and/or stimulation of memory B cells originally developed in response to

circulating coronaviruses. In contrast, the high anti-SARS-CoV levels seen in COVID-19 convalescent subjects, which did not change over time, are probably due to cross-reactive anti-SARS-CoV-2 antibodies, since the Wisconsin cohort was almost certainly not exposed to SARS-CoV.

Similar to recent reports [21-23, 32-34], we demonstrated that anti-SARS-CoV-2 antibodies were highest in patients with severe disease, perhaps due to different immunophenotypes in COVID-19 patients [35] with a stronger inflammatory response in severe disease driving higher antibody titers. We also found that in non-hospitalized patients, higher antibody levels correlated with older age, male sex, higher BMI, and higher Charlson Comorbidity Index score. These factors all correlated with severe disease in our cohort as measured by hospitalization except for BMI, which others have reported to be associated with severe disease [36]. Thus, non-hospitalized subjects with these high-risk characteristics might have had relatively severe disease that our methods could not measure, driving higher antibody levels. Alternatively, these characteristics could contribute directly to increased antibody levels. However, other reports suggest that older age and obesity impair antibody responses [37], and males have no generalizable increased antibody response [38]. Of note, the correlation between anti-SARS-CoV-2 antibody titers with age, sex, and obesity has been previously reported [23, 39], but we are the first to report a correlation with the Charlson Comorbidity Index score.

In addition to disease severity, we report for the first time that specific COVID-19 symptoms correlate with higher anti-SARS-CoV-2 antibody levels. Fever, body aches, and low appetite, which consistently correlated with higher antibody levels in both univariate and multivariable analyses, can be signs of a systemic inflammatory response, which is likely key for developing a strong anti-SARS-CoV-2 antibody response. Gastrointestinal symptoms correlated with older age, higher BMI, more comorbidities, and male sex as well as higher antibody levels. Thus, it is

difficult to determine which factor is driving antibody development. Diarrhea, typically caused by enteric viral infection and damage, may directly exacerbate inflammation and COVID-19 severity [40] causing the higher antibody titers. Alternatively, diarrhea may simply be more common in severe disease, which correlates with age, BMI, Charlson Comorbidity Index score, and male sex, although we did not see increased diarrhea in our hospitalized patients.

Interestingly, loss of taste or smell, a unique feature of COVID-19, is associated with higher antibody levels only in the multiple linear regression analysis, suggesting that it is a predictor of higher antibody titers independent of disease severity and correlates of severe disease. The mechanism for loss of taste or smell remains unclear. It seems unlikely that anti-SARS-CoV-2 antibodies cause this symptom, since only a small percentage of subjects have antibodies early in disease when loss of taste and smell occurs [41]. Moreover, a mechanism by which this symptom could drive antibody levels is similarly hard to imagine. Thus, the correlation between loss of taste and smell and antibody titers is likely driven by other factors that remain to be discovered.

Many symptoms did not correlate consistently or at all with antibody levels including shortness of breath, which was associated with higher antibody levels in COVID-19 convalescent plasma donors [24]. However, that study [24] had fewer subjects than our study with plasma donated at various times post-COVID-19 and no other symptoms evaluated. Many symptoms that did not correlate with antibody levels also did not correlate with severe disease and may not be related to the inflammation that drives antibody production.

Finally, we found that antibodies persist at least three months after symptom resolution. Some antibody levels even continued to rise slightly during this time period, although neutralizing titers fell slightly in non-hospitalized subjects. Our findings are discrepant from some studies, which

reported falling antibody levels against SARS-CoV-2 within a few months of disease [12-21]. However, these studies had smaller sample sizes (particularly at later time points), variable or unclear time points as related to symptom resolution, antibody loss in subjects with mild or asymptomatic disease, or no clinical data. However, our findings are consistent with reports of persistent antibody titers at least three to six months after disease [8-11]. As time goes on, additional studies will be needed at later time points that use a variety of antibody detection methods, defined collection time points, and extensive clinical data.

There are a few caveats to our studies. COVID-19 symptoms were self-reported up to a month after symptom resolution, which could lead to recall error. Additionally, some medical records were incomplete with no recent primary care or admission note for 19% of subjects and incomplete BMI data for 14%. This gap would be biased toward non-hospitalized patients. Also, our population was relatively racially and ethnically homogeneous. However, our study is strong in its wide breadth of COVID-19 severity in 113 subjects with consistent time points and multiple types of antibody tests.

In sum, we report that anti-SARS-CoV-2 antibodies last at least three months post-symptom resolution and that antibody titers consistently correlate with fever, body aches, low appetite, older age, male sex, higher COVID-19 severity, higher BMI, and higher Charlson Comorbidity Index score. Further work is needed to determine protective antibody levels against re-infection, how long protective titers last, and the mechanisms by which COVID-19 symptoms, demographics, and comorbidities may drive higher antibody levels.

ACKNOWLEDGEMENTS

We thank the UW Office of Clinical Trials and the UW Carbone Cancer Center Translational Science BioCore as well as the human subjects who participated in this study.

FUNDING

This work was supported by a COVID-19 Response grant from the Wisconsin Partnership Program [4647] and the Department of Medicine, both at the UW School of Medicine and Public Health to M.A.S. Additional support was provided by the National Institutes of Health's National Institute on Aging to M.F.A. [T32 AG000213], National Heart, Lung, and Blood Institute [T32 HL007899] to A.M.M., and National Institute of Allergy and Infectious Disease to A.S.H. [T32 AI007414].

FIGURE LEGENDS

Figure 1. Antibodies against SARS-CoV-2 in COVID-19 convalescent subjects five weeks post-symptom resolution. IgG against the spike (S) protein from HCoV-OC43, HCoV-HKU1, HCoV-NL63, HCoV-229E, and SARS-CoV, as well as SARS-CoV-2 S, N terminal domain (NTD) of S, receptor binding domain (RBD) of S, and nucleocapsid (N) protein for convalescent (black, n=113) and naive (gray, n=87) sera (A), fold reduction of angiotensin converting enzyme (ACE)2 binding to RBD for convalescent (n=113) and naive (n=88) sera (B), and neutralizing titers for convalescent (n=113) and naive (n=30) sera (C) were compared by t test with Welch's correction. Bars represent mean, ****$p<0.0001$, and AUC: area under the curve. D. Neutralizing titers were compared with anti-SARS-CoV-2 IgG levels and RBD-ACE2 binding inhibition for convalescent subjects (n=113) with Spearman correlation coefficients (ρ) and p values listed.

Figure 2. Patients with more severe COVID-19 have higher antibody levels against SARS-CoV-2. IgG levels against SARS-CoV-2 S, NTD, RBD, and N, as well as fold reduction of RBD-ACE2 binding, and neutralizing antibodies in COVID-19 convalescent sera five weeks post-symptom resolution were compared for non-hospitalized (NH, n=94) versus hospitalized (Hosp.,

n=19) subjects by t test and among subjects with mild (score 1, n=12), moderate (2, n=82), severe (3, n=12), and critical (4, n=7) COVID-19 severity by ANOVA (anti-NTD, anti-RBD, and RBD-ACE2 binding inhibition by Welch's ANOVA with Dunnett's test; anti-S and anti-N by ANOVA with Tukey's multiple comparisons test, and neutralizing titers by Kruskal-Wallis ANOVA with Dunn's multiple comparisons test). For all panels: lines indicate mean +/- SEM; *p<0.05, **p<0.01, ***p<0.001, ****p<0.0001.

Figure 3. Visual representation of COVID-19 symptoms analysis (reported in Tables 2-4) highlight correlations with clinical features or antibody levels 5 weeks after symptom resolution. Univariate analysis of symptoms and clinical features (left panel) or symptoms and antibody levels (middle panel) were done by Kruskal-Wallis test (for age, Body Mass Index (BMI), Charlson Comorbidity Index Score (CCS), IgG against spike (S), N terminal domain (NTD), receptor binding domain (RBD), nucleocapsid (N), fold reduction in angiotensin converting enzyme two (ACE2) binding to RBD, and neutralizing antibodies (Neut)) or by chi-squared test (for sex). The shade of blue at the intersection of the two variables indicates whether the median age, BMI, S, NTD, RBD, N or ACE2 for subjects with a particular symptom was above or below the mean of all other symptoms for that clinical feature or antibody. For neutralizing titer in the univariate analysis, mean was used to indicate shade of blue. For sex, the difference in percentages of males minus females with the reported symptom was used to determine shade of blue. Multiple linear regression analysis of symptoms with antibody levels when age, BMI, CCS and sex were controlled for is represented (right panel) with shade of blue corresponding to strength of association of the variables as determined by the beta coefficient. Number of symptoms was assessed by summing the number of symptoms subjects reported and moderate disease symptoms (sx) are defined as a COVID-19 Severity Score of 2. *p<0.05, **p<0.01 and ***p<0.001

Figure 4. Antibodies against SARS-CoV-2 persist three months after COVID-19 symptom resolution. Sera from COVID-19 convalescent subjects (n=79) collected 5 weeks (w) and 3 months (m) after symptom resolution were subjected to multiplex assay to detect IgG that binds to SARS-CoV-2 S, NTD, RBD and N antigens, to RBD-ACE2 binding inhibition assay, and to SARS-CoV-2 neutralization assay. Dots, lines, and asterisks in left panel represent all (n=79) subjects, in middle panel represent hospitalized subjects (n=12) and in right panel represent non-hospitalized subjects (n=67) with lines connecting the two time points for individual subjects (*$p<0.05$ and **$p<0.01$ by paired t test).

Table 1. Median (IQR) IgG levels, fold RBD-ACE2 inhibition, and SARS-CoV-2 neutralization titers five weeks after resolution of COVID-19 symptoms according to clinical and demographic characteristics in non-hospitalized subjects

	N	Anti-Spike [a]	Anti-NTD [a]	Anti-RBD [a]	Anti-N [a]	ACE-2 Inhib.	Neut. Titer
All subjects	94	19 (7.0, 35)	0.27 (0.10, 0.69)	5.1 (1.8, 12)	31 (11, 51)	73 (20, 287)	20 (10, 40)
Age quartile		**p=0.047**	**p=0.009**	**p=0.028**	**p=0.005**	**p=0.011**	p=0.230
1 (19.2-27.6)	24	10 (3.8, 22)	0.14 (0.07, 0.42)	2.2 (1.2, 7.3)	9.6 (3.2, 35)	32 (11, 94)	10 (10, 20)
2 (29.6-42.4)	23	18 (8.4, 28)	0.25 (0.15, 0.53)	5.3 (1.8, 9.6)	29.0 (23, 56)	85 (50, 203)	20 (10, 40)
3 (42.5-54.5)	23	31 (7.9, 37)	0.51 (0.08, 1.0)	10 (2.1, 15)	37 (19, 51)	119 (15, 311)	20 (1, 40)
4 (54.8-76.5)	24	30 (8.8, 46)	0.37 (0.20, 1.7)	8.4 (3.5, 22)	44.1 (29, 63)	216 (36, 555)	20 (10, 80)
Sex		**p=0.034**	**p=0.039**	**p=0.015**	**p=0.031**	**p=0.023**	**p=0.009**
Male	32	29 (7.2, 43)	0.46 (0.15, 0.89)	9.6 (2.5, 16)	44 (23, 66)	121 (43, 344)	40 (10, 80)
Female	62	17 (7.0, 32)	0.21 (0.08, 0.47)	4.1 (1.6, 10)	29 (8.7, 44)	51 (15, 219)	15 (10, 40)
BMI [b] (lb/in^2)		**p=0.041**	**p=0.011**	**p=0.020**	p=0.091	p=0.067	**p=0.027**
1 (<25)	22	11 (5.0, 20)	0.16 (0.09, 0.27)	3.1 (1.3, 6.4)	22 (10, 40)	38 (20, 121)	10 (10, 20)
2 (25-29.99)	27	21 (7.9, 43)	0.41 (0.12, 1.0)	6.9 (2.2, 16)	43 (16, 51)	72 (17, 328)	10 (10, 40)
3 (≥30)	30	27 (15, 38)	0.41 (0.18, 0.86)	9.1 (4.8, 13)	43 (23, 85)	139 (45, 298)	40 (10, 80)
Charlson		**p=0.021**	**p=0.001**	**p=0.010**	**p=0.010**	**p=0.009**	p=0.072
> 2	30	33 (8.8, 45)	0.46 (0.25, 1.4)	9.8 (4.1, 20)	45 (30, 63)	217 (34, 489)	30 (10, 80)

[a] Values are $x10^5$

[b] Data missing for 15 subjects

Table 2. Clinical and demographic features according to clinical symptoms in non-hospitalized subjects

Symptom	N	Age in years Median (IQR)	BMI[a] in lb/in^2 Median (IQR)	CCS Median (IQR)	Sex % males - % females (% of F, % of M)
All subjects	94	42.4 (27.6, 54.8)	27.7 (24.7, 32.4)	1 (0, 2)	-31.9 (66.0, 34.0)
Fever	59	44.3 (29.6, 55.4)	28.4 (25.2, 32.4)	**1 (0, 2)***	9.1 (59.7, 68.8)
Chills [b]	59	42.5 (29.6, 54.5)	29.3 (25.2, 34.1)	1 (0, 2)	15.7 (59.3, 75.0)
Productive cough	37	43.6 (27.0, 52.9)	31.3 (25.6, 34.1)	1 (0, 2)	**25.6 (30.7, 56.3)***
Dry cough	58	42.1 (31.4, 54.0)	28.5 (24.8, 32.5)	1 (0, 2)	15.4 (56.5, 71.9)
Shortness of breath	47	44.1 (36.3, 54.8)	29.4 (25.0, 32.5)	1 (0, 2)	18.9 (43.6, 62.5)
Chest tightness	60	41.2 (29.8, 54.7)	28.2 (24.7, 32.3)	1 (0, 2)	12.2 (59.7, 71.9)
Sore throat	45	43.3 (27.6, 54.8)	29.0 (24.6, 32.9)	1 (0, 2)	-1.5 (48.4, 46.9)
Loss of taste or smell	58	40.4 (26.6, 52.9)	27.3 (24.2, 32.3)	0 (0, 2)	1.2 (61.3, 62.5)
Runny or stuffed nose	54	39.3 (26.6, 54.0)	28.0 (25.0, 33.1)	0 (0, 2)	-1.8 (58.1, 56.3)
Body aches	69	42.4 (27.5, 54.5)	28.0 (25.1, 32.5)	1 (0, 2)	**21.4 (66.1, 87.5)***
Headaches	68	40.4 (27.2, 54.3)	27.7 (24.1, 32.4)	0.5 (0, 2)	-0.7 (72.6, 71.9)
Low appetite	59	43.4 (30.1, 54.8)	28.3 (25.0, 32.5)	1 (0, 2)	9.1 (59.7, 68.8)
Nausea	32	44.1 (32.5, 55.3)	27.0 (24.8, 35.4)	1 (0, 2.5)	0.5 (33.9, 34.4)
Vomiting	13	51.3 (32.3, 54.8)	**32.4 (30.0, 36.0)***	2 (0, 3)	-2 (14.5, 12.5)
Abdominal pain	17	**54.8 (42.5, 62.5)****	31.2 (26.0, 32.4)	**2 (1, 3)*****	15.2 (12.9, 28.1)
Diarrhea	42	43.8 (36.3, 54.8)	**31.4 (25.4, 34.3)****	1 (0, 2)	**27 (35.5, 62.5)***

[a]BMI data missing for 15 subjects
[b]Chills data missing for two subjects

Table 3. Median (IQR) IgG levels, fold RBD-ACE2 inhibition, and SARS-CoV-2 neutralization titers five weeks after resolution of COVID-19 symptoms according to clinical symptoms in non-hospitalized subjects

	N	Anti-Spike [a]	Anti-NTD [a]	Anti-RBD [a]	Anti-N [a]	ACE-2 Inhib.	Neut. Titer
All subjects	94	19 (7.0, 35)	0.27 (0.10, 0.69)	5.1 (1.8, 12)	31 (11, 51)	73 (20, 287)	20 (10, 40)
Fever	59	**29 (7.9, 39)****	**0.41 (0.17, 0.86)****	**9.2 (2.8, 14)****	**40 (23, 54)***	**121 (37, 328)****	**20 (10, 80)*****
Chills [b]	59	21 (7.9, 39)	0.32 (0.14, 0.82)	5.9 (2.1, 14)	38 (16, 53)	73 (34, 305)	**20 (10, 80)***
Productive cough	37	26 (10, 38)	**0.44 (0.18, 0.74)***	**8.7 (3.2, 13)***	42 (23, 55)	**131 (42, 305)***	**20 (10, 80)****
Dry cough	58	**26 (10, 38)****	**0.32 (0.17, 0.73)***	**7.4 (2.8, 13)****	39 (21, 53)	**124 (37, 298)***	**20 (10, 40)***
Shortness of breath	47	26 (6.7, 38)	0.27 (0.12, 0.74)	5.9 (1.8, 13)	27 (11, 56)	85 (22, 305)	20 (10, 80)
Chest tightness	60	21 (7.2, 35)	0.26 (0.09, 0.71)	5.8 (1.8, 13)	36 (12, 56)	79 (21, 287)	20 (10, 40)
Sore throat	45	22 (8.4, 35)	0.34 (0.17, 0.68)	6.9 (2.4, 12)	38 (14, 53)	73 (20, 298)	20 (10, 40)
Loss of taste or smell	58	21 (8.0, 36)	0.33 (0.10, 0.73)	5.0 (1.8, 13)	31 (14, 54)	73 (22, 298)	20 (10, 40)
Runny or stuffed nose	54	20 (6.7, 37)	0.28 (0.09, 0.69)	5.5 (1.7, 12)	35 (16, 53)	73 (20, 279)	20 (10, 40)
Body aches	69	**24 (8.4, 39)****	**0.29 (0.14, 0.86)***	**6.9 (2.2, 14)****	38 (16, 53)	**93 (28, 298)***	**20 (10, 80)***
Headaches	68	**24 (9.1, 35)***	**0.31 (0.16, 0.71)***	**6.8 (2.9, 13)****	36 (18, 53)	92 (26, 293)	**20 (10, 40)***
Low appetite	59	**27 (9.8, 43)*****	**0.41 (0.18, 1.0)*****	**8.7 (2.9, 16)*****	**40 (22, 56)****	**123 (28, 311)****	**20 (10, 80)*****
Nausea	32	**29 (9.2, 46)***	**0.45 (0.26, 1.1)****	**9.1 (3.5, 14)***	**42 (26, 56)***	95 (19, 332)	20 (10, 80)
Vomiting	13	**30 (20, 43)***	**0.93 (0.44, 1.1)*****	**10 (4.8, 20)***	**48 (42, 82)****	131 (26, 376)	40 (10, 80)
Abdominal pain	17	**35 (17, 47)***	**1.0 (0.28, 1.6)****	**14 (5.6, 20)***	**48 (29, 69)***	**310 (47, 756)***	**80 (20, 80)****
Diarrhea	42	**28 (13, 43)****	**0.44 (0.23, 0.93)****	**8.9 (4.1, 14)***	**41 (23, 82)****	**124 (47, 392)****	**30 (10, 80)***

[a] Values are $x10^5$

[b] Data missing for three subjects

*p<0.05, **p<0.01, ***p<0.001

Table 4. Multiple linear regression of symptoms associated with antibody levels, ACE-2 inhibition, and viral neutralization titers five weeks after resolution of COVID-19 symptoms in nonhospitalized subjects

	sqrt[IgG(Spike)]				log[IgG(NTD)]				sqrt[IgG(RBD)]			
Symptom [a]	β	95% CI	P	Adj. R^2	β	95% CI	P	Adj. R^2	β	95% CI	P	Adj. R^2
Fever	313.6	13.0, 614.2	0.041	0.14	0.726	0.163, 1.289	0.012	0.19	253.5	54.7, 452.4	0.013	0.21
Chills	207.1	-124.4, 538.7	0.217	0.12	0.279	-0.357, 0.915	0.385	0.13	143.3	-79.9, 366.5	0.205	0.16
Productive cough	167.2	-152.3, 486.7	0.300	0.10	0.491	-0.110, 1.092	0.108	0.14	82.4	-132.6, 297.4	0.448	0.14
Dry cough	362.9	59.7, 666.1	0.020	0.15	0.683	0.106, 1.260	0.021	0.18	163.8	-43.9, 371.4	0.120	0.16
Shortness of breath	71.4	-228.9, 371.8	0.637	0.09	-0.016	-0.588, 0.556	0.955	0.11	-2.3	-204.1, 199.5	0.982	0.14
Chest tightness	193.1	-117.0, 503.1	0.219	0.11	0.110	-0.485, 0.705	0.713	0.11	87.4	-121.7, 296.6	0.407	0.14
Sore throat	51.3	-243.5, 346.1	0.730	0.09	-0.056	-0.616, 0.505	0.844	0.11	9.8	-188.1, 207.7	0.922	0.14
Loss of taste or smell	419.3	123.5, 715.1	0.006	0.18	0.699	0.130, 1.269	0.017	0.18	279.1	80.5, 477.7	0.007	0.22
Runny or stuffed nose	41.8	-263.5, 347.1	0.786	0.09	-0.029	-0.610, 0.551	0.920	0.11	25.9	-178.9, 230.7	0.802	0.14
Body aches	637.9	308.3, 967.5	<0.001	0.24	1.071	0.430, 1.711	0.001	0.23	376.7	150.6, 602.8	0.001	0.25
Headaches	511.8	202.5, 821.0	0.002	0.21	0.862	0.265, 1.460	0.005	0.20	284.9	72.7, 497.1	0.009	0.21
Low appetite	526.9	239.3, 814.5	<0.001	0.23	1.051	0.510, 1.593	<0.001	0.26	351.1	158.0, 544.3	0.001	0.27
Nausea	238.0	-67.1, 543.1	0.124	0.12	0.617	0.045, 1.189	0.035	0.17	123.7	-82.3, 329.7	0.235	0.15
Vomiting	204.9	-224.7, 634.5	0.345	0.10	1.015	0.229, 1.802	0.012	0.19	171.3	-115.9, 458.5	0.238	0.15
Abdominal pain	196.6	-194.4, 587.7	0.320	0.10	0.319	-0.426, 1.064	0.396	0.12	144.2	-117.8, 406.1	0.276	0.15
Diarrhea	258.5	-51.6, 568.6	0.101	0.12	0.212	-0.387, 0.810	0.483	0.12	143.0	-66.2, 352.3	0.177	0.16
Moderate disease sx	482.2	33.9, 930.5	0.035	0.14	0.575	-0.294, 1.443	0.191	0.13	301.8	-0.1, 603.7	0.050	0.18
Number of symptoms	95.1	52.0, 138.2	<0.001	0.28	0.168	0.084, 0.251	<0.001	0.27	56.3	26.5, 86.1	<0.001	0.28

[a] All models adjusted for age, sex, BMI, and Charlson Comorbidity Index score.
Adj., adjusted; CI, confidence interval; sqrt, square root.

Table 4. Multiple linear regression of symptoms associated with antibody levels, ACE-2 inhibition, and viral neutralization titers five weeks after resolution of COVID-19 symptoms in nonhospitalized subjects (continued)

	sqrt[IgG(Nucleocapsid)]				log[ACE2 Inhibition]				log[viral neutralization]			
Symptom [a]	β	95% CI	p	Adj. R^2	β	95% CI	p	Adj. R^2	β	95% CI	p	Adj. R^2
Fever	340.3	-40.4, 721.0	0.079	0.15	0.805	0.133, 1.477	0.020	0.20	1.154	0.503, 1.804	0.001	0.22
Chills	256.9	-162.1, 675.8	0.226	0.14	0.469	-0.274, 1.212	0.212	0.18	0.523	-0.226, 1.272	0.168	0.13
Productive cough	121.4	-282.2, 525.0	0.551	0.11	0.457	-0.261, 1.175	0.209	0.16	0.780	0.084, 1.477	0.029	0.15
Dry cough	150.1	-244.1, 544.3	0.450	0.12	0.723	0.033, 1.413	0.040	0.19	0.710	0.020, 1.399	0.044	0.14
Shortness of breath	-222.4	-597.0, 152.2	0.241	0.13	-0.034	-0.712, 0.645	0.922	0.14	-0.023	-0.707, 0.661	0.947	0.09
Chest tightness	158.3	-233.8, 550.4	0.424	0.12	0.215	-0.489, 0.920	0.544	0.14	0.367	-0.339, 1.074	0.304	0.11
Sore throat	-111.5	-481.5, 258.5	0.550	0.11	-0.061	-0.727, 0.604	0.855	0.14	-0.031	-0.698, 0.635	0.926	0.09
Loss of taste or smell	380.1	-1.4, 761.6	0.051	0.15	0.726	0.044, 1.408	0.037	0.19	0.871	0.185, 1.556	0.014	0.16
Runny or stuffed nose	129.0	-253.8, 511.9	0.504	0.11	-0.073	-0.761, 0.616	0.834	0.14	-0.053	-0.735, 0.630	0.879	0.09
Body aches	405.7	-38.9, 850.4	0.073	0.15	0.885	0.096, 1.674	0.029	0.20	1.165	0.388, 1.942	0.004	0.19
Headaches	423.0	18.1, 827.9	0.041	0.16	0.887	0.169, 1.606	0.016	0.21	1.095	0.407, 1.784	0.002	0.20
Low appetite	428.9	48.6, 809.1	0.028	0.17	0.993	0.326, 1.659	0.004	0.23	1.082	0.414, 1.751	0.002	0.20
Nausea	327.8	-54.5, 710.0	0.092	0.14	0.008	-0.691, 0.708	0.981	0.14	0.336	-0.358, 1.029	0.338	0.11
Vomiting	517.3	-12.5, 1047.1	0.055	0.15	-0.125	-1.100, 0.850	0.799	0.14	0.160	-0.833, 1.152	0.749	0.10
Abdominal pain	109.7	-384.6, 603.9	0.660	0.11	0.253	-0.633, 1.139	0.571	0.14	0.626	-0.219, 1.471	0.144	0.12
Diarrhea	316.5	-73.7, 706.6	0.110	0.14	0.429	-0.277, 1.134	0.230	0.16	0.396	-0.312, 1.104	0.269	0.11
Moderate disease sx	476.2	-94.1, 1046.5	0.100	0.14	1.349	0.355, 2.343	0.008	0.22	1.232	0.206, 2.259	0.019	0.16
Number of symptoms	76.8	18.6, 135.1	0.010	0.19	0.144	0.040, 0.248	0.007	0.22	0.188	0.091, 0.285	<0.001	0.24

[a] All models adjusted for age, sex, BMI, and Charlson Comorbidity Index score.
Adj., adjusted; CI, confidence interval; sqrt, square root.

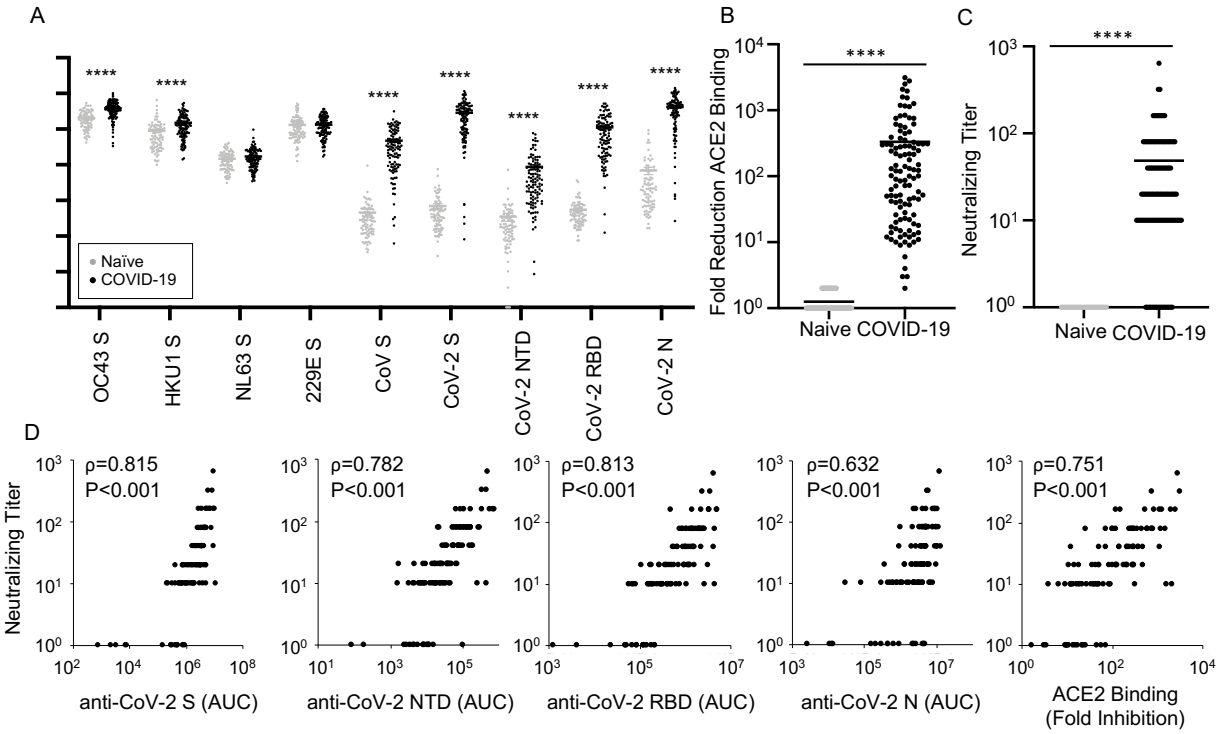

Figure 1. Antibodies against SARS-CoV-2 in COVID-19 convalescent subjects five weeks post-symptom resolution. IgG against the spike (S) protein from HCoV-OC43, HCoV-HKU1, HCoV-NL63, HCoV-229E, and SARS-CoV, as well as SARS-CoV-2 S, N terminal domain (NTD) of S, receptor binding domain (RBD) of S, and nucleocapsid (N) protein for convalescent (black, n=113) and naive (gray, n=87) sera (A), fold reduction of angiotensin converting enzyme (ACE)2 binding to RBD for convalescent (n=113) and naive (n=88) sera (B), and neutralizing titers for convalescent (n=113) and naive (n=30) sera (C) were compared by t test with Welch's correction. Bars represent mean, ****p<0.0001, and AUC: area under the curve. D. Neutralizing titers were compared with anti-SARS-CoV-2 IgG levels and RBD-ACE2 binding inhibition for convalescent subjects (n=113) with Spearman correlation coefficients (ρ) and p values listed.

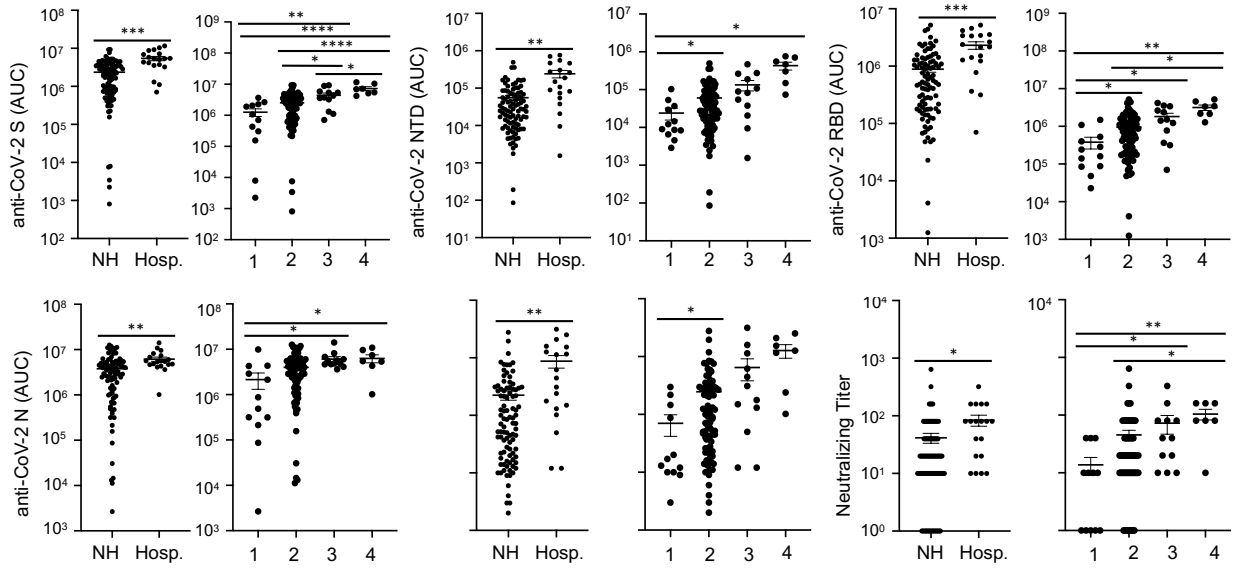

Figure 2. Patients with more severe COVID-19 have higher antibody levels against SARS-CoV-2. IgG levels against SARS-CoV-2 S, NTD, RBD, and N, as well as fold reduction of RBD-ACE2 binding, and neutralizing antibodies in COVID-19 convalescent sera five weeks post-symptom resolution were compared for non-hospitalized (NH, n=94) versus hospitalized (Hosp., n=19) subjects by t test and among subjects with mild (score 1, n=12), moderate (2, n=82), severe (3, n=12), and critical (4, n=7) COVID-19 severity by ANOVA (anti-NTD, anti-RBD, and RBD-ACE2 binding inhibition by Welch's ANOVA with Dunnett's test; anti-S and anti-N by ANOVA with Tukey's multiple comparisons test, and neutralizing titers by Kruskal-Wallis ANOVA with Dunn's multiple comparisons test). For all panels: lines indicate mean +/- SEM; *p<0.05, **p<0.01, ***p<0.001, ****p<0.0001.

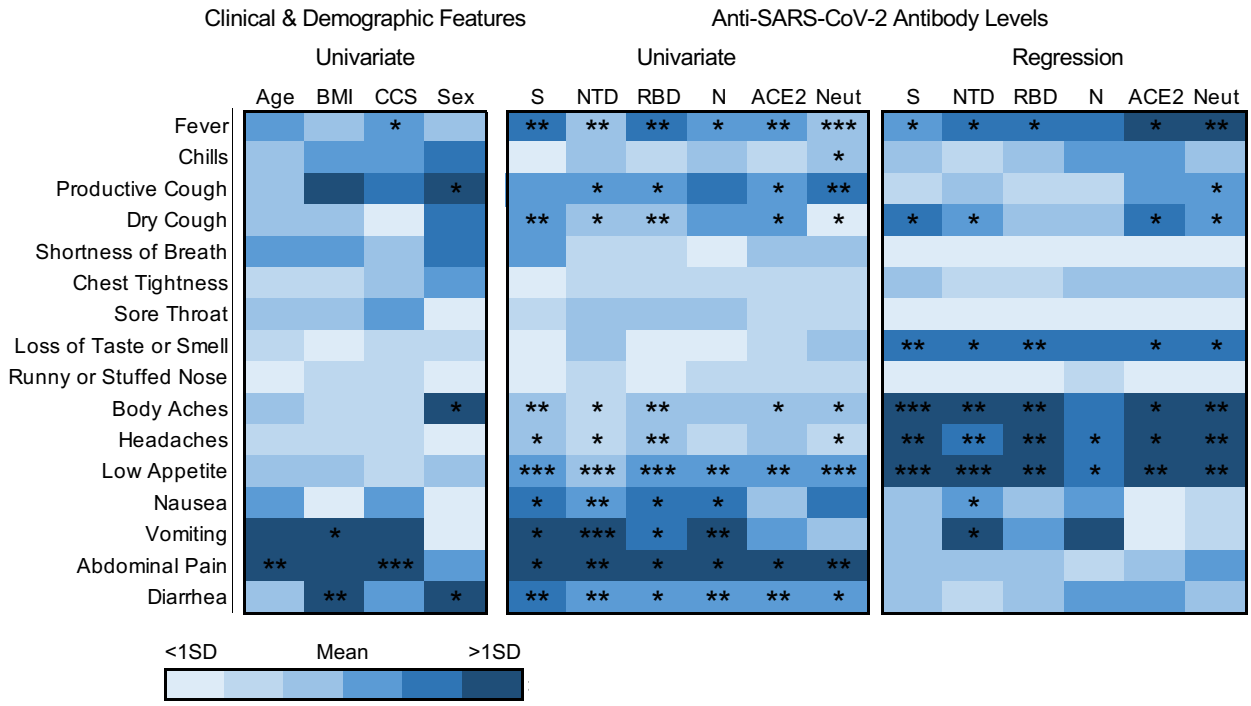

Figure 3. Visual representation of COVID-19 symptoms analysis (reported in Tables 2-4) highlight correlations with clinical features or antibody levels 5 weeks after symptom resolution. Univariate analysis of symptoms and clinical features (left panel) or symptoms and antibody levels (middle panel) were done by Kruskal-Wallis test (for age, Body Mass Index (BMI), Charlson Comorbidity Index Score (CCS), IgG against spike (S), N terminal domain (NTD), receptor binding domain (RBD), nucleocapsid (N), fold reduction in angiotensin converting enzyme two (ACE2) binding to RBD, and neutralizing antibodies (Neut)) or by chi-squared test (for sex). The shade of blue at the intersection of the two variables indicates whether the median age, BMI, S, NTD, RBD, N or ACE2 for subjects with a particular symptom was above or below the mean of all other symptoms for that clinical feature or antibody. For neutralizing titer in the univariate analysis, mean was used to indicate shade of blue. For sex, the difference in percentages of males minus females with the reported symptom was used to determine shade of blue. Multiple linear regression analysis of symptoms with antibody levels when age, BMI, CCS and sex were controlled for is represented (right panel) with shade of blue corresponding to strength of association of the variables as determined by the beta coefficient. Number of symptoms was assessed by summing the number of symptoms subjects reported and moderate disease symptoms (sx) are defined as a COVID-19 Severity Score of 2. *p<0.05, **p<0.01 and ***p<0.001

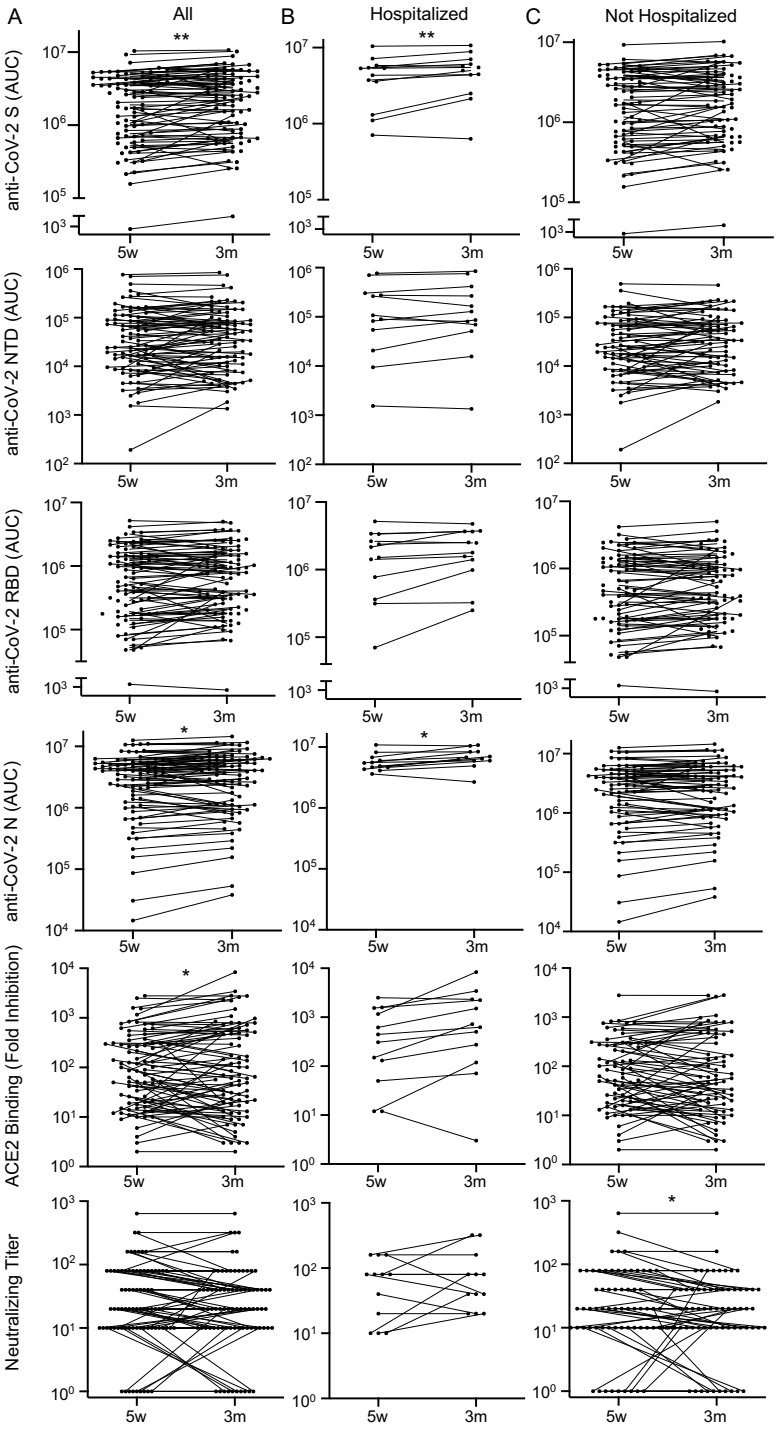

Figure 4. Antibodies against SARS-CoV-2 persist three months after COVID-19 symptom resolution. Sera from COVID-19 convalescent subjects (n=79) collected 5 weeks (w) and 3 months (m) after symptom resolution were subjected to multiplex assay to detect IgG that binds to SARS-CoV-2 S, NTD, RBD and N antigens, to RBD-ACE2 binding inhibition assay, and to SARS-CoV-2 neutralization assay. Dots, lines, and asterisks in left panel represent all (n=79) subjects, in middle panel represent hospitalized subjects (n=12) and in right panel represent non-hospitalized subjects (n=67) with lines connecting the two time points for individual subjects (*p<0.05 and **p<0.01 by paired t test).

Supplementary Table 1. Clinical and demographic characteristics of 113 COVID-19 convalescent subjects

Characteristic	All subjects (N=113)	Not hospitalized (N=94)	Hospitalized (N=19)	p-value
Age (years), median (IQR)	44.3 (32.3, 56.9)	42.4 (27.6, 54.8)	61.8 (48.2, 70.5)	**<0.001**
Male sex, n (%)	47 (41.6)	32 (34.0)	15 (79.0)	**<0.001**
Race, n (%)				0.370
White	103 (91.2)	86 (91.5)	17 (89.5)	
Black	4 (3.5)	4 (4.3)	0 (0.0)	
Asian	6 (5.3)	4 (4.3)	2 (10.5)	
Hispanic ethnicity, n (%)	5 (4.4)	5 (5.3)	0 (0.0)	0.304
Area deprivation index score, median (IQR)	30 (21, 41)	31.5 (21, 42)	30 (15, 40)	0.332
Body-mass index [a] (lb/in^2), median (IQR)	27.8 (25.0, 32.8)	27.7 (24.7, 32.4)	29.8 (26.1, 34.4)	0.239
Charlson score, median (IQR)	1 (0, 2)	1 (0, 2)	2 (0, 5)	**0.005**
Active cancer, n (%)	5 (4.4)	4 (4.3)	1 (5.3)	0.846
Diabetes [b], n (%)	11 (9.7)	7 (7.5)	4 (21.1)	0.068
Vascular disease [c], n (%)	10 (8.9)	4 (4.3)	6 (31.6)	**<0.001**
Asthma, n (%)	22 (19.5)	22 (23.4)	0 (0.0)	**0.019**
Immunosuppressive medication, n (%)	7 (6.2)	7 (7.5)	0 (0.0)	0.219
Inhaled steroid, n (%)	28 (24.8)	25 (26.6)	3 (15.8)	0.320
Symptoms, n (%)				
Fever	76 (67.3)	59 (62.8)	17 (89.5)	**0.024**
Chills	72 (65.5)	59 (64.8)	13 (68.4)	0.765
Productive cough	48 (42.5)	37 (39.4)	11 (57.9)	0.136
Dry cough	73 (64.6)	58 (61.7)	15 (79.0)	0.152
Shortness of breath	61 (54.0)	47 (50.0)	14 (73.7)	0.059
Chest tightness	66 (58.4)	60 (63.8)	6 (31.6)	**0.009**
Sore throat	48 (42.5)	45 (47.9)	3 (15.8)	**0.010**
Loss of taste or smell	67 (59.3)	58 (61.7)	9 (47.4)	0.246
Runny or stuffed nose	62 (54.9)	54 (57.5)	8 (42.1)	0.220
Body aches	80 (70.8)	69 (73.4)	11 (57.9)	0.175
Headaches	75 (66.4)	68 (72.3)	7 (36.8)	**0.003**
Low appetite	72 (63.7)	59 (62.8)	13 (68.4)	0.640
Nausea	38 (33.6)	32 (34.0)	6 (31.6)	0.836
Vomiting	15 (13.3)	13 (13.8)	2 (10.5)	0.699
Abdominal pain	21 (18.6)	17 (18.1)	4 (21.1)	0.762
Diarrhea	52 (46.0)	42 (44.7)	10 (52.6)	0.526
Intubated, n (%)	7 (6.2)	--	7 (36.8)	--

[a] Data missing for 16 individuals (16 missing height; 8 missing weight)

[b] 10 of 11 subjects with HgbA1c$\geq$7

[c] Eight subjects had a history of myocardial infarction, four with peripheral vascular disease, three with congestive heart failure, two with cerebrovascular disease (not mutually exclusive)

Supplementary Table 2. Median (IQR) IgG levels, fold RBD-ACE2 inhibition, and SARS-CoV-2 neutralization titers five weeks after resolution of COVID-19 symptoms according to clinical and demographic characteristics in non-hospitalized subjects

	N	Anti-S [a]	Anti-NTD [a]	Anti-RBD [a]	Anti-N [a]	ACE-2 Inhib.	Neut. Titer
All subjects	94	19 (7.0, 35)	0.27 (0.10, 0.69)	5.1 (1.8, 12)	31 (11, 51)	73 (20, 287)	20 (10, 40)
Race		p=0.580	p=0.716	p=0.530	p=0.179	p=0.683	p=0.235
White	86	18 (6.7, 35)	0.25 (0.09, 0.73)	4.9 (1.7,12)	30 (10, 51)	72 (22, 268)	20 (10, 40)
Black	4	26 (14, 40)	0.31 (0.23, 0.86)	7.0 (3.4, 14)	52 (41, 86)	186 (15.5, 421)	30 (15, 60)
Asian	4	31 (15, 40.5)	0.47 (0.20, 0.67)	10 (4.2, 19)	26 (15, 34)	346 (75, 569)	60 (25, 120)
Hispanic ethnicity		**p=0.048**	p=0.097	p=0.100	p=0.136	p=0.056	p=0.057
	5	39 (30, 46)	0.77 (0.56, 1.1)	13 (10, 14)	53 (44, 55)	310 (245, 376)	40 (40, 80)
ADI tertile		p=0.478	p=0.642	p=0.471	p=0.544	p=0.573	p=0.662
1 (4, 24)	33	19 (8.4, 31)	0.23 (0.11, 0.66)	4.8 (1.7, 11)	27 (12, 51)	52 (17, 131)	20 (10, 80)
2 (26, 40)	33	15 (5.3, 36)	0.26 (0.08, 0.62)	4.4 (1.6, 13)	31 (8.5, 49)	86 (21, 273)	20 (10, 40)
3 (41, 99)	32	23 (8.0, 43)	0.32 (0.13, 0.93)	7.2 (2.8, 14)	42 (25, 54)	100 (37, 310)	20 (10, 40)
Active Cancer		p=0.190	p=0.925	p=0.349	p=0.779	p=0.210	p=0.312
	4	10.3 (3.7, 19)	0.30 (0.18, 0.40)	3.5 (1.9, 5.4)	36 (19, 41)	28 (16, 88)	10 (6, 25)
Diabetes		p=0.424	p=0.589	p=0.416	p=0.069	p=0.074	p=0.320
	7	33 (23, 77)	0.32 (0.06, 1.7)	10 (6.7, 42)	47 (30, 118)	219 (45, 1186)	40 (10, 80)
Vascular disease		p=0.155	p=0.059	p=0.144	p=0.269	p=0.056	p=0.155
	4	47 (23, 71)	1.4 (0.63, 3.3)	23 (10, 33)	59 (28, 94)	790 (387, 1801)	80 (41, 360)
Asthma		p=0.382	p=0.755	p=0.443	p=0.106	p=0.512	p=0.813
	22	13 (5.0, 38)	0.29 (0.06, 0.82)	4.4 (1.1, 14)	24 (6.5, 38)	50 (14, 353)	15 (10, 40)
Immunosup. medication		p=0.376	p=0.512	p=0.338	p=0.835	p=0.412	p=0.372
	7	8.0 (5.2, 32)	0.12 (0.07, 0.73)	2.8 (1.2, 12)	37 (19, 44)	28 (15, 279)	10 (1, 20)
Inhaled steroid		p=0.112	**p=0.018**	p=0.101	p=0.935	p=0.325	p=0.050
	25	33 (8.0, 43)	0.47 (0.24, 1.0)	9.2 (2.9, 15)	33 (16, 46)	203 (34, 310)	20 (10, 80)

[a] Values are area under the curve x10^5

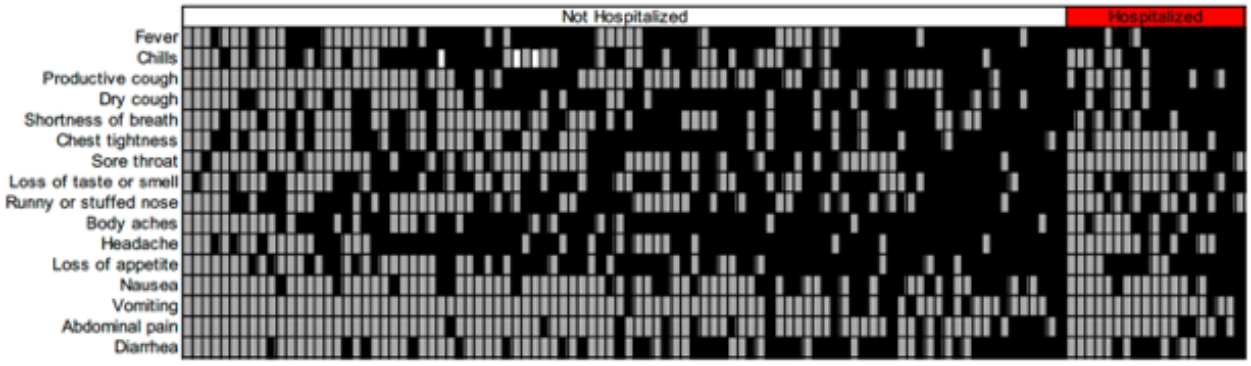

Supplementary Figure 1. Self-reported symptoms during COVID-19. Upon initial recruitment, subjects were asked about each symptom listed on the left during their COVID-19 illness. Each column represents a subject (n=113) with hospitalized subjects under the red bar. Black square, symptom experienced; gray square, symptom not experienced; white square, data not collected.

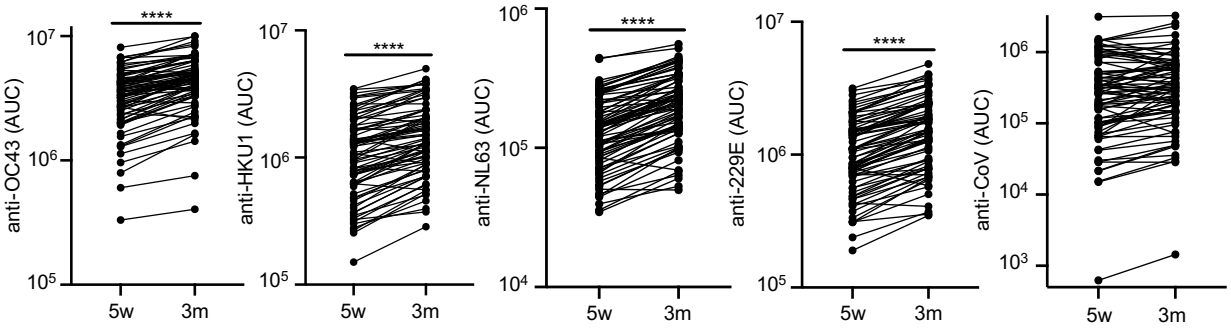

Supplementary Figure 2. Antibodies to seasonal coronaviruses and SARS-CoV do not decline from five weeks to three months post COVID-19 symptom resolution. Sera from COVID-19 convalescent subjects five weeks (w) and three months (m) post symptom resolution were evaluated for IgG (reported as area under the curve, AUC) that bound to the spike protein of common cold coronaviruses OC43, HKU1, NL63 and 229E as well as SARS-CoV by multiplex assay. Lines connect time points for individual subjects (n=79). Paired t tests were performed ****p<0.0001.

REFERENCES

1. Novel Coronavirus (2019-nCoV) Situation Report. World Health Organization **2020**:5.
2. Fu L, Wang B, Yuan T, et al. Clinical characteristics of coronavirus disease 2019 (COVID-19) in China: A systematic review and meta-analysis. J Infect **2020**; 80:656-65.
3. worldometer. https://wwwworldometersinfo/coronavirus/.
4. Haleem A, Javaid M, Vaishya R. Effects of COVID-19 pandemic in daily life. Curr Med Res Pract **2020**; 10:78-9.
5. Chang SC, Wang JT, Huang LM, et al. Longitudinal analysis of Severe Acute Respiratory Syndrome (SARS) coronavirus-specific antibody in SARS patients. Clin Diagn Lab Immunol **2005**; 12:1455-7.
6. Shi Y, Wan Z, Li L, et al. Antibody responses against SARS-coronavirus and its nucleocaspid in SARS patients. J Clin Virol **2004**; 31:66-8.
7. Liu L, Xie J, Sun J, et al. Longitudinal profiles of immunoglobulin G antibodies against severe acute respiratory syndrome coronavirus components and neutralizing activities in recovered patients. Scand J Infect Dis **2011**; 43:515-21.
8. Dan JM, Mateus J, Kato Y, et al. Immunological memory to SARS-CoV-2 assessed for up to 8 months after infection. Science **2021**.
9. Wu J, Liang B, Chen C, et al. SARS-CoV-2 infection induces sustained humoral immune responses in convalescent patients following symptomatic COVID-19. medRxiv, **2020**.
10. Pradenas E, Trinité B, Urrea V, et al. Stable neutralizing antibody levels six months after mild and severe COVID-19 episode. bioRxiv, **2020**.
11. Rodda LB, Netland J, Shehata L, et al. Functional SARS-CoV-2-Specific Immune Memory Persists after Mild COVID-19. Cell **2021**; 184:169-83.e17.
12. Korte W, Buljan M, Rösslein M, et al. SARS-CoV-2 IgG and IgA antibody response is gender dependent; and IgG antibodies rapidly decline early on. J Infect **2020**.
13. Yin S, Tong X, Huang A, et al. Longitudinal anti-SARS-CoV-2 antibody profile and neutralization activity of a COVID-19 patient. J Infect **2020**.
14. Röltgen K, Wirz OF, Stevens BA, et al. SARS-CoV-2 Antibody Responses Correlate with Resolution of RNAemia But Are Short-Lived in Patients with Mild Illness. medRxiv **2020**.
15. Seow J, Graham C, Merrick B, et al. Longitudinal observation and decline of neutralizing antibody responses in the three months following SARS-CoV-2 infection in humans. Nat Microbiol **2020**; 5:1598-607.
16. Ibarrondo FJ, Fulcher JA, Goodman-Meza D, et al. Rapid Decay of Anti-SARS-CoV-2 Antibodies in Persons with Mild Covid-19. N Engl J Med **2020**.
17. Long QX, Tang XJ, Shi QL, et al. Clinical and immunological assessment of asymptomatic SARS-CoV-2 infections. Nat Med **2020**.
18. Liu A, Li Y, Peng J, Huang Y, Xu D. Antibody responses against SARS-CoV-2 in COVID-19 patients. J Med Virol **2020**.
19. Girardin RC, Dupuis AP, Payne AF, et al. Temporal Analysis of Serial Donations Reveals Decrease in Neutralizing Capacity and Justifies Revised Qualifying Criteria for COVID-19 Convalescent Plasma. J Infect Dis **2021**.
20. Wajnberg A, Amanat F, Firpo A, et al. Robust neutralizing antibodies to SARS-CoV-2 infection persist for months. Science **2020**; 370:1227-30.
21. Bonifacius A, Tischer-Zimmermann S, Dragon AC, et al. COVID-19 immune signatures reveal stable antiviral T cell function despite declining humoral responses. Immunity **2021**; 54:340-54.e6.
22. Marklund E, Leach S, Axelsson H, et al. Serum-IgG responses to SARS-CoV-2 after mild and severe COVID-19 infection and analysis of IgG non-responders. PLoS One **2020**; 15:e0241104.
23. Klein SL, Pekosz A, Park HS, et al. Sex, age, and hospitalization drive antibody responses in a COVID-19 convalescent plasma donor population. J Clin Invest **2020**; 130:6141-50.

24. Salazar E, Kuchipudi SV, Christensen PA, et al. Convalescent plasma anti-SARS-CoV-2 spike protein ectodomain and receptor binding domain IgG correlate with virus neutralization. J Clin Invest **2020**.
25. Rijkers G, Murk JL, Wintermans B, et al. Differences in antibody kinetics and functionality between severe and mild SARS-CoV-2 infections. J Infect Dis **2020**.
26. Holmes CL, Peyton CG, Bier AM, et al. Reduced IgG titers against pertussis in rheumatoid arthritis: Evidence for a citrulline-biased immune response and medication effects. PLoS One **2019**; 14:e0217221.
27. Kind AJH, Buckingham WR. Making Neighborhood-Disadvantage Metrics Accessible - The Neighborhood Atlas. N Engl J Med **2018**; 378:2456-8.
28. Charlson ME, Pompei P, Ales KL, MacKenzie CR. A new method of classifying prognostic comorbidity in longitudinal studies: development and validation. J Chronic Dis **1987**; 40:373-83.
29. Alkhouli M, Nanjundappa A, Annie F, Bates MC, Bhatt DL. Sex Differences in Case Fatality Rate of COVID-19: Insights From a Multinational Registry. Mayo Clin Proc **2020**; 95:1613-20.
30. Zhou P, Yang XL, Wang XG, et al. A pneumonia outbreak associated with a new coronavirus of probable bat origin. Nature **2020**; 579:270-3.
31. Fonville JM, Wilks SH, James SL, et al. Antibody landscapes after influenza virus infection or vaccination. Science **2014**; 346:996-1000.
32. Wang P, Liu L, Nair MS, et al. SARS-CoV-2 neutralizing antibody responses are more robust in patients with severe disease. Emerg Microbes Infect **2020**; 9:2091-3.
33. Chen X, Pan Z, Yue S, et al. Disease severity dictates SARS-CoV-2-specific neutralizing antibody responses in COVID-19. Signal Transduct Target Ther **2020**; 5:180.
34. Wang Y, Zhang L, Sang L, et al. Kinetics of viral load and antibody response in relation to COVID-19 severity. J Clin Invest **2020**; 130:5235-44.
35. Mathew D, Giles JR, Baxter AE, et al. Deep immune profiling of COVID-19 patients reveals distinct immunotypes with therapeutic implications. Science **2020**; 369.
36. Hussain A, Mahawar K, Xia Z, Yang W, El-Hasani S. Obesity and mortality of COVID-19. Meta-analysis. Obes Res Clin Pract **2020**; 14:295-300.
37. Frasca D, Diaz A, Romero M, Blomberg BB. Ageing and obesity similarly impair antibody responses. Clin Exp Immunol **2017**; 187:64-70.
38. Kumakura S, Shibata H, Onoda K, Nishimura N, Matsuda C, Hirose M. Seroprevalence survey on measles, mumps, rubella and varicella antibodies in healthcare workers in Japan: sex, age, occupational-related differences and vaccine efficacy. Epidemiol Infect **2014**; 142:12-9.
39. Petersen LR, Sami S, Vuong N, et al. Lack of antibodies to SARS-CoV-2 in a large cohort of previously infected persons. Clin Infect Dis **2020**.
40. Wang F, Zheng S, Zheng C, Sun X. Attaching clinical significance to COVID-19-associated diarrhea. Life Sci **2020**; 260:118312.
41. Long QX, Liu BZ, Deng HJ, et al. Antibody responses to SARS-CoV-2 in patients with COVID-19. Nat Med **2020**; 26:845-8.

Chapter 3: Anti-membrane antibodies persist at least one year and discriminate between past COVID-19 infection and vaccination

Maya F. Amjadi[1], Ryan R. Adyniec[1], Srishti Gupta[1], S. Janna Bashar[1], Aisha M. Mergaert[1,2], Katarina M. Braun[3], Gage K. Moreno[2], David H. O'Connor[2], Thomas C. Friedrich[3], Nasia Safdar[1], Sara S. McCoy[1], Miriam A. Shelef[1,4]

[1] Department of Medicine, University of Wisconsin (UW)-Madison, Madison, 53705 USA

[2] Department of Pathology and Laboratory Medicine, UW-Madison, Madison, 53705 USA

[3] Department of Pathobiological Sciences, UW-Madison, Madison, 53705 USA

[4] William S. Middleton Memorial Veterans Hospital, Madison, 53705 USA

J Infect Dis. 2022 Nov 28;226(11):1897-1902. doi: 10.1093/infdis/jiac263. PMID: 35758987; PMCID: PMC9278254.

Contributions: I performed and analyzed all immunoassays and ELISAs, made the figures, wrote the first draft of the manuscript, and assisted in editing the manuscript.

ABSTRACT

The consequences of past COVID-19 infection for personal and population health are emerging, but accurately identifying distant infection is a challenge. Anti-spike antibodies rise after both vaccination and infection and anti-nucleocapsid antibodies rapidly decline. We evaluated anti-membrane antibodies in COVID-19 naïve, vaccinated, and convalescent subjects to determine if they persist and accurately detect distant infection. We found that anti-membrane antibodies persist for at least a year and are a sensitive and specific marker of past COVID-19 infection. Thus, anti-membrane and anti-spike antibodies together can differentiate between COVID-19 convalescent, vaccinated, and naïve states to advance public health and research.

INTRODUCTION

The cardinal features and challenges of the COVID-19 pandemic have changed. Initially, the pandemic was defined by SARS-CoV-2 infections in an immunologically naive population, Now, immunity from vaccination, infection, or both is common, reducing the severity of future infection waves. However, identifying infection for research and public health efforts is limited by the need to perform viral testing during acute infection (which may not occur during asymptomatic disease or pandemic surges that deplete resources) and by shortcomings in serologic testing [1]. Anti-nucleocapsid antibodies often decline to seronegativity just months after infection [2-4]. Anti-spike antibodies persist at least a year post-infection [5, 6] but typically cannot differentiate between infection and vaccination [7-9]. Anti-membrane antibodies develop soon after SARS-CoV-2 infection [10-12], but they are rarely assessed and their longevity is unknown. Here, we evaluated antibodies against the receptor binding domain (RBD) of spike, nucleocapsid, and membrane antigens in naïve, COVID-19 vaccinated, and COVID-19 convalescent subjects up to a year post symptom resolution to evaluate the persistence of anti-membrane antibodies and to identify antigens that discriminate between distant infection, vaccination, and naïve states.

MATERIALS AND METHODS

Human subjects

Human studies were approved by the UW Institutional Review Board and human subjects provided written informed consent. Sera and data collected before 2019 from 60 COVID-19 naïve adults without inflammatory disease (exception: one subject with psoriatic arthritis using adalimumab to match two COVID-19 convalescent subjects using adalimumab) were obtained from the University of Wisconsin (UW) Rheumatology Biorepository [13].

COVID-19 convalescent sera and data were obtained from the UW COVID-19 Convalescent Biorepository [14]. Briefly, in spring of 2020, adults with a positive SARS-CoV-2 PCR test at UW Health were invited to participate until 121 subjects were recruited. Demographic and clinical information were collected by questionnaire and electronic medical record (EMR) abstraction. COVID-19 severity was diverse: mild (n=12), moderate (n=86), severe (n=15) and critical (n=8) as we previously defined [14]. Subjects provided blood and clinical information 5 weeks (n=121), 3 months (n=115), 6 months (n=98) and 12 months (n=100) +/- 3 weeks after symptom resolution. One sample collected >3 weeks from the 3 month timepoint and subjects for whom the 5 week time point was collected >3 weeks from the intended timepoint (n=1) or missed >1 blood draw (n=16) were excluded from comparative analyses, generating sample sizes of 104 (5 weeks), 101 (3 months), 97 (6 months), and 98 (12 months). Based on anti-RBD Ig elevation timing post-vaccination (Supplementary Figure 1), COVID-19 convalescent subjects at 12 months were considered vaccinated if they received 1 vaccine dose $\geq$5 days before sample collection (n=77) and unvaccinated if they received no vaccine (n=17) or their first or only vaccine dose <5 days before sample collection (n=4).

Vaccinated individuals without past COVID-19 (n=21) were recruited by flyers at UW Health in summer of 2021. Complete vaccination (>3 weeks after two mRNA vaccine doses or one Ad26.COV2.S dose) and lack of known COVID-19 was confirmed by questionnaire and EMR review.

Limited clinical data, sera, and SARS-CoV-2 lineages were provided by UW Health Infection Control for 20 completely vaccinated healthcare workers with breakthrough COVID-19 (positive PCR and symptoms) in spring of 2021. Blood collection occurred ~1 day after SARS-CoV-2 PCR (range 0-4 days) and ~3 days after symptom onset (range 0-5 days). Four breakthrough cases also had PCR positive COVID-19 prior to vaccination completion and 3-6 months prior to breakthrough infection. Healthcare workers with breakthrough infections were invited to participate in the longitudinal study, and 3 provided blood ~8 weeks (range 37-70 days) after the initial collection.

Anti-RBD Ig Immunoassay

Anti-RBD Ig was detected by Lumit™ SARS-CoV-2 Immunoassay (Promega, Madison, USA) according to kit instructions using a TEMPEST® Liquid Handler (Formulatrix, Bedford, MA) and a PHERAstar FS plate reader (BMG Labtech, Ortenberg, Germany). Sera were diluted 1:10 to use the recommended sample/calibrator cutoff of 1 for seropositivity. At 1:10, the highest anti-RBD Ig values were above the linear range, but results were overall similar to a 1:200 dilution (Supplementary Figure 2), at which higher values were within the linear range.

Anti-membrane and anti-nucleocapsid IgG enzyme-linked immunosorbent assay (ELISA)

ELISAs were performed as previously to detect IgG against SARS-CoV-2 membrane (aa 8-23, ITVEELKKLLEQWNLV-K-biotin) and nucleocapsid (aa 390-405, QTVTLLPAADLDDFSK-K-biotin) peptides [10] with the following modifications: blocking for >2.5 instead of 1 hour and serum dilution of 1:50 (nucleocapsid) or 1:500 (membrane), instead of 1:200 to maximally utilize the linear range. Relative absorbance values (IgG binding to uncoated wells subtracted from coated wells for each subject and values normalized across plates using a serum standard) of 0 were plotted as 0.0001 to allow a log scale for graphs.

Statistics

Statistical analyses were performed using Prism (GraphPad, San Diego, CA) and JMP (SAS Institute, Cary, NC) software. Antibody levels were compared between naïve or vaccinated subjects versus all other groups by Kruskal-Wallis One-Way ANOVA with Dunn's multiple comparisons test. Antibody levels in unvaccinated versus vaccinated 12 month convalescent samples were compared by Mann-Whitney U test. Matched antibody levels across multiple timepoints in convalescent subjects were compared by Friedman test with Dunn's multiple comparisons test. Antibody levels in breakthrough infection subjects were compared at ~3 days post symptom onset versus ~8 weeks later by Wilcoxon signed rank test. Antibody positivity was compared between two groups with Fisher's exact test and among multiple groups with a chi-square test. P values <0.05 were considered significant.

RESULTS

We quantified antibodies against RBD, nucleocapsid, and membrane antigens in sera from the following subjects: naïve, vaccinated with no known COVID-19 infection, COVID-19

convalescent with sera collected 5 weeks, 3 months, 6 months, and 12 months post symptom resolution (all initially unvaccinated), and vaccinated with subsequent SARS-CoV-2 breakthrough infection. Clinical and demographic information is in Supplementary Table 1.

For anti-RBD Ig, the chemiluminescent assay had an area under the receiver operator curve (AUC) of 0.973, 90% sensitivity, and 97% specificity (Supplementary Figure 3A), comparable to other assays [14]. Convalescent and vaccinated individuals had significantly higher anti-RBD Ig than naïve subjects, with no significant difference in antibody levels or percent seropositivity between vaccinated subjects and unvaccinated convalescent subjects (Figure 1A and 1B). In a matched analysis of the 88 subjects who provided serum at all 4 timepoints (Figure 1C), anti-RBD Ig levels were statistically different between timepoints, but the extremely small difference in medians is unlikely to be biologically meaningful. Further, the percent of seropositive subjects at 5 weeks (91%) versus 6 months (88%) was not significantly different (Figure 1B). Because only 21 convalescent subjects remained unvaccinated at 12 months, this timepoint was not compared to the 5 week timepoint. Not surprisingly, anti-RBD Ig levels in 12 month convalescent subjects were significantly higher for those who received at least one dose of a vaccine compared with no vaccine (Figure 1A and Supplementary Figure 1B). Finally, all vaccinated subjects, with or without past or breakthrough infections, were seropositive for anti-RBD Ig, with no significant differences in antibody levels between vaccinated subjects with or without breakthrough infections (Figure 1A and 1B). Overall, these data suggest that anti-RBD antibodies are detectable in the vast majority of vaccinated and convalescent subjects at least a year after infection, but cannot differentiate between past infection, vaccination, and vaccination with breakthrough infection.

Next, we evaluated anti-nucleocapsid IgG. The ELISA had an AUC of 0.919, 91% sensitivity, and 88% specificity (Supplementary Figure 3B). The low specificity of this test is consistent with

other anti-nucleocapsid tests, likely due to cross-reactivity with common cold coronavirus nucleocapsid [14, 15]. Nonetheless, as expected, there was no difference in anti-nucleocapsid IgG levels between naïve versus vaccinated subjects or between 12 month convalescent vaccinated versus unvaccinated subjects (Figure 1D). Also as expected, compared to either vaccinated or naïve subjects, anti-nucleocapsid IgG levels were higher in subjects with past infection (Figure 1D). However, in a matched analysis of convalescent subjects, anti-nucleocapsid IgG levels fell significantly over time (Figure 1F) with 34% of subjects seronegative by 6 months and 48% by 12 months, a significant increase in seronegativity compared to 8% at 5 weeks (Figure 1E). Interestingly, none of the four breakthrough cases who also had COVID-19 before vaccination were seropositive for anti-nucleocapsid IgG at the time of breakthrough infection and only one of three subjects was seropositive eight weeks after breakthrough infection (Figure 1E). Together, these data highlight the rapid decline of anti-nucleocapsid antibodies.

Last, we evaluated anti-membrane IgG. The ELISA had an AUC of 0.956, 88% sensitivity, and 95% specificity (Supplementary Figure 3C). As expected, anti-membrane IgG levels and percent seropositivity did not differ between naïve and vaccinated subjects or between 12 month convalescent vaccinated and unvaccinated subjects, but were significantly higher in convalescent subjects (Figure 1G and 1H). In a matched analysis over time (Figure 1I), anti-membrane IgG levels remained stable at 6 months with an extremely small decline at 12 months. However, at 12 months, 94% of convalescent samples were seropositive for anti-membrane IgG, as compared to 88% at 5 weeks (Figure 1H). Interestingly, all four vaccine breakthrough infection subjects with prior COVID-19 and no breakthrough subjects without prior COVID-19 were seropositive for anti-membrane IgG during acute infection (Figure 1I). Together, these data demonstrate that anti-membrane IgG persists at least a year and can be a sensitive and specific marker of past COVID-19 infection.

Finally, we compared antibody levels at 5 weeks and 12 months post-symptom resolution across disease severity groups. As expected [10, 14], levels of all three antibodies were generally higher in subjects with more severe COVID-19 at both time points (Figure 2).

DISCUSSION

Here, in addition to confirming that anti-RBD antibodies last at least a year and anti-nucleocapsid IgG declines over months [2-6], we demonstrate that anti-membrane IgG is present in the vast majority of COVID-19 convalescent patients and persists at least a year. Our findings are consistent with findings for IgG against a recombinant membrane antigen (polypeptide of aa 1-19 and 101-222) in the early convalescent period [11]. In contrast, Jörrißen and colleagues found that only ~20% of non-hospitalized COVID-19 convalescent subjects had IgG against a membrane peptide in the early convalescent period [12]. Our non-hospitalized subjects alone were 88% positive for anti-membrane IgG at 5 weeks (n=83) and 94% at 12 months (n=77) post symptom resolution. This discrepancy may be due to their smaller sample size (n=30) or use of a different peptide (aa 1-20).

Given the absence of anti-RBD and anti-membrane antibodies in naïve subjects, the presence of only anti-RBD antibodies in vaccinated subjects, and the presence of both in COVID-19 convalescent subjects up to 12 months after infection, our study suggests that a combination of anti-RBD and anti-membrane antibody testing could be used to detect past COVID-19 infection and vaccination at a population and individual level. An analogous testing strategy for hepatitis B uses anti-surface antibodies to detect past infection or vaccination and anti-core antibodies to detect past infection. While SARS-CoV-2 does not appear to cause persistent infection like hepatitis B, the long-term consequences of COVID-19 are still emerging and revealing a previously undetected infection may prove important. At minimum, detecting unknown past

infections may relieve personal anxiety about future infections in some individuals. Moreover, accurate assessment of past infection in a population could enhance the prediction of and interpretation of COVID-19 surge outcomes and inform public health policy.

Limitations of this study include that samples were collected only up to 12 months post COVID-19 and that we quantified IgG, not IgM or IgA, that binds membrane and nucleocapsid peptides versus total Ig that binds RBD. Also, subjects were infected by ancestral SARS-CoV-2 lineages (early 2020) or alpha and delta variants (breakthrough infections, Supplementary Figure 4), whereas the omicron variant has a single amino acid difference in the membrane peptide (ITVEELKKLLE**E**WNLV). Finally, sample sizes for breakthrough infections were small with samples collected ~3 days after symptom onset, possibly allowing an early antibody response. Future studies are needed to evaluate later time points, multiple antibody isotypes, larger cohorts, and antibodies after omicron infections.

Nonetheless, we demonstrate that anti-membrane antibodies persist at least a year and, together with anti-RBD antibodies, can accurately identify past-COVID-19 infection and vaccination.

ACKNOWLEDGEMENTS

The authors thank Gene Ananiev and Song Guo at UW's Small Molecules Screening Facility and Laura Perez-Brenner, Samantha Lewis and Melanie Dart from Promega for technical advice, UW Health Infection Control and Employee Health Services, the UW Clinical Research Office, and the participating human subjects.

FUNDING

This work was supported by a Wisconsin Partnership Program COVID-19 Response grant [4647] and a UW Department of Medicine COVID-19 Pilot Award to MAS, by the CDC [75D30120C09870, 75D30121C11060] to DHO and TCF, and by NIAID [R24OD017850] to DHO. Additional support includes NIA [T32 AG000213] and MSTP [T32 GM140935] to MFA, NHLBI [T32 HL007899] to AMM, NCATS [1KL2TR002374] to SSM, and NIAID [1DP2AI144244-01] to NS. DHO and TCF are members of the Upper Midwest Regional Accelerator for Genomic Surveillance funded by the Rockefeller Foundation.

FIGURE LEGENDS

Figure 1. Anti-RBD, anti-nucleocapsid, and anti-membrane antibodies after COVID-19 vaccination and infection. Anti-RBD Ig was detected by immunoassay (reported as sample/calibrator, S/C) and anti-nucleocapsid and anti-membrane IgG were quantified by ELISA reported as relative absorbance, rel. abs.) in sera from the following subjects: naive (n=60), vaccinated with no known COVID-19 infection (Vax, n=21), COVID-19 convalescent 5 weeks (5w, n=104), 3 months (3m, n=101), 6 months (6m, n=97), and 12 months (12m, n=98) post-symptom resolution either vaccinated (12m Vax, n=77) or not (12m Unvax, n=21), vaccinated with breakthrough COVID-19 ~3 days (Vax BT ~3d, n=20) and ~8 weeks (Vax BT ~8w, n=3) after symptom onset including 4 subjects with previous COVID-19 infection (PI). Anti-RBD Ig (A), anti-nucleocapsid IgG (D), and anti-membrane IgG (G) for all groups were graphed and compared to naive (blue) or Vax (gray) by Kruskal-Wallis and Dunn's multiple comparisons tests and 12m Unvax was compared to 12m Vax by Mann-Whitney test (brackets). Vax BT with both ~3d and ~8w timepoints are represented with triangles or squares and Vax BT subjects with PI in red symbols. Percent positive (black) and negative (gray) for anti-RBD Ig (B), anti-nucleocapsid IgG (E), and anti-membrane IgG (H) were graphed and compared between

selected groups by Fisher's exact (line) or chi-square (bracket encompassing compared groups) tests. Matched anti-RBD Ig (C), anti-nucleocapsid IgG (F) and anti-membrane IgG (I) levels were compared across all time points for COVID-19 convalescent subjects (n=88) by Friedman test with Dunn's multiple comparisons test. For all panels: bars indicate medians, dashed lines indicate cutoffs, *p<0.05, **p<0.01, ***p<0.001, ****p<0.0001, or not significant (ns).

Figure 2. Anti-SARS-CoV-2 antibody levels are higher after more severe COVID-19. Anti-RBD Ig (A), anti-nucleocapsid IgG (B), and anti-membrane IgG (C) were compared across disease severity groups by Kruskal-Wallis with Dunn's Multiple Comparisons test at indicated time points (mild: n=11 5w, n=10 6m, n=9 12m; moderate (mod.): n=72 5w, n=68 6m, 12m, severe, n=15 5w, n=13 6m, n=15 12m, critical: n=6 5w, 6m, 12m). For all panels: bars represent medians, *p<0.05, **p<0.01, ***p<0.001, ****p<0.0001.

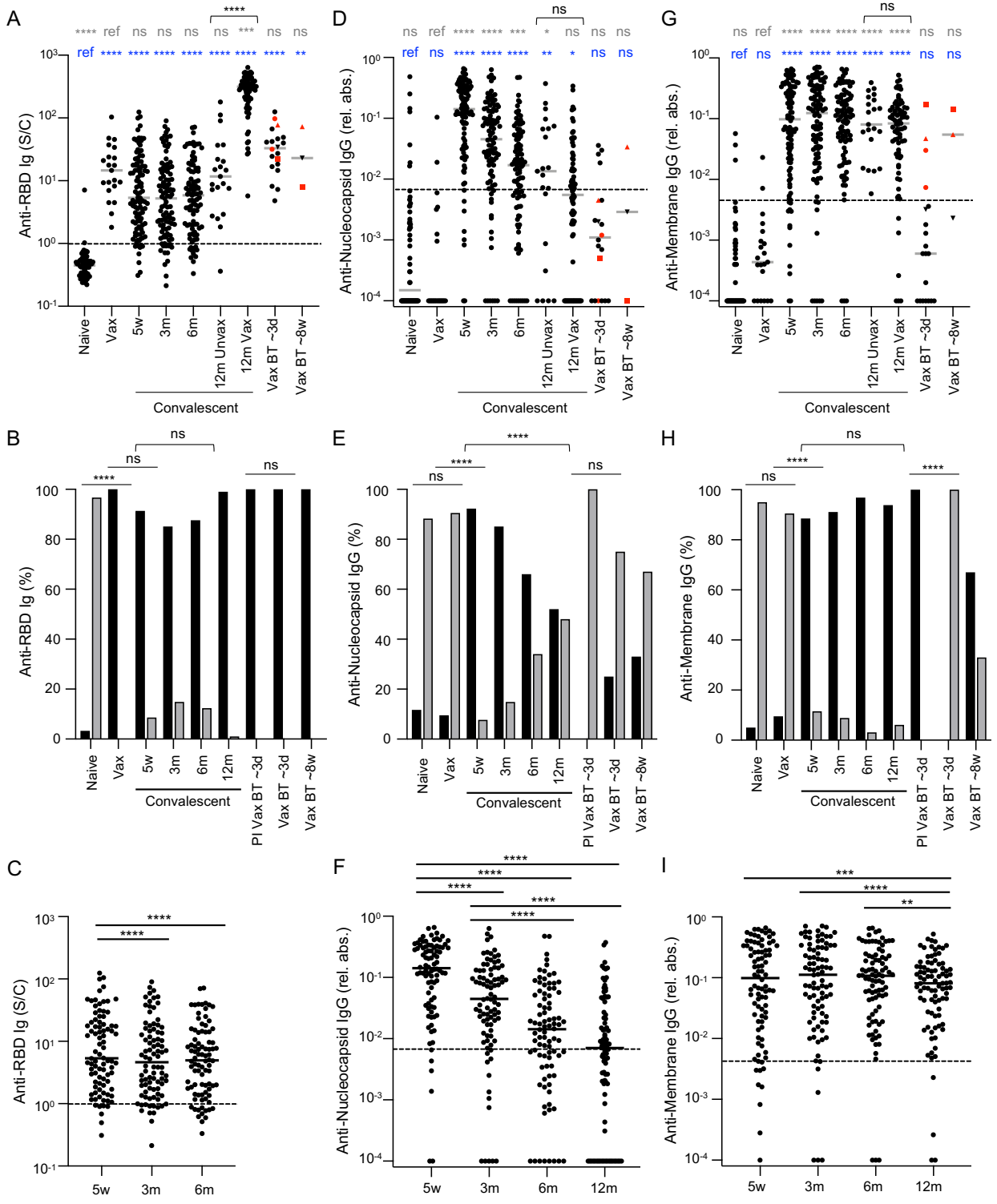

Figure 1. Anti-RBD, anti-nucleocapsid, and anti-membrane antibodies after COVID-19 vaccination and infection. Anti-RBD Ig was detected by immunoassay (reported as sample/calibrator, S/C) and anti-nucleocapsid and anti-membrane IgG were quantified by ELISA reported as relative absorbance, rel. abs.) in sera from the following subjects: I (n=60), vaccinated with no known COVID-19 infection (Vax, n=21), COVID-19 convalescent 5 weeks (5w, n=104), 3 months (3m, n=101), 6 months (6m, n=97), and

12 months (12m, n=98) post-symptom resolution either vaccinated (12m Vax, n=77) or not (12m Unvax, n=21), vaccinated with breakthrough COVID-19 ~3 days (Vax BT ~3d, n=20) and ~8 weeks (Vax BT ~8w, n=3) after symptom onset including 4 subjects with previous COVID-19 infection (PI). Anti-RBD Ig (A), anti-nucleocapsid IgG (D), and anti-membrane IgG (G) for all groups were graphed and compared to I (blue) or Vax (gray) by Kruskal-Wallis and Dunn's multiple comparisons tests and 12m Unvax was compared to 12m Vax by Mann-Whitney test (brackets). Vax BT with both ~3d and ~8w timepoints are represented with triangles or squares and Vax BT subjects with PI in red symbols. Percent positive (black) and negative (gray) for anti-RBD Ig (B), anti-nucleocapsid IgG I, and anti-membrane IgG (H) were graphed and compared between selected groups by Fisher's exact (line) or chi-square (bracket encompassing compared groups) tests. Matched anti-RBD Ig (C), anti-nucleocapsid IgG (F) and anti-membrane IgG (I) levels were compared across all time points for COVID-19 convalescent subjects (n=88) by Friedman test with Dunn's multiple comparisons test. For all panels: bars indicate medians, dashed lines indicate cutoffs, *p<0.05, **p<0.01, ***p<0.001, ****p<0.0001, or not significant (ns).

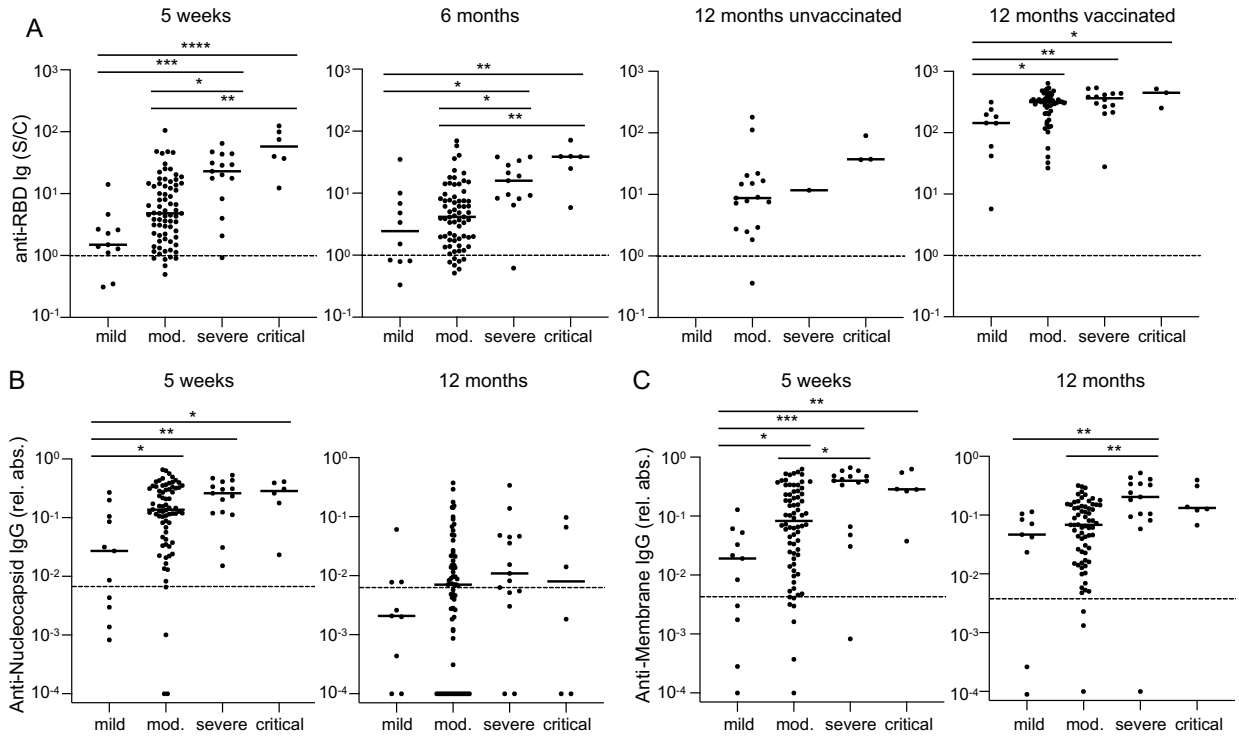

Figure 2. Anti-SARS-CoV-2 antibody levels are higher after more severe COVID-19. Anti-RBD Ig (A), anti-nucleocapsid IgG (B), and anti-membrane IgG (C) were compared across disease severity groups by Kruskal-Wallis with Dunn's Multiple Comparisons test at indicated time points (mild: n=11 5w, n=10 6m, n=9 12m; moderate (mod.): n=72 5w, n=68 6m, 12m, severe, n=15 5w, n=13 6m, n=15 12m, critical: n=6 5w, 6m, 12m). For all panels: bars represent medians, *p<0.05, **p<0.01, ***p<0.001, ****p<0.0001.

Supplementary Table 1. Clinical and Demographic Data for Subjects.

Cohort	n	Age	Sex (%)			Days since 1st vaccine
		Median (IQR)	F	M	NB	Median (IQR)
Naïve	60	49 (37, 63)	65	35	0	-
Vaccinated	21	41 (33, 56)	90	5	5	186 (170, 206)
COVID-19 Convalescent						
5 weeks	104	48 (33, 58)	58	42	0	-
3 months	101	45 (33, 58)	56	44	0	-
6 months	97	47 (34, 59)	60	40	0	-
12 months, unvaccinated	21	44 (38, 58)	48	52	0	-
12 months, vaccinated	77	50 (34, 58)	60	40	0	73 (40, 98)
Vaccinated with breakthrough COVID-19	20	35 (29, 41)	80	15	5	125 (104, 154)
Post-breakthrough, 8 weeks	3	47 (35, 57)	67	33	0	173 (153, 185)

NB: non-binary

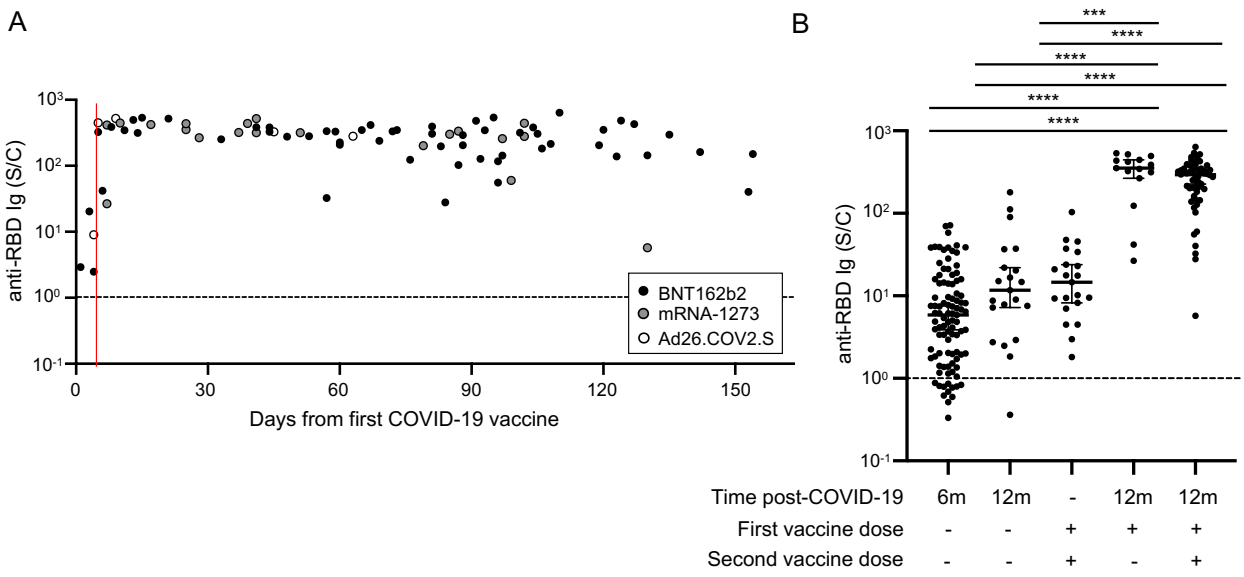

Supplementary Figure 1. Rise in anti-RBD Ig in response to vaccination in COVID-19 convalescent subjects. A. Serum anti-RBD Ig levels (reported as sample/calibrator, S/C) for COVID-19 convalescent individuals 12 months after symptom resolution were plotted according to the time of receipt of the first BNT162b2 vaccine dose (n=58), the first mRNA-1273 vaccine dose (n=20), or the only Ad26.COV2.S vaccine dose (n=5). Red line indicates day >5, the cutoff selected for vaccinated versus unvaccinated post COVID-19. B. Serum anti-RBD Ig levels for unvaccinated COVID-19 convalescent individuals 6 months (n=97) or 12 months (n=21) post symptom resolution, fully vaccinated individuals with no known COVID-19 (n=21), and 12 month convalescent subjects who received either 1 (n=15) or 2 (n=58) vaccine doses of BNT162b2 or mRNA-1273 were compared by Kruskal-Wallis One-way ANOVA with Dunn's multiple comparisons test (***p<0.001, ****p<0.0001). Median and 95% CI are shown. For all panels, black dashed lines indicate the antibody detection cutoff.

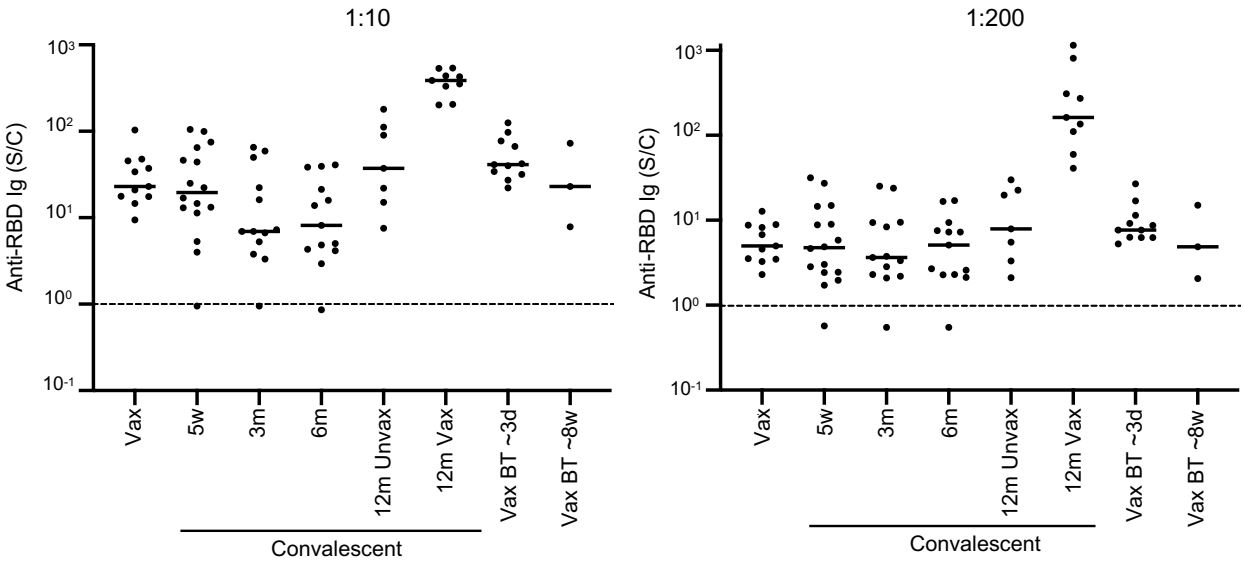

Supplementary Figure 2. Similar results for anti-RBD Ig detection at different serum dilutions. Anti-RBD Ig levels (sample/calibrator, S/C) detected by immunoassay in sera from COVID-19 vaccinated subjects with no known COVID-19 infection (Vax n=11), COVID-19 convalescent patients collected 5 weeks (5w, n=16), 3 months (3m, n=13), 6 months (6m, n=13), and 12 months post symptom resolution (n=7 unvaccinated, 12m Unvax; n=9 vaccinated, 12m Vax), vaccinated subjects with breakthrough COVID-19 (n=11) collected ~3 days (Vax BT ~3d) and ~8 weeks (Vax BT ~8w, n=3) after symptom onset showed similar trends when evaluated at 1:10 and 1:200 serum dilutions. Black solid lines indicate medians and black dashed lines represent antibody detection cutoffs.

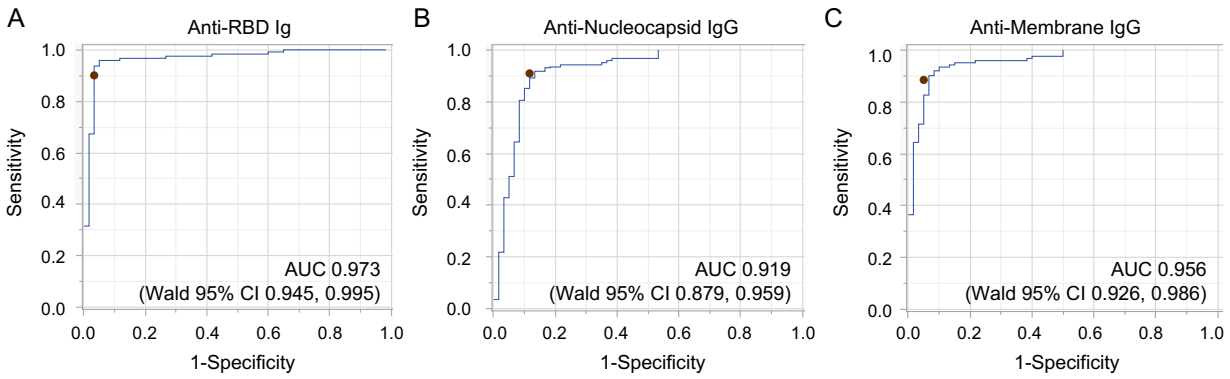

Supplementary Figure 3. Receiver operator curves for antibody detection assays. Anti-RBD Ig (A) was detected by immunoassay and anti-nucleocapsid (B) and anti-membrane (C) IgG were quantified by ELISA for naive (n=60) and ~5 week COVID-19 convalescent (n=121) sera with receiver operator curves for antibody levels shown. Dots indicate cutoffs for seropositivity, which were selected by identifying thresholds that maximized sensitivity and specificity as a starting point and then favoring higher specificity to be more conservative in claiming positive results. Selected optimal cutoffs were a sample/calibrator value of 1 for anti-RBD Ig (90% sensitivity and 97% specificity) which is identical to the value suggested by the manufacturer, a relative absorbance of 0.0067 for anti-nucleocapsid IgG (91% sensitivity and 88% specificity), and a relative absorbance of 0.0043 for anti-membrane IgG (88% sensitivity and 95% specificity).

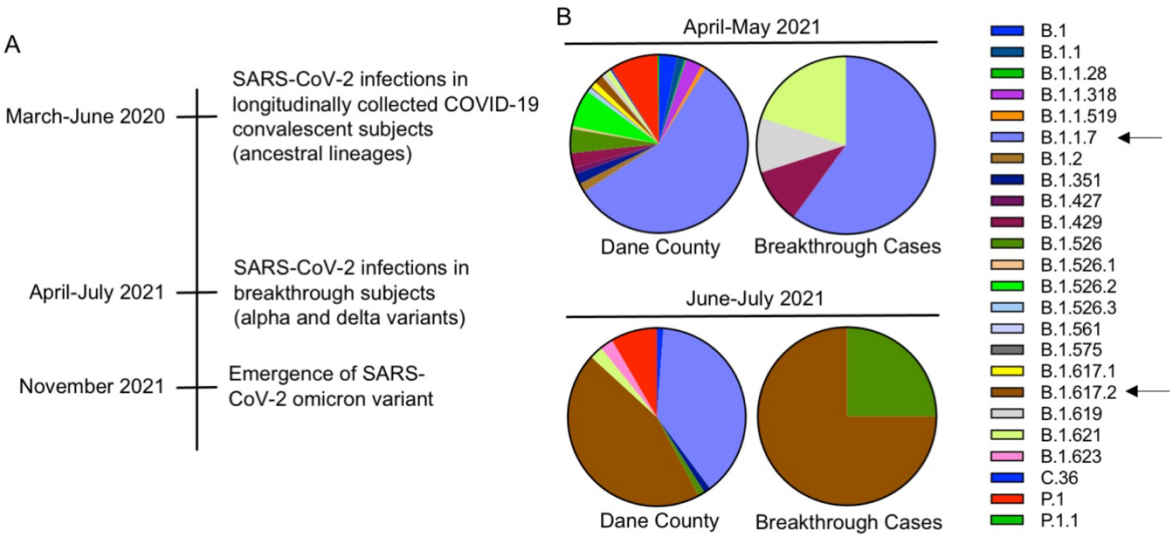

Supplementary Figure 4. SARS-CoV-2 lineages in study subjects. A. Timeline of study subject infections and SARS-CoV-2 lineages. B. Samples from PCR positive COVID-19 cases in 2021 in Dane County (n=367 April-May, n=83 June-July) and vaccinated subjects with breakthrough COVID-19 (n=10 April-May, n=4 June-July), who were also located in Dane County, were sequenced to determine viral lineages. Pie charts show percentage of each lineage sequenced out of the total sequenced for each group. Arrows indicate the most common lineages (B.1.1.7, alpha variant, and B.1.617.2, delta variant). Six of twenty breakthrough samples could not be sequenced. Similar SARS-CoV-2 lineages were sequenced in breakthrough and total infections in Dane County.

REFERENCES

1. Gong F, Wei HX, Li Q, Liu L, Li B. Evaluation and Comparison of Serological Methods for COVID-19 Diagnosis. Front Mol Biosci **2021**; 8:682405.
2. Ripperger TJ, Uhrlaub JL, Watanabe M, et al. Orthogonal SARS-CoV-2 Serological Assays Enable Surveillance of Low-Prevalence Communities and Reveal Durable Humoral Immunity. Immunity **2020**; 53:925-33.e4.
3. Liu A, Li Y, Peng J, Huang Y, Xu D. Antibody responses against SARS-CoV-2 in COVID-19 patients. J Med Virol **2020**.
4. Bolotin S, Tran V, Osman S, et al. SARS-CoV-2 Seroprevalence Survey Estimates Are Affected by Anti-Nucleocapsid Antibody Decline. J Infect Dis **2021**; 223:1334-8.
5. Gallais F, Gantner P, Bruel T, et al. Evolution of antibody responses up to 13 months after SARS-CoV-2 infection and risk of reinfection. EBioMedicine **2021**; 71:103561.
6. Wang Z, Muecksch F, Schaefer-Babajew D, et al. Naturally enhanced neutralizing breadth against SARS-CoV-2 one year after infection. Nature **2021**; 595:426-31.
7. Wang Z, Schmidt F, Weisblum Y, et al. mRNA vaccine-elicited antibodies to SARS-CoV-2 and circulating variants. Nature **2021**; 592:616-22.
8. Doria-Rose N, Suthar MS, Makowski M, et al. Antibody Persistence through 6 Months after the Second Dose of mRNA-1273 Vaccine for Covid-19. N Engl J Med **2021**; 384:2259-61.
9. Sadoff J, Gray G, Vandebosch A, et al. Safety and Efficacy of Single-Dose Ad26.COV2.S Vaccine against Covid-19. N Engl J Med **2021**; 384:2187-201.
10. Heffron AS, McIlwain SJ, Amjadi MF, et al. The landscape of antibody binding in SARS-CoV-2 infection. PLoS Biol **2021**; 19:e3001265.
11. Lopandić Z, Protić-Rosić I, Todorović A, et al. IgM and IgG Immunoreactivity of SARS-CoV-2 Recombinant M Protein. Int J Mol Sci **2021**; 22.
12. Jörrißen P, Schütz P, Weiand M, et al. Antibody Response to SARS-CoV-2 Membrane Protein in Patients of the Acute and Convalescent Phase of COVID-19. Front Immunol **2021**; 12:679841.
13. Holmes CL, Peyton CG, Bier AM, et al. Reduced IgG titers against pertussis in rheumatoid arthritis: Evidence for a citrulline-biased immune response and medication effects. PLoS One **2019**; 14:e0217221.
14. Amjadi MF, O'Connell SE, Armbrust T, et al. Specific COVID-19 Symptoms Correlate with High Antibody Levels against SARS-CoV-2. Immunohorizons **2021**; 5:466-76.
15. Noda K, Matsuda K, Yagishita S, et al. A novel highly quantitative and reproducible assay for the detection of anti-SARS-CoV-2 IgG and IgM antibodies. Sci Rep **2021**; 11:5198.

Chapter 4: Novel and unique rheumatoid factors that cross-react with viral epitopes develop in COVID-19

Maya F. Amjadi[1], Maxwell H. Parker[1], Ryan R. Adyniec[1], Zihao Zheng[1,2], Alex Robbins[1], Michael F. Denny[1], Sara M. McCoy[1], Irene M. Ong[3,4,5], Miriam A. Shelef[1,6]

[1]Department of Medicine, University of Wisconsin-Madison, Madison, Wisconsin, USA

[2]Department of Statistics, University of Wisconsin-Madison, Madison, Wisconsin, USA

[3]Department of Biostatistics and Medical Informatics, University of Wisconsin-Madison, Madison, WI, United States of America

[4]University of Wisconsin Carbone Comprehensive Cancer Center, University of Wisconsin-Madison, Madison, WI, United States of America

[5]Department of Obstetrics and Gynecology, University of Wisconsin-Madison, Madison, WI, United States of America

[6]William S. Middleton Memorial Veterans Hospital, Madison, Wisconsin, USA

Contributions: I performed and analyzed the experiments in Supplementary Figure 1B and Figures 6C, 7, and 8, and I closely mentored a student who performed the experiments in Supplementary Figures 3 and 4. I also analyzed data and made Figures 2, 3, 5-8 and Supplementary Figures 3-5, wrote the first draft of the manuscript, and assisted in editing the manuscript.

ABSTRACT

Rheumatoid factors (RFs), polyreactive antibodies known to bind conformational epitopes of IgG Fc, are a hallmark of rheumatoid arthritis but also develop in other inflammatory conditions and infections. Recently, unique linear IgG epitopes were identified in rheumatoid arthritis, but specific IgG epitopes bound by infection-induced RFs remain undefined. Here, we identified novel IgG epitopes bound primarily by IgM in COVID-19 that were not bound in rheumatoid arthritis or other inflammatory conditions. Moreover, one RF was polyreactive, binding two IgG and several viral peptides based on a motif (G/A/R/K-D-S/T), as well as IgG Fc and SARS-CoV-2 spike proteins. In contrast, a rheumatoid arthritis IgG-RF (known to be polyreactive with thousands of rheumatoid arthritis autoantigens based on a different motif) bound IgG Fc, but not G/A/R/K-D-S/T peptides or spike. Thus, polyreactive RFs from different conditions have unique reactivities that reflect the overall antibody repertoire of their milieu. Moreover, a motif underlies COVID-19-induced RF polyreactivity, providing evidence that motifs and not protein identity may underly antigenic similarity and thus molecular mimicry. These findings provide new insights into how viral infection can contribute to partial immune tolerance loss for IgG with potential implications for rheumatoid arthritis development and millions of people post-COVID-19.

INTRODUCTION

Rheumatoid factors (RFs) are antibodies of any isotype that bind the Fc region of IgG. Initially discovered in 1939 [1], RFs are found so frequently in rheumatoid arthritis that they are used as a diagnostic marker with 60-90% sensitivity [2, 3]. However, RFs have also been identified in other inflammatory conditions, including autoimmune diseases like Sjogren's disease [4] and lupus [5] as well as in smokers [6]. Further, RFs transiently increase with vaccination and acute infection [7-9] and can persist in about half of people with chronic infections like hepatitis B or C

[10, 11]. In total, ~4% of Caucasians have RFs [2] even though RFs are considered a hallmark of rheumatoid arthritis.

Canonically, RFs bind two epitopes in the constant region of IgG: the Ga determinant (a conformational epitope comprised of loops from the CH2 and CH3 domains) [12] and a conformational epitope in the hinge (a flexible region that connects the CH1 and CH2 domains) [13]. Of note, RFs do not bind native, circulating IgG; rather IgG must be enzymatically cleaved, bind antigen, or be otherwise modified to allow RF binding [14]. Recently, citrullinated and homocitrullinated linear IgG epitopes were found to be bound by IgG in rheumatoid arthritis and not in other autoimmune diseases, while a linear native IgG epitope in the hinge region was bound in Sjogren's Disease [15, 16], suggesting that different IgG epitopes may be uniquely bound by RFs in different conditions. However, which, if any, unique IgG epitopes are bound by RFs in infection is unknown.

In addition to binding IgG, RFs are commonly polyreactive, binding a variety of self and non-self antigens [17-20]. For example, IgM-RFs (RFs of the IgM isotype) from both rheumatoid arthritis and periodontitis patients can bind both IgG and some, but not all, oral bacteria [20]. To date, the specific epitopes bound by poly-reactive RFs in infection have not been explored. However, defining infection-induced RF poly-reactivity could provide insights into how immune tolerance could be lost after an infection, an important area given the links between infections, RFs, and the development of rheumatoid arthritis [21, 22].

Unfortunately, studying infection-induced RFs in humans is challenging due to the difficulty of generating a uniform study cohort. However, in 2020, severe acute respiratory syndrome coronavirus two (SARS-CoV-2) emerged. In addition to causing the devasting coronavirus disease 2019 (COVID-19) pandemic, SARS-CoV-2 created a large cohort of individuals who

generated a primary immune response to the same virus at a similar time. Also, RFs develop in 5-20% of COVID-19 patients [23-25]. Thus, COVID-19 presents a unique opportunity to study infection-induced RFs. Moreover, since >680 million people were infected with SARS-CoV-2 [26], millions of people experienced a rheumatoid arthritis risk factor and developed RFs, adding importance to the study of RFs in COVID-19.

In this study, we evaluated antibody binding to IgG and viral epitopes to reveal novel and unique features of SARS-CoV-2-induced RF reactivity.

MATERIALS AND METHODS

Human Subjects

This study was conducted in accordance with the Declaration of Helsinki and was approved by the Institutional Review Board at the University of Wisconsin. Serum and clinical information from COVID-19 convalescent subjects (positive SARS-CoV-2 PCR test and ~5 weeks post-symptom resolution) were obtained from the University of Wisconsin (UW) COVID-19 Convalescent Biorepository [27], and serum and plasma from subjects with acute COVID-19 (hospitalized at UW Health with a positive SARS-CoV-2 test and COVID-19 symptom onset <3 weeks prior to sample collection) were obtained from the UW Carbone Cancer Center Translational Science BioCore BioBank. Serum and clinical information for subjects with rheumatologist-diagnosed rheumatoid arthritis, systemic lupus erythematosus, Sjogren's disease, and age- and sex-matched controls with no autoimmune or inflammatory disease were obtained from the UW Rheumatology Biorepository [28]. Healthy control and rheumatoid arthritis sera were collected prior to 2019 and lupus and Sjogren's disease subjects had no known positive COVID-19 tests. Rheumatoid arthritis subjects either had negative clinical testing for

anti-cyclic citrullinated peptide (CCP) and RF or had anti-CCP and RF levels greater than 2x the upper limit of normal. Lupus and Sjogren's disease subjects had a positive clinical test for RF.

High Density Peptide Array

IgA, IgM, and IgG binding to an array that contained the constant regions of the heavy chains of IgG1-4 (Uniprot P01857, P0859, P01860, P01861), tiled as 16 amino acid peptides overlapping by 15 amino acids was quantified as previously described [29]. Additionally, the array contained peptides from the following proteins tiled in an identical manner: the proteomes of 7 human coronaviruses including SARS-CoV-2, proteomes and spike proteins from other coronaviruses, and proteins from poliovirus, 7 strains of rhinovirus, and human cytomegalovirus [29]. Antibody binding data to viral peptides on this array as well as IgA, IgM, and IgG binding data from an array containing the constant regions of the heavy chains of IgG1-4 (Uniprot P01857, P0859, P01860, P01861) tiled as 12 amino acid peptides overlapping by 11 amino acids [15] were used in secondary analysis.

Enzyme Linked Immunosorbent Assay (ELISA)

For peptide ELISA, Costar 96-well high binding ELISA plates (Corning, Corning, NY) were coated with 5µg/ml streptavidin (Thermo Scientific Pierce, Waltham, MA) in phosphate buffered saline (PBS) overnight at 4°C, washed twice with PBS, and coated with either 0.1uM peptide (Supplementary Table 1) conjugated to biotin at the C terminus (Biomatik, Cambridge, Ontario, Canada or Peptide 2.0, Chantilly, VA) in PBS or PBS alone (uncoated wells) for one hour at room temperature. Plates were washed three times with wash buffer (PBS with 0.2% Tween 20), blocked with blocking solution (5% nonfat dehydrated milk in wash buffer) for at least 2.5 hours at room temperature, and then incubated with serum (diluted 1:100 in blocking solution) or purified antibodies (20ng/ml or as indicated) overnight at 4°C. Plates were then washed four

times with wash buffer, incubated for one hour at room temperature with mouse anti-human IgG, goat anti-human IgM, or goat F(ab')2 anti-human kappa and goat F(ab')2 anti-human lambda all conjugated to horse radish peroxidase (Southern Biotechnology, Birmingham, AL) diluted 1:5000 in blocking solution. Plates were washed four times with wash buffer, developed with tetramethylbenzidine substrate solution (Thermo Scientific Pierce) and the reaction was stopped using 0.18M sulfuric acid. Endpoint absorbance (450-562nm) was read on a FilterMax F3 spectrophotometer (Molecular Devices, San Jose, CA) and absorbance values from uncoated wells were subtracted from coated wells for each sample as nonspecific binding.

For protein ELISA, human IgG Fc fragment (MilliporeSigma, Burlington, MA) was depleted of contaminating light chain and IgM using streptavidin magnetic beads coated with biotinylated goat F(ab')2 anti-human kappa, goat F(ab')2 anti-human lambda, and goat F(abs')2 anti-human IgM (Southern Biotechnology). Plates (Corning) were coated with 2.5 µg/ml human Fc fragment or SARS-CoV-2 spike protein (GenScript USA, Piscataway, NJ) in PBS or with PBS alone. Plates were washed as described above and blocked overnight at 4°C. Serum or plasma (diluted 1:5000) or purified antibodies in blocking solution were added to the wells and incubated overnight at 4°C. Plates were washed as above, goat F(ab')2 anti-human kappa and lambda conjugated to horse radish peroxidase (Southern Biotechnology) at 1:5000 in blocking solution were added for one hour at room temperature. Plates were washed, developed, and absorbance was recorded as described above.

A standard curve was used for some ELISAs. After the above streptavidin and wash steps, wells were either incubated with biotinylated goat F(ab')2 anti-human kappa and lambda (Southern Biotechnology) diluted 1:5000 in PBS for one hour at room temperature followed by washing, blocking, and incubation with serially diluted human IgG (Bethyl Laboratories, Montgomery, TX) or IgM (Fitzgerald Industries, Acton, MA) overnight at 4°C or incubated with

serially diluted biotinylated human IgM and human IgG (Novus Biologicals, Englewood, CO) in PBS for one hour at room temperature. Plates were washed, incubated with detection antibody, developed and absorbance determined as above. Four parameter logistic curve was used on myassays.com to determine concentration from absorbance values.

Antibody Purification

Streptavidin sepharose beads (BioVision, San Francisco, CA or Abcam, Waltham, MA) were washed three times with tris buffered saline (TBS) (Fisher Bioreagent, Pittsburgh, PA) and then incubated with 0.05mM biotinylated peptide in TBS and tumbled at 4°C for two hours. Peptide-labeled beads were resuspended in blocking solution and loaded onto a frit membrane in a spin column (G-Biosciences, St. Louis, MO) and washed with blocking solution. Columns were stoppered, and sera diluted 1:5 in blocking solution were added. Columns were capped and stored overnight at 4°C, washed twice with blocking solution, then conditioned with conditioning buffer (Classic IP Kit, Thermo Scientific Pierce). Elution buffer (100mM glycine pH 2.6) was added and antibodies collected into neutralizing buffer (Tris HCl pH 8.7). Columns were centrifuged briefly at 8000xg and the elution step was repeated. The concentration of purified antibodies was approximated by ELISA using the above-described standard curve.

Statistical analysis

Statistical analysis was performed using Prism (Graphpad, San Diego, CA). To avoid making distributional assumptions, we used nonparametric tests. A Kruskal Wallis test with Dunn's multiple comparisons test was used to compare >2 groups and a Mann-Whitney test was used to compare 2 groups. $P<0.05$ was considered significant for both. A Wilcoxon matched-pairs signed rank test was used when two sets of data were paired, and $p=0.0625$, the lowest

possible p value for n=5, was considered significant. Motif analysis was performed with Meme Suite [30].

RESULTS

To evaluate RFs in COVID-19, first we quantified total RFs by IgG Fc ELISA. As shown in Supplementary Figure 1, 4% of our subjects acutely ill with COVID-19 and 5% of our COVID-19 convalescent subjects had higher levels of RFs than age- and sex-matched controls. We then investigated antibody binding to all possible linear native peptides along the length of the constant region of the IgG heavy chain in COVID-19 convalescent and control sera using high density peptide array. As shown in Figure 1 and Supplemental Figure 2, there were several sites of high IgG and IgM binding to the constant region of IgG, whereas IgA binding was overall low in COVID-19 convalescent sera. To determine if the regions of IgG bound by antibodies post-COVID-19 would also be bound in rheumatoid arthritis, we performed a secondary analysis of previously obtained IgA, IgM, and IgG binding data to the same region of IgG for subjects with the four serotypes of rheumatoid arthritis: a positive anti-CCP test (a marker for anti-citrullinated protein antibodies, the second hallmark autoantibody of rheumatoid arthritis), a positive RF test, neither test positive, and both tests positive) [15]. For all rheumatoid arthritis serotypes, there was similar antibody binding to the IgG peptides as controls (Figure 1 and Supplemental Figure 2).

Next, we selected peptides derived from IgG1, the most abundant IgG in humans [31], that were bound at high levels after COVID-19 to confirm by ELISA, specifically peptides starting at amino acid positions 104 (in the hinge region), 131 (in the CH2 region), and 238 and 293 (both in the CH3 region). As shown in Figure 2, the hinge region peptide 104 was bound at a similar level in COVID-19 convalescent and control subjects. However, the three peptides from the CH2 and CH3 regions showed significantly higher binding by COVID-19 convalescent compared to

control sera, with IgG1-131 and IgG1-238 highly bound by IgM and IgG1-293 moderately bound by both IgM and IgG. These results identify novel linear epitopes of IgG bound by IgM in COVID-19.

Given the common presence of RFs in other conditions, especially rheumatoid arthritis, we next evaluated antibody binding to the four IgG1 peptides in rheumatoid arthritis (anti-CCP+RF+ and anti-CCP-RF-), RF+ Sjogren's disease, RF+ lupus, and smokers. We found that in rheumatoid arthritis, antibody binding to IgG1-131, IgG1-238 and IgG1-293 was not different from controls. However, the hinge region IgG1-104 peptide had significantly higher IgG binding in anti-CCP+RF+ rheumatoid arthritis compared with controls (Figure 3). A similar pattern was seen in Sjogren's disease with elevated IgG binding to IgG1-104 and no significantly increased binding to the other IgG1 peptides, apart from a trend towards increased IgM binding to IgG1-104 (Supplementary Figure 3). In lupus and smokers, there was no increased antibody binding to any of the four IgG1 peptides (Supplementary Figures 4 and 5). Taken together, these data suggest that unique linear epitopes of IgG are bound primarily by IgM after COVID-19 that are not bound in other RF+ conditions. In contrast, the peptide at position 104 of IgG1 (hinge region) is bound prominently in Sjogren's disease and rheumatoid arthritis.

We then more fully characterized when and in which COVID-19 patients RFs develop. We tested sera from patients with acute COVID-19 by ELISA for IgM against all four IgG1 peptides and IgG against IgG1-104 and IgG1-293. We found that patients with acute COVID-19 had higher IgM binding to IgG1-131, IgG1-238 and IgG1-293 compared to controls (Figure 5A). No increased binding was seen for IgM or IgG to IgG1-104 or for IgG to IgG1-293. Also, IgM levels against IgG1-131, IgG1-238, and IgG1-293 rose significantly by 2-3 weeks post-symptom onset (Figure 5B). Finally, we found that subjects with age >60 years, male sex, and severe disease had higher IgG levels against IgG1-293 (Figure 4) with no significant difference between groups

for antibodies that bound the other IgG1 peptides. In our cohort, males were older than females (mean 49 versus 43, p = 0.045 by Mann-Whitney test) and older males were more likely to have severe or critical disease [27]. However, within the moderate severity group, which had an approximately equal distribution of sex and age, IgG anti-IgG1-293 was not different between sexes (p = 0.161, Mann-Whitney test) but was significantly higher in adults >60 years old compared to <40 years old when comparing three groups as in Figure 5A (p = 0.007, Kruskal-Wallis with Dunn's multiple comparisons test). Thus, age may be the underlying risk factor for anti-IgG1-293. Taken together, these data suggest that RFs develop soon after SARS-CoV-2 infection, persist for at least 5 weeks post-symptoms resolution, and in some cases, may be driven by older age.

Having characterized the development and unique reactivity of these IgG1-binding antibodies in COVID-19, we then evaluated cross-reactivity. First, we noticed that typically the same subjects had elevated IgM anti-IgG1-131 and anti-IgG1-238 with limited overlap with IgM anti-IgG1-293 (Figure 6A). Further, both IgG1-131 and IgG1-238 had a positively charged amino acid in position one and an aspartic acid in position two (Figure 6B). Hypothesizing that a single antibody might bind to both IgG1-131 and IgG1-238, but not IgG1-293, we purified antibodies that bound to IgG1-131 or IgG1-238 from COVID-19 convalescent sera and evaluated their binding to IgG1-131 and IgG1-238, as well as to IgG1-293, homocitrullinated (J) IgG1-219J and IgG1-289J (two peptides highly bound by IgG in rheumatoid arthritis [16]), and a SARS-CoV-2 membrane peptide that is highly bound in COVID-19 [29] that we selected as a negative control. As shown in Figure 6C, antibodies purified by binding to IgG1-131 or IgG1-238 bound to both IgG1-131 and IgG1-238, but not to any of the other peptides. We then performed similar experiments with antibodies purified from COVID-19 convalescent sera that bound to IgG1-293 and antibodies from rheumatoid arthritis sera that bound to IgG1-219J and IgG1-289J (Figure 6C). Anti-IgG1-293 did not bind to any of the IgG1 peptides apart from IgG1-293, but did bind

the SARS-CoV-2 membrane peptide, potentially due to sequence similarities (Figure 6B). The rheumatoid arthritis anti-219J and anti-289J antibodies cross-reacted to some extent with each other, as expected [16, 32], but not with any other peptide. Together, these data suggest that two cross-reactive antibodies develop in COVID-19 that bind native linear IgG1 peptides, but not the homocitrullinated IgG1 peptides bound by RFs in rheumatoid arthritis.

Next, we evaluated the cross-reactivity of the anti-IgG1-131/238 antibodies with viral peptides. The array that contained the IgG peptides also contained peptides derived from proteins and proteomes from several coronaviruses (including SARS-CoV-2) and other viruses [29]. We performed a secondary analysis of this array data to determine which peptides were bound by IgM in subjects who had high levels of IgM that bound IgG1-131 or IgG1-238. We divided the COVID-convalescent subjects into two groups: subjects with high IgM binding to IgG1-131 or IgG1-238 (>1 standard deviation above mean IgM binding to all IgG1-derived peptides) and subjects with low binding (<1 standard deviation above the mean). We then evaluated which peptides were bound >5x more by IgM in the high binding group (n=10) as compared to the low binding group (n=30). We excluded peptides with increased binding by IgG (>1.5 fold) to reduce the possibility of detecting IgM-RFs bound to IgG bound to viral peptides. We found that COVID-19 convalescent sera with high levels of IgM that bound IgG1-131 or IgG1-238 also had IgM that bound 18 peptides from 15 proteins from 11 viruses, including 2 peptides in the SARS-CoV-2 spike protein >5x greater than the low binding group (Supplemental Table 2, locFDR<0.1). Moreover, these 18 peptides had a strong motif with an aspartic acid (D) at position 2 in every peptide (Figure 7A). Notably, despite the uniform presence of aspartic acid in position 2, not all array peptides with this “second D” are highly bound by COVID convalescent sera with high levels of IgM anti-IgG1-131 or IgG1-238, but second D motif peptides are bound more overall (Supplemental Figure 6).

Given the binding of multiple peptides with a similar motif by subjects with IgM anti-IgG1-131/238, we evaluated cross-reactivity with three virus-derived peptides with the second D motif. We purified antibodies that bound IgG1-131 and IgG1-238 from COVID-19 convalescent sera and evaluated binding to SARS-CoV-2 open reading frame 1ab (ORF1ab)-32, SARS-CoV-2 spike-570, and genome polyprotein of poliovirus 1 (polio)-112 (all with the second D motif) or two SARS-CoV-2 peptides previously found to be highly bound by antibodies in COVID-19 without the motif (nucleocapsid-390 and spike-1253) [29]. We found that antibodies that bound IgG1-131 and IgG1-238 also bound the three second D motif viral peptides and not the viral peptides without the motif (Figure 7B). This cross-reactivity was limited to anti-IgG1-131/238, since antibodies purified based on binding to IgG1-293, IgG1-219J, and IgG1-289J (peptides that do not contain the second D motif) generally did not bind any viral peptides (Figure 7B).

Next, we evaluated if anti-IgG1-131 is a RF, i.e. able to bind IgG Fc protein. As shown in Figure 8A, with increasing concentration of anti-IgG1-131 purified from five COVID-19 convalescent subjects, increased binding to IgG Fc was detected. Further, anti-IgG1-131 purified from each subject bound IgG Fc more than a negative control peptide, although, binding was variable with an average of only 13% of the level of binding to the IgG1-131 peptide used to purify the antibody (Figure 8B). To compare with an antibody that binds a linear IgG1 epitope in rheumatoid arthritis, we purified anti-IgG1-219J from five rheumatoid arthritis subjects. As expected, with increasing concentration of purified anti-IgG1-219J, increased binding to IgG Fc was detected, and anti-IgG1-219J bound IgG Fc more than the negative control peptide (Figure 8A and 8B). However, at the same concentration, anti-IgG1-219J bound IgG Fc more consistently, on average at 51% of the level of binding to IgG1-219J peptide (Figure 8B).

Given the low RF activity of some anti-IgG1-131 antibodies (Figure 8A) and their polyreactivity, including with the spike-570 peptide (Figure 7A), this antibody may have been generated in a

poly-reactive response to SARS-CoV-2 spike, whereas a rheumatoid arthritis RF that was generated prior to the emergence of COVID-19, would not have formed in this manner. To evaluate this possibility further, we determined the comparative abilities of antibodies purified based on binding to spike-570, IgG1-131, IgG1-219J, and mem-8 to bind SARS-CoV-2 spike protein and IgG Fc. As expected, anti-mem-8 had minimal binding to either protein (Figure 8C). Anti-spike-570 and anti-IgG1-131 generally clustered together, as expected given their cross-reactivity, with all ten antibodies binding spike protein more than IgG Fc (Figures 8C and 8D). However, antibodies purified based on binding to IgG1-131 bound spike and IgG Fc relatively similarly, whereas antibodies purified based on binding to spike-570 had more distinctly increased binding to spike than IgG Fc (Figure 8D). In contrast, all five rheumatoid arthritis anti-IgG1-219J antibodies bound IgG Fc more than spike (Figures 8C and 8D). Taken together, the data in Figure 8 suggest that COVID-19 induces poly-reactive antibodies that are both RFs and anti-SARS-CoV-2 spike protein antibodies, whereas rheumatoid arthritis antibodies that bind linear IgG epitopes have relatively high RF activity and minimal binding to spike protein.

DISCUSSION

In this manuscript, we report that SARS-CoV-2 induces unique cross-reactive RFs that bind novel IgG epitopes and multiple viral antigens. While RFs are known to develop in SARS-CoV-2 and other infections [11, 24, 25], specific IgG epitopes have not been evaluated. Here, we identified three linear epitopes in the CH2 and CH3 regions of IgG1 bound post-COVID-19 (Figures 1 and 2). IgG1-131 and IgG1-238 appear to be novel IgG epitopes for RFs, with both of these epitopes bound by the same antibody that can also bind IgG Fc at a relatively low level, consistent with polyreactive IgM-RFs in a variety of conditions [18, 33]. Part of IgG1-293 was identified in an array of seven amino acid linear epitopes derived from the CH2 and CH3 regions of IgG bound by rheumatoid arthritis IgM-RFs [34, 35]. Interestingly, the seven amino acids

identified as bound by rheumatoid arthritis RFs, WQQGNV, were not the amino acids similar to the SARS-CoV-2 membrane peptide (Figure 6B). We did not detect binding to IgG1-293 in rheumatoid arthritis, perhaps due to differences in conformation of their seven amino acid peptide [36] versus our longer peptide. Indeed, we did not detect binding of any of the three COVID-19-related linear IgG epitopes in rheumatoid arthritis, Sjogren's disease, lupus, or smokers (Figure 3, Supplemental Figures 3-5), suggesting that they are unique to COVID-19. In contrast, IgG-RFs in anti-CCP+RF+ rheumatoid arthritis uniquely bind linear citrullinated and homocitrullinated IgG epitopes [15, 16]. Also, rheumatoid arthritis and Sjogren's disease IgG bound IgG1-104 (Figure 3 and Supplemental Figure 3), consistent with binding by Sjogren's disease IgG to an overlapping hinge peptide (IgG1-109) [16]. However, in that study, rheumatoid arthritis IgG did not have increased binding to IgG1-109 [16], a discrepancy likely due to the slightly different peptide and increased sample size in the current study. Together, these findings support the idea that RFs with different reactivities can develop in different conditions, a phenomenon that could be leveraged to generate more specific clinical RF assays.

Of the COVID-19 RFs that we identified, anti-IgG1-131/238 is polyreactive, and anti-IgG1-293 is at least cross-reactive. RF polyreactivity is well-known [17-20] and is attributed generally to antigenic similarity [20] with specific epitopes undefined. Here, we identified specific peptides as well as a short motif underlying polyreactive RFs post-COVID-19. Polyreactivity driven by a motif also was shown for a subset of pathogenic anti-DNA antibodies in lupus (D/E-W-D/E-Y-S/G) [37, 38] and for some anti-citrullinated protein antibodies in rheumatoid arthritis (citrulline-glycine, citrulline-serine, or homocitrulline-glycine pairs) [15, 32]. Motif-containing peptides bound by IgM post-COVID-19 were derived from SARS-CoV-2 as well as viruses that our subjects were extremely unlikely to have been exposed to, like MERS-CoV, suggesting that the motif, and not protein identity underlies reactivity. Polyreactivity due to motifs, seemingly independent of protein identity, is a substantial departure from how antigenic similarity, as well

as molecular mimicry, typically refers to a small number of similar proteins [39]. For example, peptides from both myelin basic protein and a hepatitis B protein that contain YGSLPQ can drive encephalitis, leading to the conclusion of molecular mimicry between these two proteins [40]. However, a correlation between hepatitis B and multiple sclerosis has not been observed, and YGSLPQ is present in thousands of proteins in fish, birds, reptiles, insects, worms, plants, fungi, bacteria, viruses, and mammals. Thus, a polyreactive antibody that binds those two antigens due to the motif seems more likely than hepatitis B driving multiple sclerosis due to molecular mimicry between two proteins. Our finding of a motif-driven polyreactive RF post-COVID-19 adds to a growing body of evidence that polyreactivity due to motifs may drive autoreactivity more than protein identity.

The development of post-COVID-19 RFs is likely due to a polyreactive antibody response to SARS-CoV-2. Consistent with this idea, anti-IgG1-131 binds spike protein more than IgG Fc (Figure 8), and the post-COVID-19 RFs in general have similar kinetics and demographics (Figures 4 and 5) as other anti-SARS-CoV-2 antibodies [27, 41]. Polyreactive antibodies are common in infection, both in the early IgM response and the later IgG response [42-44]. For example, broadly neutralizing antibodies, i.e., antibodies that neutralize similar strains of the same virus, can be polyreactive [42, 43]. However, the cost of polyreactivity is self-reactivity, and an inability for some people to generate broadly neutralizing antibodies against some viruses may be due to peripheral tolerance mechanisms [42-44]. Tolerance in the T cell compartment likely explains the absence of IgG-RFs that bind IgG1-131/238 post-COVID-19, even at 5 weeks post-symptom resolution. In contrast, the unique RFs in rheumatoid arthritis are IgG-RFs. Consistent with this observation, T cell tolerance for IgG has previously been shown to be intact in health and lost in rheumatoid arthritis [45, 46].

Like the different IgG epitopes bound by RFs in different conditions, their polyreactivity also differs. Rheumatoid arthritis RFs that bind IgG1-219J do not bind spike protein well (Figure 8) but do bind thousands of citrullinated and homocitrullinated antigens, the same antigens that are bound by the second hallmark autoantibody in rheumatoid arthritis, namely anti-citrullinated protein antibodies [16, 32, 47]. Similarly, neither IgM nor IgG from subjects with lupus, Sjogren's disease, or rheumatoid arthritis bind the second D containing IgG1-131 or IgG1-238 peptides, despite extensive polyreactivity in their B cell compartments [32, 48, 49]. This observation is particularly interesting given the negative charge of the second D motif, DNA, and the D/E-W-D/E-Y-S/G motif noted above for some anti-DNA antibodies in lupus. Perhaps the polyreactive antibodies against second D peptides that are present in ~40% of COVID-19 patients (Figure 2) might not only contribute to the development of RFs, but also anti-nuclear antibodies, which have been reported in ~30% of COVID-19 patients [25, 50, 51]. Consistent with this possibility, cross-reactivity of RFs with DNA has been reported [18, 52] and DNA can drive RF+ B cell expansion via TLR signaling [53], which perhaps occurred for the COVID-19 IgM-RFs given the likely absence of T cell help. Also, similar to the different RFs in RA versus COVID-19, anti-nuclear antibodies in COVID-19 are different from those in lupus and Sjogren's disease given the lack of reactivity against extractable nuclear antigens in COVID-19 [50]. Taken together, these observations suggest that the polyreactivity of RFs (and possibly anti-nuclear antibodies) in different conditions reflects the broader immune responses of those conditions, an observation that perhaps could be utilized to reveal causative antigens in autoimmune disease.

There are several caveats to our study. First, the peptide array contained only linear native epitopes derived from viruses and human IgG heavy chain. We did not evaluate conformational, post-translationally modified, or human non-IgG epitopes. Also, since very few COVID-19 subjects generated high levels of anti-IgG1-293, we were limited in further evaluation of this antibody's cross-reactivity. Finally, the only infectious disease we evaluated was COVID-19, so

it remains unknown if the RFs that we identified are unique to SARS-CoV-2 or are elicited by other pathogens. However, in evaluating RFs that develop in response to other pathogens, to truly compare with SARS-CoV-2, a cohort of adults developing a primary immune response would be needed. In support of this idea, four times as many COVID-19 patients develop anti-nuclear antibodies compared to other causes of fever and/or pneumonia [50], but whether this difference is due to a unique property of SARS-CoV-2 versus an increased production of polyreactive B cells in a primary immune response is not known. Thus, future studies are needed to evaluate additional self antigens bound by antibodies that bind the second D motif, additional motifs such as what may underlie anti-IgG1-293 reactivity, and RF epitopes in other primary and secondary immune responses to infections.

Despite these limitations, we present novel, unique, cross-reactive RFs in COVID-19. The implications of these RFs are unknown. They may be simply the side effects of polyreactive antiviral antibodies with little functional impact. However, RFs are often polyreactive, and previously have been shown to bind virus-antibody immune complexes to enhance neutralization by complement and uptake by macrophages [54, 55], suggesting a possible beneficial role. Alternatively, RFs that develop in COVID-19 could be harmful. Infections not only induce RFs but are also risk factors for rheumatoid arthritis [8, 9, 21, 22]. RFs typically appear several years prior to arthralgias and ultimately rheumatoid arthritis [56], during a pre-clinical period. Interestingly, in this period, anti-Epstein-Barr virus (EBV) antibodies are sometimes elevated in association with increased IgM-RF [57]. Perhaps this correlation is due to a polyreactive anti-EBV response that generates IgM-RFs, similar to what we observed in COVID-19. However, anti-CCP also correlated with anti-EBV [57], and only 2 of our 120 COVID-19 convalescent subjects had anti-CCP (data not shown). Thus, consistent with the absence of reports of a dramatic rise in rheumatoid arthritis cases post-COVID-19, COVID-19 is not likely to induce imminent rheumatoid arthritis in the majority of people. Also consistent with this idea,

promiscuous autoantibodies in COVID-19 have shown limited functional activity [58]. However, loss of tolerance for IgG could be a first step in immune tolerance loss [59] with epitope spreading and/or changes in polyreactivity leading to the development of increased and more pathogenic autoantibodies, a typical chronology for autoimmune disease [33]. Also, for individuals who already have anti-CCP, SARS-CoV-2 could trigger further progression. Indeed, arthralgia, autoantibodies, and elevated cytokines [23, 60, 61] have been reported in long COVID, raising the possibility that a subset of this condition could be late pre-clinical rheumatoid arthritis. Further studies are needed to evaluate both the antiviral properties of post-COVID-19 RFs as well as the development of rheumatoid arthritis-related antibodies in long COVID and over time post-COVID-19. Such studies may reveal important antiviral roles for RFs as well as how immune tolerance is maintained or lost post-COVID-19.

ACKNOWLEDGEMENTS

The author(s) thank the human subjects who participated as well as the University of Wisconsin Carbone Cancer Center BioBank, supported by P30 CA014520, for use of its facilities and services.

FUNDING

Funding for this work was provided by the U.S. Army Medical Research Acquisition Activity through the Peer Reviewed Medical Research Program [W81XWH-18-1-0717] and the UW School of Medicine and Public Health from the Wisconsin Partnership Program [5084] to M.A.S.. Additional support was provided by the National Institutes of Health's National Institute on Aging [T32 AG000213] and MSTP funding [T32 GM140935] to M.F.A.

FIGURE LEGENDS

Figure 1. COVID-19 convalescent, but not rheumatoid arthritis, serum IgM and IgG bind to linear native IgG1-derived peptides. Serum IgA, IgM and IgG binding to linear native peptides from the constant region of the heavy chain of IgG1 were quantified for subjects 5 weeks post-COVID-19 (n=40) and matched controls (n=20) as well as rheumatoid arthritis (RA, n=12 anti-CCP+RF+, anti-CCP+RF- anti-CCP-RF+, and anti-CCP-RF-) and matched controls (n=12) by high density peptide array and reported as fold change.

Figure 2. IgG1 epitopes bound by COVID-19 convalescent sera. COVID-19 convalescent sera (5 weeks post-COVID-19, n=120) and sera from matched controls (n=54) were assayed by ELISA to determine IgM or IgG binding (reported in absorbance (abs)) to four IgG1-derived peptides starting at amino acid positions 104, 131, 238 and 293. Dots indicate individual serum samples, lines indicate medians, and ***p<0.001, ****p<0.0001. A Mann-Whitney test was used to compare groups.

Figure 3. Only the hinge region peptide is bound by rheumatoid arthritis sera. Sera from 32 anti-CCP+RF+ rheumatoid arthritis (RA+), 24 anti-CCP-RF- rheumatoid arthritis (RA-), and 20 matched controls were tested by ELISA for IgM or IgG binding to IgG1-derived peptides starting at amino acid positions 104, 131, 238, and 293. Dots indicate individual serum samples, lines indicate medians, and **p<0.01. Absorbance (abs) values were compared using a Kruskal Wallis test with Dunn's multiple comparisons test.

Figure 4. IgM that binds linear epitopes of IgG1 rise in acute COVID-19. IgM that binds IgG1-104, IgG1-131, IgG1-238, and IgG1-293 and IgG that binds IgG1-104 and IgG1-293 were quantified by ELISA for serum or plasma from individuals with acute COVID-19 and controls. A. COVID-19 (n=51) versus controls (n=51) were compared by Mann-Whitney test. B. Controls

(n=51) were compared to COVID-19 (57 samples from 51 subjects), one (n=19), two (n=23), and three (n=15) weeks post-symptom onset by Kruskal-Wallis with Dunn's multiple comparisons test. For all panels: dots indicate individual serum samples, bars indicate medians, *p<0.05, **p<0.01, ***p<0.001, ****p<0.0001.

Figure 5. Higher anti-IgG1-293 levels in older, male subjects with more severe disease. Sub-analyses of absorbance (abs) values for COVID-19 convalescent subjects by age (<40 years n=47, 40-60 years n=47, >60 years n=26), sex (females n=68, males n=52) and disease severity (mild n=12, moderate n=85, severe n=14, critical n=8) were assessed by Kruskal-Wallis test with Dunn's multiple comparisons test (A and C) or Mann-Whitney test (B). Dots represent individual subjects, lines indicate medians, and *p<0.05, **p<0.01.

Figure 6. Cross-reactivity among antibodies that bind IgG1 epitopes. A. Binding of IgM to IgG1-131, IgG1-238, and IgG1-293 that was quantified by ELISA for 120 COVID-19 convalescent subjects was plotted to compare binding for each peptide for each subject. B. Comparison of peptide sequences (orange: same amino acid, same position; green: related amino acid, same position; blue: homocitrulline; gray: neighboring serine or glycine). C. Purified antibodies that bound to IgG1-131, IgG1-238, IgG1-293, IgG1-219J, and IgG1-289J were evaluated by ELISA for binding to IgG1-131, IgG1-238, IgG1-293, IgG1-219J, IgG1-289J, and a SARS-CoV-2 membrane (mem) peptide (binding level of indicated purified antibody on y axis, antigen on X axis). Groups were compared to the first column in each graph by Kruskal-Wallis with Dunn's multiple comparisons test. Dots represent individual experiments using 5 unique subjects, boxes indicate mean +/- SEM, and *p<0.05, **p<0.01.

Figure 7. Cross-reactive binding of antibodies to IgG1 and viral peptides. A. Motif for 18 peptides bound at a high level by IgM from COVID-19 convalescent serum that also had high

levels of IgM that bound IgG1-131 or IgG1-238. B. Antibodies that bound to IgG1-131 or IgG1-238 (B) or IgG1-293, IgG1-219J, or IgG1-289J (C) were purified and evaluated by ELISA for binding to the IgG1 peptide (striped column) or viral peptides with the second D motif (SARS-CoV-2 orf1ab-32, SARS-CoV-2 spike-570, poliovirus 1 genome polyprotein-112) and without the motif (SARS-CoV-2 nucleocapsid (nucl)-390 and spike-1253). The binding level of the indicated purified antibody is on the y axis and the antigens are on X axis. Groups were compared to the first column in each graph by Kruskal-Wallis with Dunn's multiple comparisons test. Dots represent individual experiments with individual subjects (n=5), boxes indicate mean +/- SEM and *p<0.05, **p<0.01 and ***p<0.001.

Figure 8. Cross-reactive antibodies in COVID-19 bind both IgG Fc and spike protein. A. Increasing concentrations of anti-IgG1-131 purified from 5 COVID-19 convalescent subjects or anti-219J purified from 5 rheumatoid arthritis subjects were used to assess binding to the peptide against which the antibody was purified, IgG Fc, or a negative control peptide (spike-1253, based on Figure 7) by ELISA. Symbols represent mean +/- SEM. B. For the 333ng concentration of the purified antibodies, binding to the negative control peptide and IgG Fc were divided by binding to the peptide used to purify the antibody with percent binding compared by Wilcoxon matched-pairs signed rank test. Each symbol represents a different subject and #p=0.0625. C and D. Antibodies were purified based on binding to spike-570, IgG1-131, IgG1-219J, and mem-8 (n=5). Binding of each purified antibody (250ng) to SARS-CoV-2 spike protein and IgG Fc was determined by ELISA. C. Results are displayed in a scatter plot. D. Binding to spike versus IgG Fc was compared by Wilcoxon matched-pairs signed rank test (#p=0.0625).

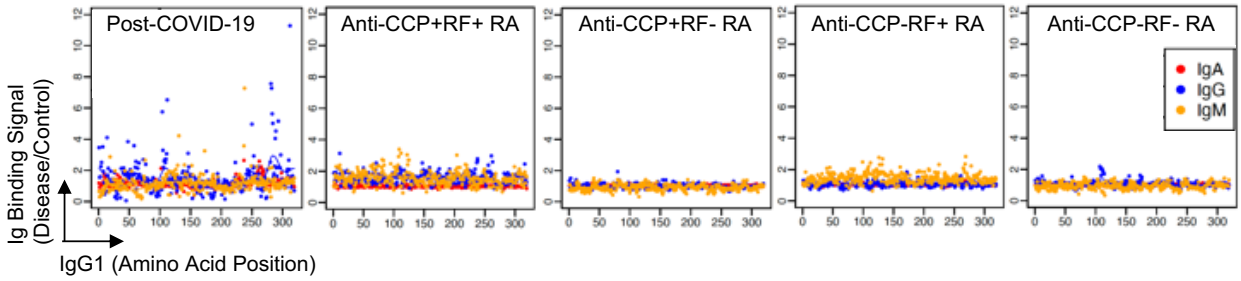

Figure 1. COVID-19 convalescent, but not rheumatoid arthritis, serum IgM and IgG bind to linear native IgG1-derived peptides. Serum IgA, IgM and IgG binding to linear native peptides from the constant region of the heavy chain of IgG1 were quantified for subjects 5 weeks post-COVID-19 (n=40) and matched controls (n=20) as well as rheumatoid arthritis (RA, n=12 anti-CCP+RF+, anti-CCP+RF- anti-CCP-RF+, and anti-CCP-RF-) and matched controls (n=12) by high density peptide array and reported as fold change.

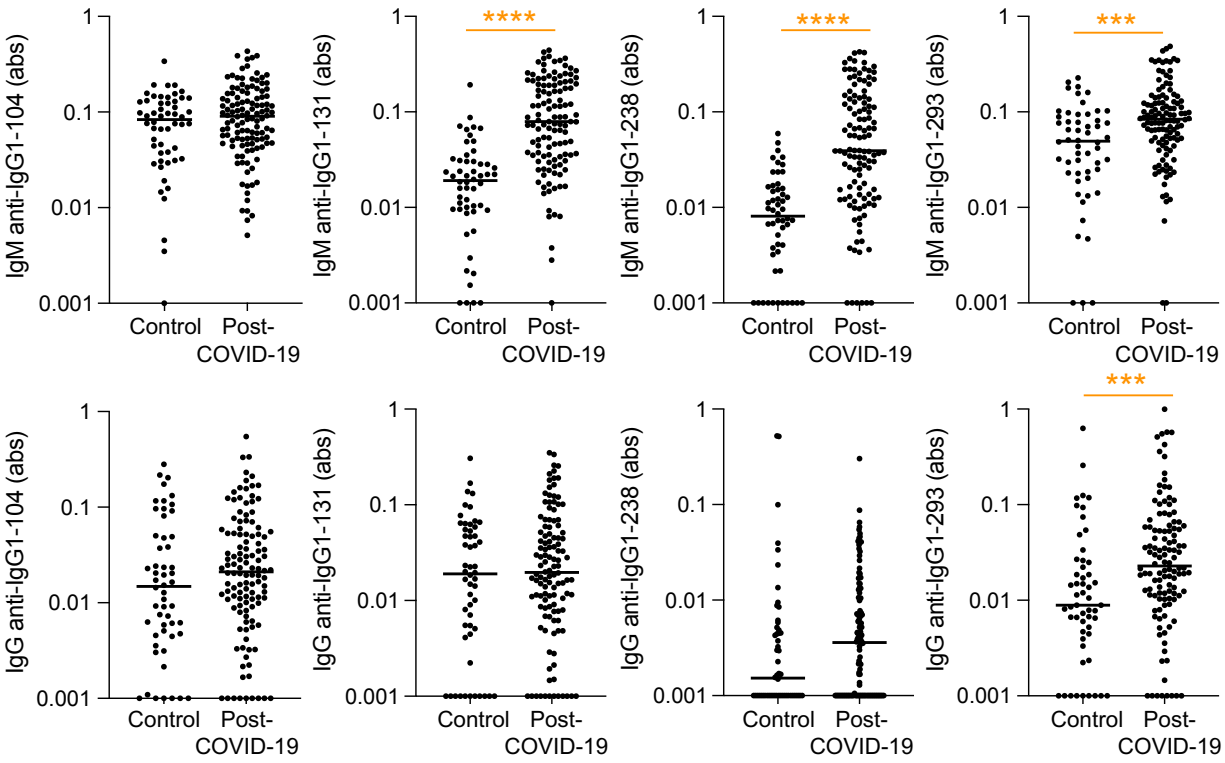

Figure 2. IgG1 epitopes bound by COVID-19 convalescent sera. COVID-19 convalescent sera (5 weeks post-COVID-19, n=120) and sera from matched controls (n=54) were assayed by ELISA to determine IgM or IgG binding (reported in absorbance (abs)) to four IgG1-derived peptides starting at amino acid positions 104, 131, 238 and 293. Dots indicate individual serum samples, lines indicate medians, and ***p<0.001, ****p<0.0001. A Mann-Whitney test was used to compare groups.

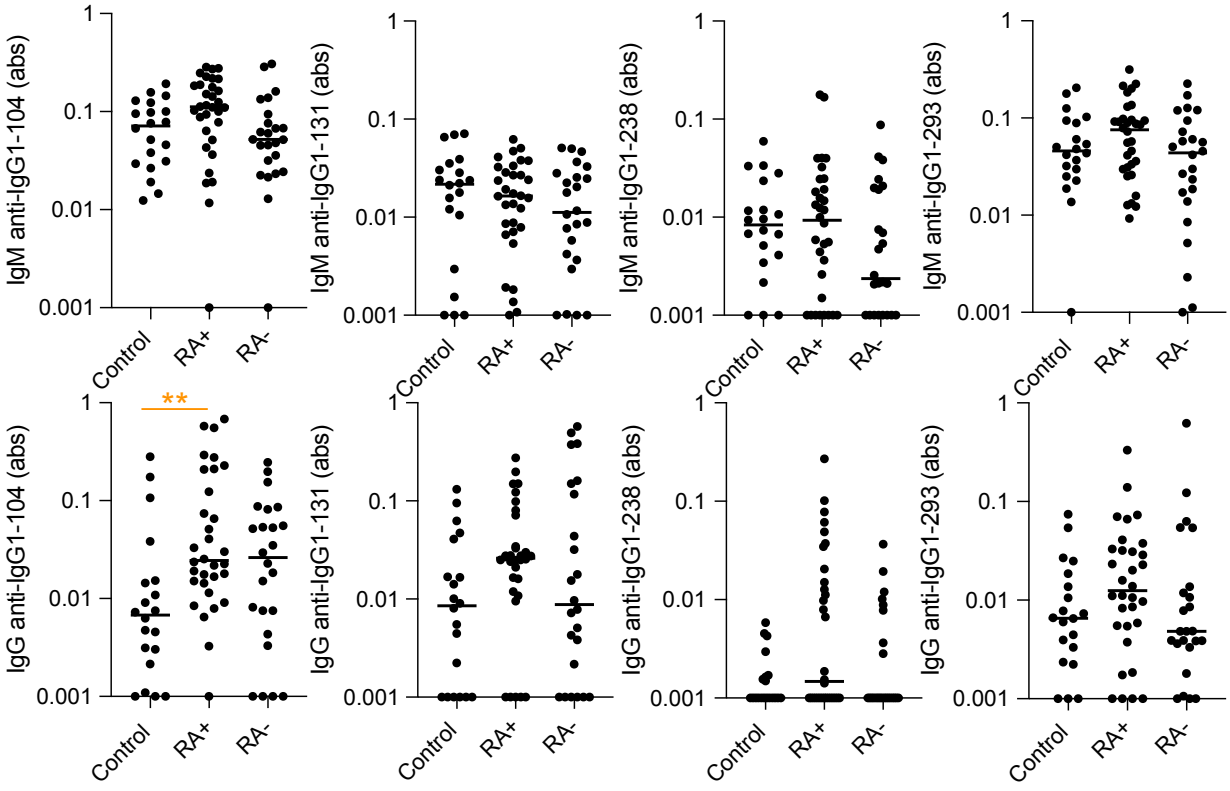

Figure 3. Only the hinge region peptide is bound by rheumatoid arthritis sera. Sera from 32 anti-CCP+RF+ rheumatoid arthritis (RA+), 24 anti-CCP-RF- rheumatoid arthritis (RA-), and 20 matched controls were tested by ELISA for IgM or IgG binding to IgG1-derived peptides starting at amino acid positions 104, 131, 238, and 293. Dots indicate individual serum samples, lines indicate medians, and **p<0.01. Absorbance (abs) values were compared using a Kruskal Wallis test with Dunn's multiple comparisons test.

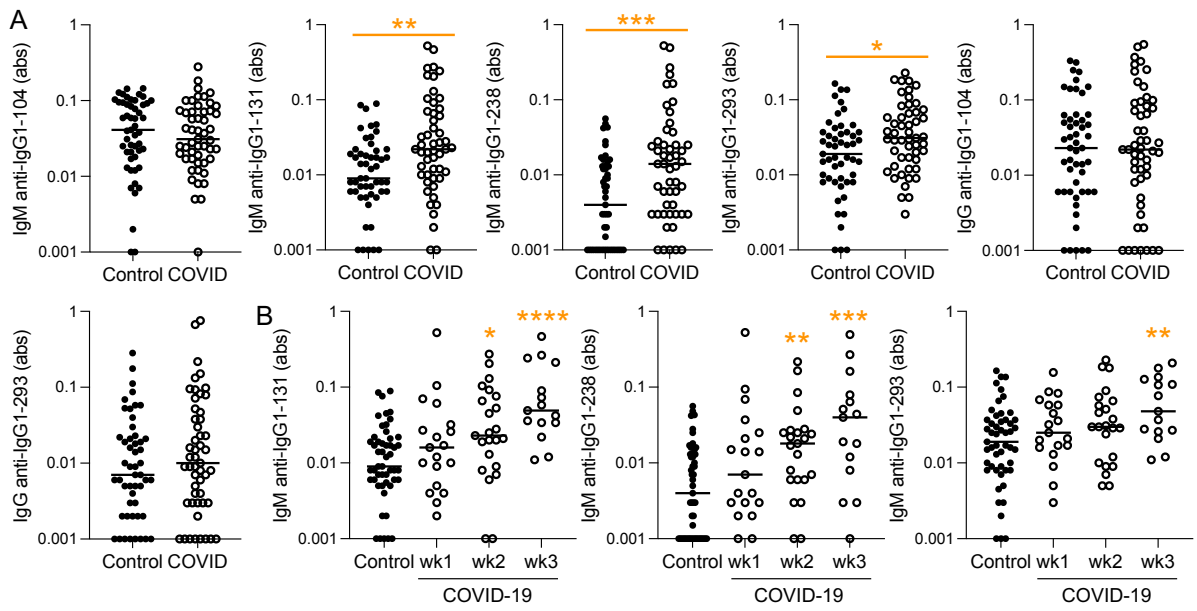

Figure 4. IgM that binds linear epitopes of IgG1 rise in acute COVID-19. IgM that binds IgG1-104, IgG1-131, IgG1-238, and IgG1-293 and IgG that binds IgG1-104 and IgG1-293 were quantified by ELISA for serum or plasma from individuals with acute COVID-19 and controls. A. COVID-19 (n=51) versus controls (n=51) were compared by Mann-Whitney test. B. Controls (n=51) were compared to COVID-19 (57 samples from 51 subjects), one (n=19), two (n=23), and three (n=15) weeks post-symptom onset by Kruskal-Wallis with Dunn's multiple comparisons test. For all panels: dots indicate individual serum samples, bars indicate medians, *p<0.05, **p<0.01, ***p<0.001, ****p<0.0001.

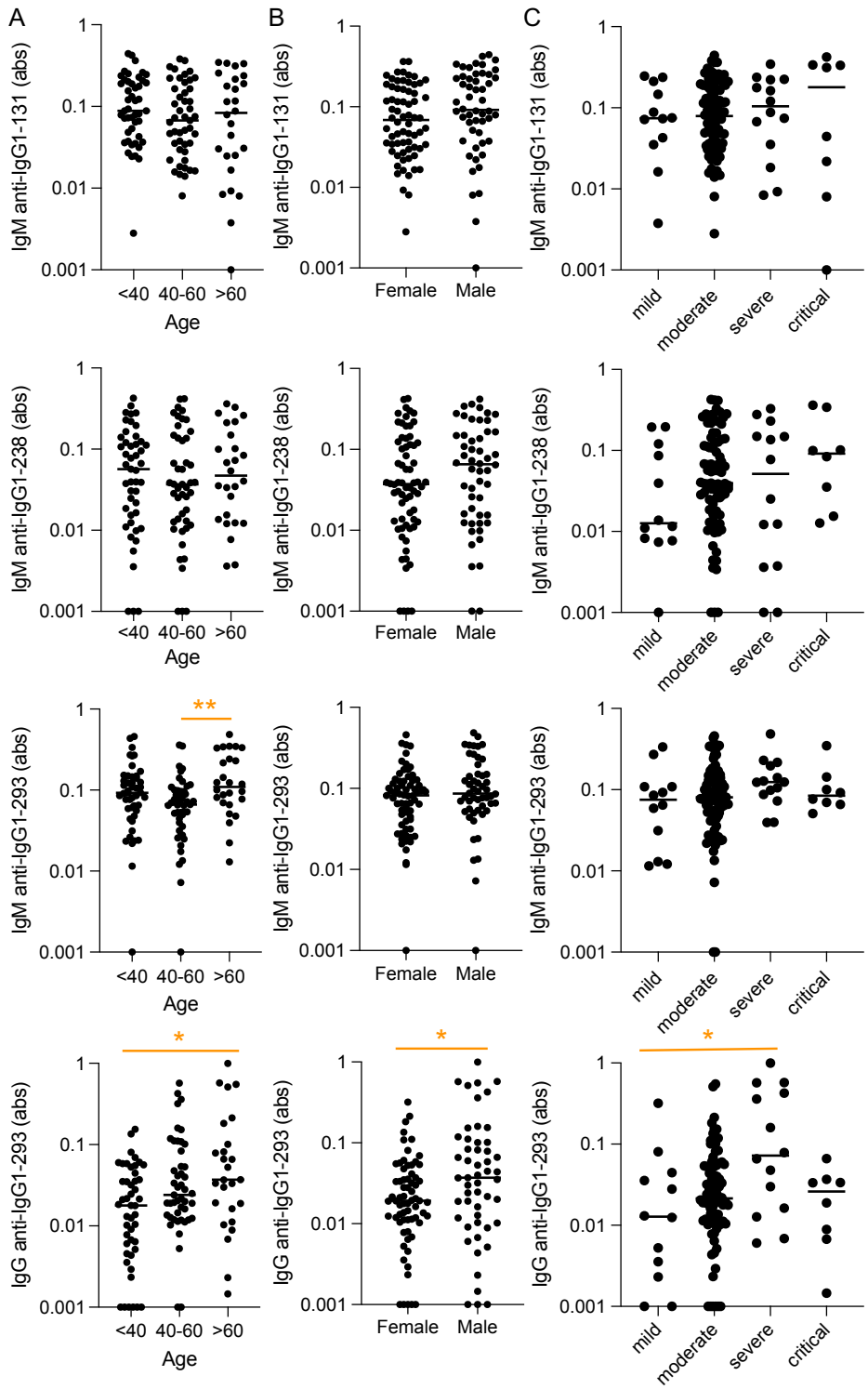

Figure 5. Higher anti-IgG1-293 levels in older, male subjects with more severe disease. Sub-analyses of absorbance (abs) values for COVID-19 convalescent subjects by age (<40 years n=47, 40-60 years n=47, >60 years n=26), sex (females n=68, males n=52) and disease severity (mild n=12, moderate n=85, severe n=14, critical n=8) were assessed by Kruskal-Wallis test with Dunn's multiple comparisons test (A and C) or Mann-Whitney test (B). Dots represent individual subjects, lines indicate medians, and *p<0.05, **p<0.01.

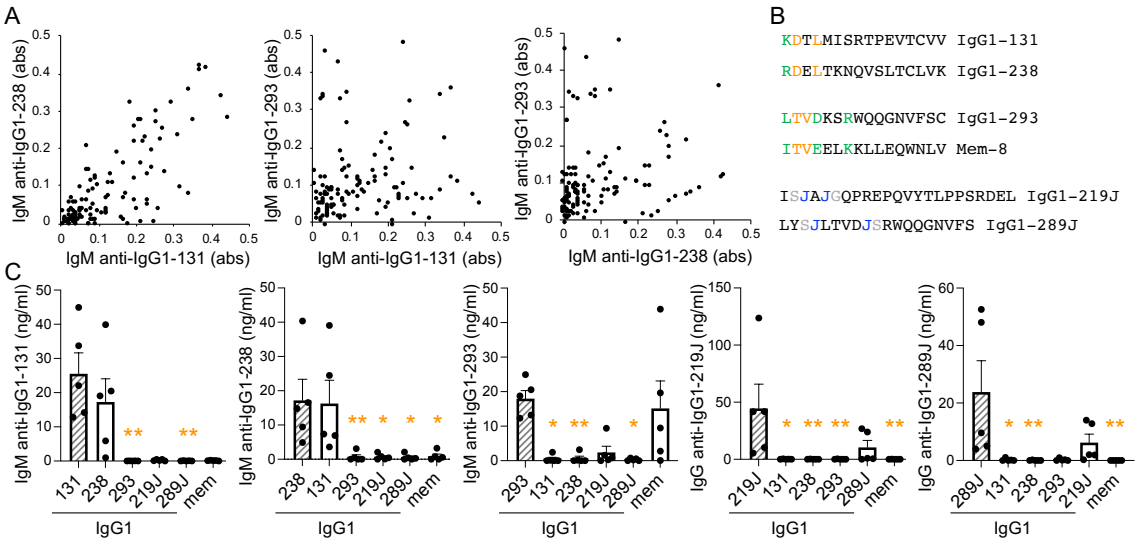

Figure 6. Cross-reactivity among antibodies that bind IgG1 epitopes. A. Binding of IgM to IgG1-131, IgG1-238, and IgG1-293 that was quantified by ELISA for 120 COVID-19 convalescent subjects was plotted to compare binding for each peptide for each subject. B. Comparison of peptide sequences (orange: same amino acid, same position; green: related amino acid, same position; blue: homocitrulline; gray: neighboring serine or glycine). C. Purified antibodies that bound to IgG1-131, IgG1-238, IgG1-293, IgG1-219J, and IgG1-289J were evaluated by ELISA for binding to IgG1-131, IgG1-238, IgG1-293, IgG1-219J, IgG1-289J, and a SARS-CoV-2 membrane (mem) peptide (binding level of indicated purified antibody on y axis, antigen on X axis). Groups were compared to the first column in each graph by Kruskal-Wallis with Dunn's multiple comparisons test. Dots represent individual experiments using 5 unique subjects, boxes indicate mean +/- SEM, and *p<0.05, **p<0.01.

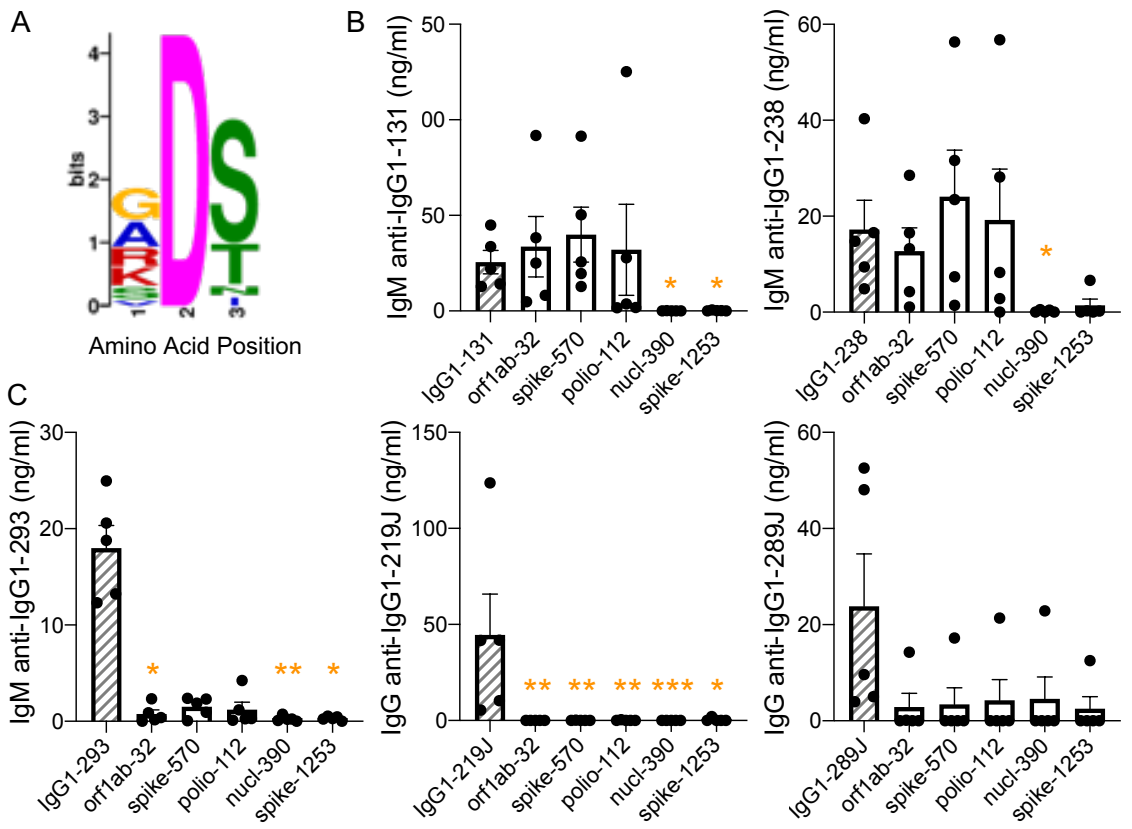

Figure 7. Cross-reactive binding of antibodies to IgG1 and viral peptides. A. Motif for 18 peptides bound at a high level by IgM from COVID-19 convalescent serum that also had high levels of IgM that bound IgG1-131 or IgG1-238. B. Antibodies that bound to IgG1-131 or IgG1-238 (B) or IgG1-293, IgG1-219J, or IgG1-289J (C) were purified and evaluated by ELISA for binding to the IgG1 peptide (striped column) or viral peptides with the second D motif (SARS-CoV-2 orf1ab-32, SARS-CoV-2 spike-570, poliovirus 1 genome polyprotein-112) and without the motif (SARS-CoV-2 nucleocapsid (nucl)-390 and spike-1253). The binding level of the indicated purified antibody is on the y axis and the antigens are on X axis. Groups were compared to the first column in each graph by Kruskal-Wallis with Dunn's multiple comparisons test. Dots represent individual experiments with individual subjects (n=5), boxes indicate mean +/- SEM and *p<0.05, **p<0.01 and ***p<0.001.

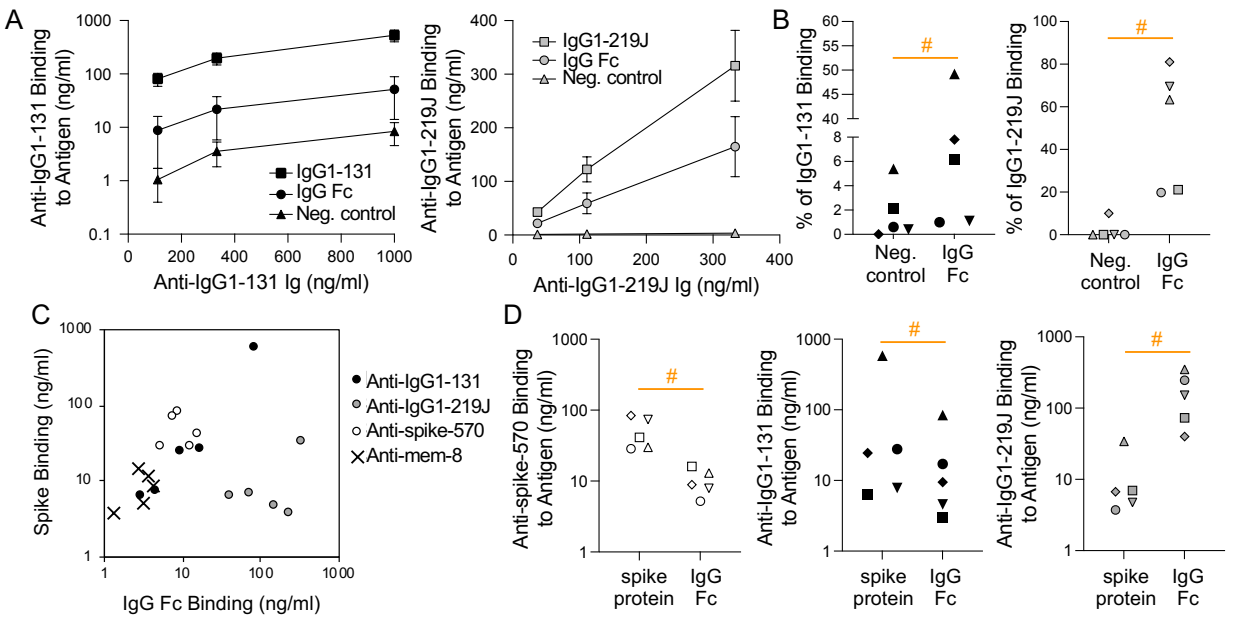

Figure 8. Cross-reactive antibodies in COVID-19 bind both IgG Fc and spike protein. A. Increasing concentrations of anti-IgG1-131 purified from 5 COVID-19 convalescent subjects or anti-219J purified from 5 rheumatoid arthritis subjects were used to assess binding to the peptide against which the antibody was purified, IgG Fc, or a negative control peptide (spike-1253, based on Figure 7) by ELISA. Symbols represent mean +/- SEM. B. For the 333ng concentration of the purified antibodies, binding to the negative control peptide and IgG Fc were divided by binding to the peptide used to purify the antibody with percent binding compared by Wilcoxon matched-pairs signed rank test. Each symbol represents a different subject and #p=0.0625. C and D. Antibodies were purified based on binding to spike-570, IgG1-131, IgG1-219J, and mem-8 (n=5). Binding of each purified antibody (250ng) to SARS-CoV-2 spike protein and IgG Fc was determined by ELISA. C. Results are displayed in a scatter plot. D. Binding to spike versus IgG Fc was compared by Wilcoxon matched-pairs signed rank test (#p=0.0625).

Supplemental Table 1. Peptide Sequences

Protein-starting amino acid	Species	Uniprot Number	Sequence
IgG1-104 *	Human	P01857	DKTHTCPPCPAPELLG
IgG1-131	Human	P01857	KDTLMISRTPEVTCVV
IgG1-238	Human	P01857	RDELTKNQVSLTCLVK
IgG1-293	Human	P01857	LTVDKSRWQQGNVFSC
IgG1-219J **	Human	P01857	ISJAJGQPREPQVYTLPPSRDEL
IgG1-289J	Human	P01857	LYSJLTVDJSRWQQGNVFS
Genome polyprot-112	Poliovirus 1	P03300	RDSEANPVDQPTEPDV
Membrane-8	SARS-CoV-2	P0DTC5	ITVEELKKLLEQWNLV
Nucleocapsid-390	SARS-CoV-2	P0DTC9	QTVTLLPAADLDDFSK
ORF1ab-32 ***	SARS-CoV-2	A0A6V7ALW7	GDSVEEVLSEARQHLK
Spike-570	SARS-CoV-2	P0DTC2	ADTTDAVRDPQTLEIL
Spike-1253	SARS-CoV-2	P0DTC2	CCKFDEDDSEPVLKGV

* IgG1: constant region of the heavy chain of IgG1
** J: homocitrulline
*** ORF: open reading frame

Supplemental Table 2. Peptides Bound by IgM in COVID-19 Convalescent Serum that also has high levels of IgM anti-IgG1-131 and IgG1-238.

Protein	First amino acid	Species	Uniprot Number	Sequence
Genome polyprot.	1159	Rhinovirus A1	A0A2H4UK13	ADSATQEKIKCEIDTL
Genome polyprot.	112	Poliovirus 1	P03300	RDSEANPVDQPTEPDV
HA-E*	281	HCoV-OC43	A0A0K0L9C4	KDFTPVQVVDSRWNNA
NS3**	49	MERS-CoV	R9UMM5	ADTAGLYTNFRIDVPS
Nucleocapsid	223	HCoV-HKU1	Q5MQC6	SDSIVKPDMADEIANL
ORF1ab***	32	Pangolin CoV	A0A6G6A2G5	GDSVEEALSEARQHLL
ORF1ab	32	Bat SARS-rCoV		GDTVEEALAEAREHLK
ORF1ab	32	Bat CoV RaTG13	A0A6B9WIQ1	GDSVEEALSEARQHLK
ORF1ab	32	SARS-CoV	P0C6X7	GDSVEEALSEAREHLK
ORF1ab	32	SARS-CoV-2	A0A6V7ALW7	GDSVEEVLSEARQHLK
ORF1ab	2890	HCoV-HKU1	P0C6X4	RDISVNDLCFANKFFQ
ORF1ab	1047	HCoV-NL63	P0C6X5	RDELGVRVLDQSDNNC
ORF1ab	6693	HCoV-NL63	P0C6X5	KDSDVNDMVLSLIKSG
ORF1ab	5997	HCoV-OC43	U3M6T2	RDSIGTNFPLQLGFST
ORF1ab	6268	HCoV-OC43	U3M6T2	KDSFKDGLCMFWNCNV
ORF1ab	794	SARS-CoV-2	A0A6V7ALW7	KDTEKYCALAPNMMVT
Spike	397	SARS-CoV-2	P0DTC2	ADSFVIRGDEVRQIAP
Spike	570	SARS-CoV-2	P0DTC2	ADTTDAVRDPQTLEIL

*HA-E: hemagglutinin-esterase
**NS: non-structural
***ORF: open reading frame

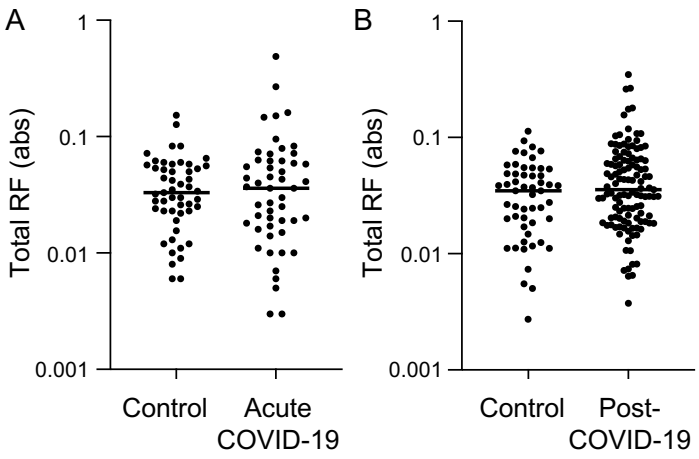

Supplemental Figure 1. Traditional RFs in COVID-19. Serum or plasma from 51 individuals with acute COVID-19 and 51 age- and sex-matched controls (A) or sera from 119 subjects 5 weeks post-COVID-19 and 53 age- and sex-matched controls (B) were assessed for RF by IgG Fc ELISA reported in absorbance (abs). Dots represent individual samples and lines indicate medians.

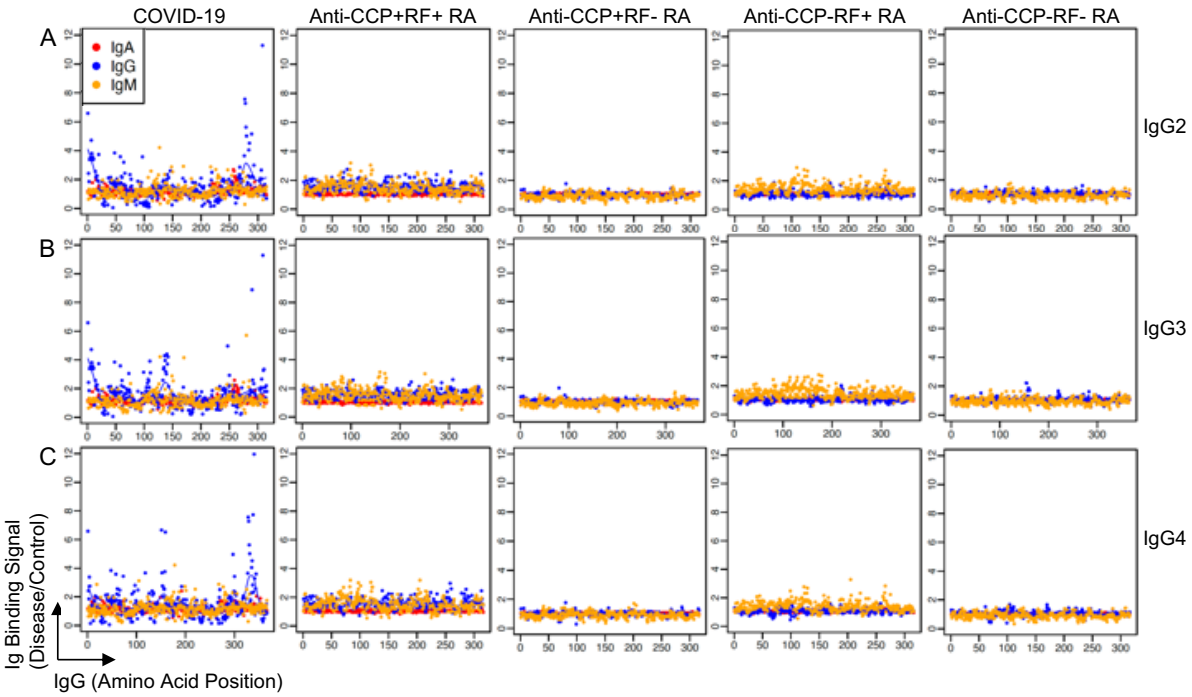

Supplemental Figure 2. COVID-19 convalescent, but not rheumatoid arthritis, serum IgM and IgG bind linear IgG-derived peptides. Serum IgA, IgM and IgG binding to linear peptides from the constant region of the heavy chain of IgG2 (A), IgG3 (B), and IgG4 (C) were quantified for subjects 5 weeks post-COVID-19 (n=40) and matched controls (n=20) as well as for rheumatoid arthritis (RA, n=12 anti-CCP+RF+, anti-CCP+RF- anti-CCP-RF+, and anti-CCP-RF-) and matched controls (n=12) by high density peptide array and reported as fold change.

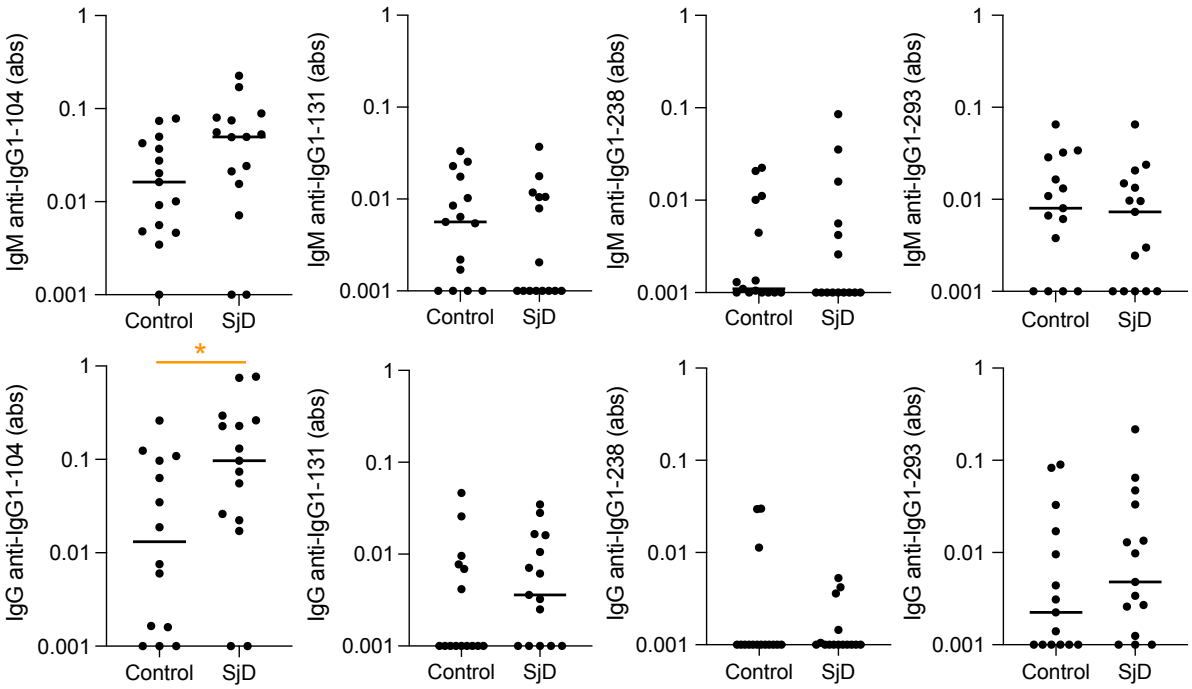

Supplemental Figure 3. Only an IgG1 hinge region peptide is bound in Sjogren's disease. Sera from RF+ Sjogren's disease subjects (n=15) or matched controls (n=15) were evaluated by ELISA for IgM and IgG binding to IgG1-104, IgG1-131, IgG1-238 and IgG1-293. Dots indicate individual serum samples and lines indicate medians. Absorbance (abs) values were compared by Mann-Whitney test, *p<0.05.

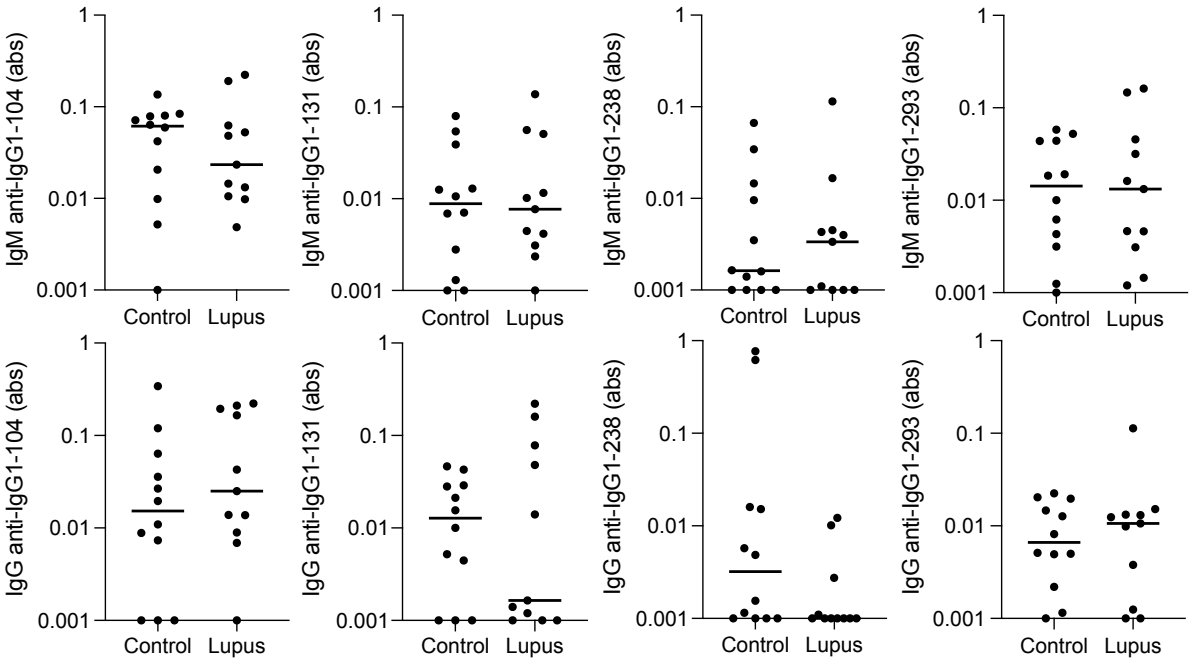

Supplemental Figure 4. Lupus serum does not contain IgM or IgG that binds the IgG1 epitopes bound in COVID-19. Sera from RF+ lupus (n=11) and matched control (n=12) subjects were tested by ELISA for IgM and IgG binding to IgG1-104, IgG1-131, IgG1-238 and IgG1-293. Dots indicate individual serum samples and lines indicate medians. Absorbance (abs) values were compared by Mann-Whitney test, and no comparisons were significant.

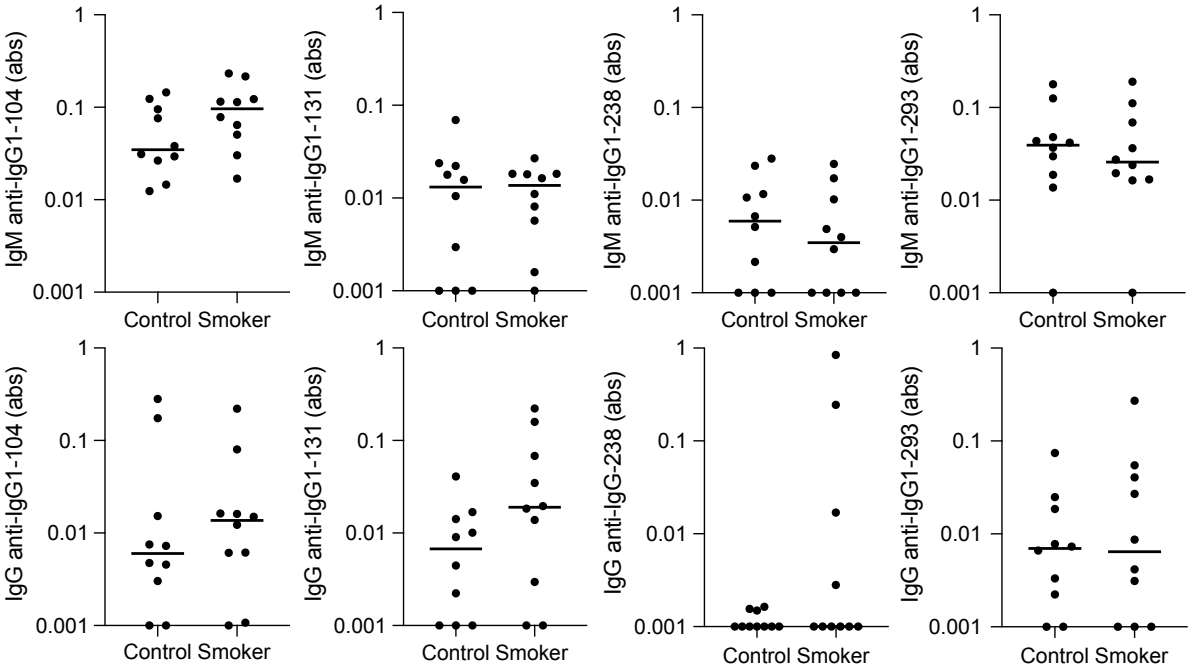

Supplemental Figure 5. Sera from smokers do not contain IgM or IgG that binds the IgG1 epitopes bound in COVID-19. Sera from smokers (n=10) and matched control subjects (n=10) were tested by ELISA for IgM and IgG binding to IgG1-104, IgG1-131, IgG1-238 and IgG1-293. Dots indicate individual serum samples and lines indicate medians. Absorbance (abs) values were compared by Mann-Whitney test, and no comparisons were significant.

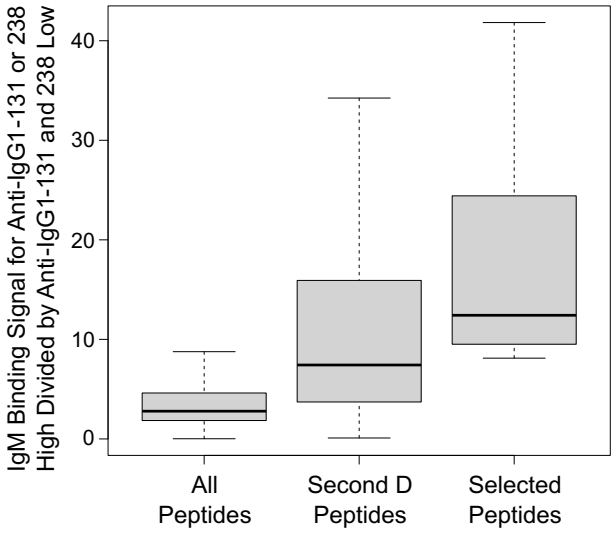

Supplemental Figure 6. IgM binding to peptides with an aspartic acid in position two. A secondary analysis was performed using IgM and IgG binding signal to 119,487 peptides derived from viral proteomes and the constant region of the heavy chains of IgG1-4 for 40 COVID-19 convalescent subjects. Subjects were divided into two groups: subjects with high IgM binding to IgG1-131 or IgG1-238 (>1 standard deviation above mean IgM binding to all IgG1-derived peptides) and subjects with low binding (<1 standard deviation above the mean). The graph depicts the fold difference in binding signal for the anti-IgG1-131/238 high group (n=10) divided by the low group (n=30) for IgM binding to all peptides (119,487), all peptides with an aspartic acid in position two (6366 “second D” peptides), and the peptides selected based on binding >5x more by IgM in the high group as compared to the low group excluding peptides with increased binding by IgG (n=18, locFDR<0.1). Boxes represent medians and 1st and 3rd quantiles of the data distribution and bars represent the maximum and minimum data, except for outliers (data points below quartile 1 minus 1.5x the interquartile range or above quartile 3 plus 1.5x the interquartile range). An ANOVA with Tukey post test on log(y) to x demonstrates a significant difference for the general ANOVA and all pairwise tests ($p< 0.0001$).

REFERENCES

1. Waaler E. On the occurrence of a factor in human serum activating the specific agglutintion of sheep blood corpuscles. 1939. APMIS **2007**; 115:422-38; discussion 39.
2. Ingegnoli F, Castelli R, Gualtierotti R. Rheumatoid factors: clinical applications. Dis Markers **2013**; 35:727-34.
3. Aletaha D, Neogi T, Silman AJ, et al. 2010 Rheumatoid arthritis classification criteria: an American College of Rheumatology/European League Against Rheumatism collaborative initiative. Arthritis Rheum **2010**; 62:2569-81.
4. Markusse HM, Otten HG, Vroom TM, Smeets TJ, Fokkens N, Breedveld FC. Rheumatoid factor isotypes in serum and salivary fluid of patients with primary Sjögren's syndrome. Clin Immunol Immunopathol **1993**; 66:26-32.
5. Witte T, Hartung K, Sachse C, et al. Rheumatoid factors in systemic lupus erythematosus: association with clinical and laboratory parameters. SLE study group. Rheumatol Int **2000**; 19:107-11.
6. Newkirk MM, Mitchell S, Procino M, et al. Chronic smoke exposure induces rheumatoid factor and anti-heat shock protein 70 autoantibodies in susceptible mice and humans with lung disease. Eur J Immunol **2012**; 42:1051-61.
7. Welch MJ, Fong S, Vaughan J, Carson D. Increased frequency of rheumatoid factor precursor B lymphocytes after immunization of normal adults with tetanus toxoid. Clin Exp Immunol **1983**; 51:299-304.
8. Salonen EM, Vaheri A, Suni J, Wager O. Rheumatoid factor in acute viral infections: interference with determination of IgM, IgG, and IgA antibodies in an enzyme immunoassay. J Infect Dis **1980**; 142:250-5.
9. Svec KH, Dingle JH. The Occurence of Rheumatoid Factor in Association with Antibody Response to Influenza A2(Asian) Virus. Arthritis Rheum **1965**; 8:524-9.
10. Lin KM, Chen WM, Tung SY, et al. Prevalence and predictive value of high-positive rheumatoid factor and anti-citrullinated protein antibody levels in nonarthritic patients with chronic hepatitis C infection. Int J Rheum Dis **2019**; 22:116-20.
11. Philémon EA, Tume C, Okomo Assoumou MC, et al. A Cross Sectional Study of the Impact of Human Immunodeficiency Virus, Hepatitis B Virus and Hepatitis C Virus on Rheumatoid Factor Production. Arch Rheumatol **2018**; 33:402-7.
12. Artandi SE, Calame KL, Morrison SL, Bonagura VR. Monoclonal IgM rheumatoid factors bind IgG at a discontinuous epitope comprised of amino acid loops from heavy-chain constant-region domains 2 and 3. Proc Natl Acad Sci U S A **1992**; 89:94-8.
13. Terness P, Kohl I, Hübener G, et al. The natural human IgG anti-F(ab')2 antibody recognizes a conformational IgG1 hinge epitope. J Immunol **1995**; 154:6446-52.
14. Maibom-Thomsen SL, Trier NH, Holm BE, et al. Immunoglobulin G structure and rheumatoid factor epitopes. PLoS One **2019**; 14:e0217624.
15. Zheng Z, Mergaert AM, Fahmy LM, et al. Disordered Antigens and Epitope Overlap Between Anti-Citrullinated Protein Antibodies and Rheumatoid Factor in Rheumatoid Arthritis. Arthritis Rheumatol **2020**; 72:262-72.
16. Mergaert AM, Zheng Z, Denny MF, et al. Rheumatoid Factor and Anti-Modified Protein Antibody Reactivities Converge on IgG Epitopes. Arthritis Rheumatol **2022**; 74:984-91.
17. Nakamura M, Burastero SE, Notkins AL, Casal P. Human monoclonal rheumatoid factor-like antibodies from CD5 (Leu-1)+ B cells are polyreactive. J Immunol **1988**; 140:4180-6.
18. Burastero SE, Casali P, Wilder RL, Notkins AL. Monoreactive high affinity and polyreactive low affinity rheumatoid factors are produced by CD5+ B cells from patients with rheumatoid arthritis. J Exp Med **1988**; 168:1979-92.
19. Schroder AK, Gharavi AE, Steinitz M, Johansson PJ, Christensen P. Binding of monoclonal IgM rheumatoid factor to streptococci via the antibody combining site. Int Arch Allergy Appl Immunol **1987**; 83:88-91.

20. The J, Ebersole JL. Rheumatoid factor from periodontitis patients cross-reacts with epitopes on oral bacteria. Oral Dis **1996**; 2:253-62.
21. Joo YB, Lim YH, Kim KJ, Park KS, Park YJ. Respiratory viral infections and the risk of rheumatoid arthritis. Arthritis Res Ther **2019**; 21:199.
22. Arleevskaya MI, Albina S, Larionova RV, Gabdoulkhakova AG, Lemerle J, Renaudineau Y. Prevalence and Incidence of Upper Respiratory Tract Infection Events Are Elevated Prior to the Development of Rheumatoid Arthritis in First-Degree Relatives. Front Immunol **2018**; 9:2771.
23. Rojas M, Rodriguez Y, Acosta-Ampudia Y, et al. Autoimmunity is a hallmark of post-COVID syndrome. J Transl Med **2022**; 20:129.
24. Xu C, Fan J, Luo Y, et al. Prevalence and Characteristics of Rheumatoid-Associated Autoantibodies in Patients with COVID-19. J Inflamm Res **2021**; 14:3123-8.
25. Anaya JM, Monsalve DM, Rojas M, et al. Latent rheumatic, thyroid and phospholipid autoimmunity in hospitalized patients with COVID-19. J Transl Autoimmun **2021**; 4:100091.
26. WHO Coronavirus Dashboard. January 23, 2023 ed. online, **2023**.
27. Amjadi MF, O'Connell SE, Armbrust T, et al. Specific COVID-19 Symptoms Correlate with High Antibody Levels against SARS-CoV-2. Immunohorizons **2021**; 5:466-76.
28. Holmes CL, Peyton CG, Bier AM, et al. Reduced IgG titers against pertussis in rheumatoid arthritis: Evidence for a citrulline-biased immune response and medication effects. PLoS One **2019**; 14:e0217221.
29. Heffron AS, McIlwain SJ, Amjadi MF, et al. The landscape of antibody binding in SARS-CoV-2 infection. PLoS Biol **2021**; 19:e3001265.
30. Bailey TL, Johnson J, Grant CE, Noble WS. The MEME Suite. Nucleic Acids Res **2015**; 43:W39-49.
31. Hjelholt A, Christiansen G, Sørensen US, Birkelund S. IgG subclass profiles in normal human sera of antibodies specific to five kinds of microbial antigens. Pathog Dis **2013**; 67:206-13.
32. Steen J, Forsstrom B, Sahlstrom P, et al. Recognition of Amino Acid Motifs, Rather Than Specific Proteins, by Human Plasma Cell-Derived Monoclonal Antibodies to Posttranslationally Modified Proteins in Rheumatoid Arthritis. Arthritis Rheumatol **2019**; 71:196-209.
33. Reed JH. Transforming mutations in the development of pathogenic B cell clones and autoantibodies. Immunol Rev **2022**; 307:101-15.
34. Peterson C, Malone CC, Williams RC, Jr. Rheumatoid-factor-reactive sites on CH3 established by overlapping 7-mer peptide epitope analysis. Mol Immunol **1995**; 32:57-75.
35. Williams RC, Jr., Malone CC. Rheumatoid-factor-reactive sites on CH2 established by analysis of overlapping peptides of primary sequence. Scand J Immunol **1994**; 40:443-56.
36. Williams RC, Jr., Malone CC, Kolaskar AS, Kulkarni-Kale U. Antigenic determinants reacting with rheumatoid factor: epitopes with different primary sequences share similar conformation. Mol Immunol **1997**; 34:543-56.
37. Gaynor B, Putterman C, Valadon P, Spatz L, Scharff MD, Diamond B. Peptide inhibition of glomerular deposition of an anti-DNA antibody. Proc Natl Acad Sci U S A **1997**; 94:1955-60.
38. DeGiorgio LA, Konstantinov KN, Lee SC, Hardin JA, Volpe BT, Diamond B. A subset of lupus anti-DNA antibodies cross-reacts with the NR2 glutamate receptor in systemic lupus erythematosus. Nat Med **2001**; 7:1189-93.
39. Cusick MF, Libbey JE, Fujinami RS. Molecular mimicry as a mechanism of autoimmune disease. Clin Rev Allergy Immunol **2012**; 42:102-11.
40. Fujinami RS, Oldstone MB. Amino acid homology between the encephalitogenic site of myelin basic protein and virus: mechanism for autoimmunity. Science **1985**; 230:1043-5.
41. Liao B, Chen Z, Zheng P, et al. Detection of Anti-SARS-CoV-2-S2 IgG Is More Sensitive Than Anti-RBD IgG in Identifying Asymptomatic COVID-19 Patients. Front Immunol **2021**; 12:724763.

42. Haynes BF, Fleming J, St Clair EW, et al. Cardiolipin polyspecific autoreactivity in two broadly neutralizing HIV-1 antibodies. Science **2005**; 308:1906-8.
43. Guthmiller JJ, Lan LY, Fernandez-Quintero ML, et al. Polyreactive Broadly Neutralizing B cells Are Selected to Provide Defense against Pandemic Threat Influenza Viruses. Immunity **2020**; 53:1230-44 e5.
44. Jones DD, DeIulio GA, Winslow GM. Antigen-driven induction of polyreactive IgM during intracellular bacterial infection. J Immunol **2012**; 189:1440-7.
45. Lang AK, Macht LM, Kirwan JR, Wraith DC, Elson CJ. Ability of T cells from patients with rheumatoid arthritis to respond to immunoglobulin G. Immunology **1999**; 98:116-22.
46. Bikoff EK. Tolerance for self IG at the level of the Ly1+ T cell. J Exp Med **1983**; 158:1868-80.
47. Sahlstrom P, Hansson M, Steen J, et al. Different hierarchies of anti-modified protein autoantibody reactivities in rheumatoid arthritis. Arthritis Rheumatol **2020**.
48. Yurasov S, Wardemann H, Hammersen J, et al. Defective B cell tolerance checkpoints in systemic lupus erythematosus. J Exp Med **2005**; 201:703-11.
49. Glauzy S, Sng J, Bannock JM, et al. Defective Early B Cell Tolerance Checkpoints in Sjogren's Syndrome Patients. Arthritis Rheumatol **2017**; 69:2203-8.
50. Pascolini S, Vannini A, Deleonardi G, et al. COVID-19 and Immunological Dysregulation: Can Autoantibodies be Useful? Clin Transl Sci **2021**; 14:502-8.
51. Muratori P, Lenzi M, Muratori L, Granito A. Antinuclear antibodies in COVID 19. Clin Transl Sci **2021**; 14:1627-8.
52. Agnello V, Arbetter A, Ibanez de Kasep G, Powell R, Tan EM, Joslin F. Evidence for a subset of rheumatoid factors that cross-react with DNA-histone and have a distinct cross-idiotype. J Exp Med **1980**; 151:1514-27.
53. Leadbetter EA, Rifkin IR, Hohlbaum AM, Beaudette BC, Shlomchik MJ, Marshak-Rothstein A. Chromatin-IgG complexes activate B cells by dual engagement of IgM and Toll-like receptors. Nature **2002**; 416:603-7.
54. Van Snick JL, Van Roost E, Markowetz B, Cambiaso CL, Masson PL. Enhancement by IgM rheumatoid factor of in vitro ingestion by macrophages and in vivo clearance of aggregated IgG or antigen-antibody complexes. Eur J Immunol **1978**; 8:279-85.
55. Ashe WK, Daniels CA, Scott GS, Notkins AL. Interaction of rheumatoid factor with infectious herpes simplex virus-antibody complexes. Science **1971**; 172:176-7.
56. Nielen MM, van Schaardenburg D, Reesink HW, et al. Specific autoantibodies precede the symptoms of rheumatoid arthritis: a study of serial measurements in blood donors. Arthritis Rheum **2004**; 50:380-6.
57. Fechtner S, Berens H, Bemis E, et al. Antibody Responses to Epstein-Barr Virus in the Preclinical Period of Rheumatoid Arthritis Suggest the Presence of Increased Viral Reactivation Cycles. Arthritis Rheumatol **2022**; 74:597-603.
58. Lebedin M, Garcia CV, Spatt L, et al. Discriminating promiscuous from target-specific autoantibodies in COVID-19. Eur J Immunol **2023**:e2250210.
59. Shelef MA. New Relationships for Old Autoantibodies in Rheumatoid Arthritis. Arthritis Rheumatol **2019**; 71:1396-9.
60. Acosta-Ampudia Y, Monsalve DM, Rojas M, et al. Persistent Autoimmune Activation and Proinflammatory State in Post-COVID Syndrome. J Infect Dis **2022**.
61. Tamariz L, Bast E, Abad M, Klimas N, Caralis P, Palacio A. Post COVID-19 joint pain: Preliminary report of the relationship with antinuclear antibodies and inflammation. J Med Virol **2022**; 94:3479-81.

Chapter 5: Conclusions and future directions

In this dissertation I have studied the antibody responses after SARS-CoV-2 infection. SARS-CoV-2 was a newly emerged pathogen in January of 2020 [1] that spread quickly and was declared a pandemic just two months later by the World Health Organization [2]. Early in the pandemic, there were many unknowns including: the persistence and protection of neutralizing antibodies, groups most likely to suffer from severe COVID-19, re-exposure risk, and the reliability of antibody tests in detecting recent SARS-CoV-2 infections. Now in the spring of 2023, the COVID-19 pandemic continues to be classified by the World Health Organization as a public health emergency of international concern [3]. The United States plans to end the public health emergency declaration on May 11, 2023. As rates of SARS-CoV-2 infections decline [4], we approach a new post-pandemic era, in which the consequences of COVID-19 have not been fully realized. New unknowns post-COVID-19 include the causes and effects of autoantibody development, long COVID, symptom persistence, elevated cytokines and other lab abnormalities, autoimmune disease development, worsening comorbidities, and other long-term complications. Future studies will need to investigate these gaps in knowledge over many years to better understand the long-term consequences of COVID-19.

Chapter 2 demonstrates many findings early in the COVID-19 pandemic. Assay development was still underway to differentiate antibodies from those recently infected with SARS-CoV-2 compared with people who had exposures to common cold causing coronaviruses. Publications varied in their use of neutralization and functional assays with small sample sizes and homogeneous cohorts [5-11]. Many studies used discarded blood products from hospitals or clinics to study the antibody responses after SARS-CoV-2, which meant that samples were not collected in uniform time frames from polymerase chain reaction (PCR) positive test or symptom onset [8, 12, 13]. By availability, samples from patients with the most severe disease were studied, whereas samples from infected individuals in the community who did not require hospitalization were not collected. Rapidly declining antibody levels were published as ominous

signs, and there was concern about lasting immunity [14-17]. Our study contributed to the field in several ways. We started a COVID-19 biobank and recruited patients who had a positive PCR test at UW Health. By formally recruiting the first 120 interested subjects into our study, we gained: a large sample size, a diverse disease severity range (from asymptomatic to intubated), uniformly timed and longitudinally collected samples, and accompanying clinical and demographic information from questionnaires and medical charts. Because we had detailed information about our samples, we could correlate anti-SARS-CoV-2 antibody levels with COVID-19 severity, age, sex, comorbidities, and symptoms. We were the first to report on symptoms correlating with antibody levels. With our large and diverse disease severity sample, we were able to demonstrate the persistence of antibodies over several months. This was expected from antibody responses in SARS-CoV, but it contrasted with many reports at the time that found declining levels.

Chapter 3 assesses the detection of antibodies against peptides from the spike, nucleocapsid, and membrane proteins of SARS-CoV-2 longitudinally over the course of a year. Limited antibody tests had received emergency use authorization. None were specific for the detection of anti-membrane antibodies, leaving a gap in our understanding of antibody detection strategies. Anti-nucleocapsid and anti-spike antibody testing were available at UW Health to detect past SARS-CoV-2 infection. However, reports of negative antibody testing following positive PCR testing questioned the utility and reliability of the anti-nucleocapsid antibody test, and the anti-spike antibody test was unable to differentiate between vaccinated and previously infected individuals. Fully vaccinated healthcare workers reported breakthrough SARS-CoV-2 infections in 2021, despite multiple exposures to antigen. For a few of these individuals, this was their second SARS-CoV-2 infection and was evidence of re-infection despite apparent immunity. Our study contributed to the field because we compared antibodies against spike, nucleocapsid, and membrane in convalescent, naive, vaccinated, breakthrough infection, and re-infection

samples. We demonstrated that anti-spike antibodies post COVID-19 persist up to 12 months and are significantly higher in individuals who had both past infection and vaccination. We showed that fully vaccinated individuals with breakthrough infections have detectable anti-spike antibodies, despite their susceptibility to infection and re-infection. We demonstrated that anti-nucleocapsid antibodies decline over the course of one year. By then, only half of convalescent individuals have detectable anti-nucleocapsid antibodies. Anti-membrane antibodies persist for 12 months, and in combination with anti-spike antibodies, can differentiate between vaccinated, convalescent, and naïve individuals, indicating their utility for community-wide seroprevalence estimations. It is unknown how long antibodies against SARS-CoV-2 will last, but antibodies against SARS-CoV were detected several years after infection [18-20]. Therefore, a future direction of this work could be to test the longitudinal antibody levels in this cohort two years and three years after recovery from COVID-19 to determine antibody persistence.

As the COVID-19 pandemic has continued, different immune system effects have emerged. Initially, attention to the immune dysregulation of cytokines and B and T cell responses was prominent. More recently, reports of autoantibodies detected after COVID-19 are further evidence of the multi-faceted effects of SARS-CoV-2 [21, 22]. Autoantibodies detected after COVID-19 could be the result of a polyreactive primary immune response, and future studies are needed to determine whether these antibodies persist and class-switch. Long COVID and autoimmune disease symptoms overlap, and it is currently unknown whether COVID-19 predisposes some individuals for autoimmune disease development.

Chapter 4 identifies rheumatoid factors post-COVID-19 and determines their novel linear epitopes. Previously, rheumatoid factor epitope identification has primarily been studied in lymphoproliferative disease and autoimmune disease. Epitopes for rheumatoid factors post-infection were unknown. A couple of reports detected rheumatoid factors in COVID-19 patient

samples [23, 24], but many knowledge gaps remained: timing of rheumatoid factor development, epitope binding, and populations affected. Our study contributed to the field because we discovered anti-IgG1 antibodies that bound unique linear epitopes in the Fc region of IgG that were not bound by rheumatoid factors from rheumatoid arthritis, Sjogren's disease, or lupus subjects. Additionally, we reported a linear peptide in the hinge of IgG1 that bound rheumatoid factors from rheumatoid arthritis and Sjogren's disease subjects, but not COVID-19 subjects. These findings provide evidence that rheumatoid factors from different conditions bind to different epitopes within IgG1. This knowledge could be leveraged into improved diagnostic tests with increased specificity. We also determined that rheumatoid factor levels post-COVID-19 increase two to three weeks from symptom onset and are associated with older age. Rheumatoid factors can be polyreactive [25], and we determined that the rheumatoid factors post-COVID-19 bound viral and self-antigens. We demonstrated that these anti-IgG1 antibodies bound IgG Fc and spike proteins, in addition to many peptide antigens. The higher binding to spike than IgG Fc suggests that SARS-CoV-2 was the antigen of origin for these rheumatoid factors, and the cross-reactivity to viral and self-antigens may represent polyreactive binding to a short motif.

Future directions of this work may investigate the duration that rheumatoid factors persist after COVID-19, their potential roles in the inflammatory response, whether they are associated with long COVID or certain symptoms, such as joint pain, and whether rheumatoid factors post-COVID-19 predispose certain groups for the development of autoimmune diseases. It is unknown how long rheumatoid factors persist after infection and whether they are associated with symptoms after initial recovery from COVID-19. We detected rheumatoid factors acutely and in the early convalescent period (five weeks and three months post symptom resolution from COVID-19). Anti-nuclear antibodies are persistently elevated 12 months after COVID-19 and are associated with symptoms, including fatigue, dyspnea, and cough severity [26].

Therefore, rheumatoid factors may also persist and be associated with symptoms. To investigate this, samples from COVID-19 convalescent individuals can be assayed for rheumatoid factors at longitudinal timepoints, including six months, one year, two years, and three years after COVID-19. Additionally, convalescent individuals can be surveyed about symptomatology (such as fatigue and arthralgias) and timing. Both longitudinal convalescent sample collection and participant surveys are ongoing, based on this dissertation's data, making these future directions possible.

Similarities in serology and symptomatology between pre-rheumatoid arthritis and long COVID patients may indicate a continuum of disease. However, future studies are needed to better understand the connection. In rheumatoid arthritis development, autoantibodies become detectable before symptom onset. Then, symptoms may occur in a pre-clinical rheumatoid arthritis stage in some patients, and ultimately diagnostic criteria for rheumatoid arthritis are met years after initial autoantibodies were detected. During the pre-rheumatoid arthritis stage, patients have detectable autoantibodies and some have symptoms (fatigue, arthralgias), similar to some patients with long COVID. For example, anti-nuclear antibodies were detected in long COVID patients a year after their infections and were associated with symptom severity [26]. In another study, patients presenting to long COVID clinics were followed for more than 100 days from symptom onset and more than a third had anti-nuclear antibody reactivity [27]. Autoantibodies detected in pre-clinical rheumatoid arthritis and long COVID are associated with inflammation. Elevated cytokines predict symptoms in long COVID at 12 months, and the number of elevated cytokines predict time to rheumatoid arthritis diagnosis [26, 28]. For these reasons, future directions of this work may aim to better determine the risk of autoimmune disease development in people with long COVID. This may require surveillance for many years. It is also possible that long COVID may accelerate autoimmune disease development due to the duration or severity of this trigger.

Our work provides evidence of a loss of tolerance to IgG after infection with COVID-19. Typically, loss of tolerance to IgG is described in rheumatoid arthritis, but it can also occur in Sjogren's disease, lupus, and other conditions. Interestingly, rheumatoid factors in rheumatoid arthritis preferentially bind linear epitopes in the CH2 and CH3 regions of IgG that are citrullinated or homocitrullinated [29]. Rheumatoid factors in rheumatoid arthritis and Sjogren's disease bind epitopes in the hinge of IgG [29], but rheumatoid factors post-COVID-19 do not bind post-translationally modified or hinge sites. A future direction of this work will be to investigate whether epitope spreading occurs, in which rheumatoid factors from COVID-19 subjects are able to recognize additional epitopes, such as citrullinated, homocitrullinated, or hinge sites. It is possible that rheumatoid factors post-infection will more closely resemble rheumatoid factors in autoimmune diseases over time, since infections and autoantibody detection are risk factors for autoimmune diseases, such as rheumatoid arthritis.

Overall, this body of work contributes to our understanding of the antibody responses that follow a novel viral infection. We defined anti-viral antibody responses using new assays that were still in development. We expanded the antigens under consideration for antibody testing by providing evidence of the benefits of membrane, while the focus in the field was on spike and nucleocapsid. And we defined the epitopes of rheumatoid factors post-COVID-19, which is a major advancement, because rheumatoid factor epitopes in infection were previously unknown. Therefore, this thesis addresses many gaps in knowledge that existed in the field. This work spurs areas for future investigations. Rheumatoid factors may propagate or resolve inflammation in infections. Future studies are required to investigate the immunologic mechanisms of rheumatoid factors in infections. Based on our findings, rheumatoid factors have different epitopes in different disease states. Future independent studies should determine whether these novel findings are reproducible. If confirmed with large, diverse samples at

multiple geographic sites, these results could be translated into the clinic. Rheumatoid factor clinical tests with enhanced epitope specificity would improve diagnostic accuracy and ultimately improve patient care.

REFERENCES

1. Wang H, Li X, Li T, et al. The genetic sequence, origin, and diagnosis of SARS-CoV-2. Eur J Clin Microbiol Infect Dis **2020**; 39:1629-35.
2. WHO Director-General's opening remarks at the media briefing on COVID-19- 11 March 2020: World Health Organization, **2020**.
3. Adam D. When will COVID stop being a global emergency? Nature **2023**; 614:201-2.
4. COVID Data Tracker Weekly Review: Centers for Disease Control and Prevention, **2023**.
5. Ma H, Zeng W, He H, et al. Serum IgA, IgM, and IgG responses in COVID-19. Cell Mol Immunol **2020**; 17:773-5.
6. Long QX, Tang XJ, Shi QL, et al. Clinical and immunological assessment of asymptomatic SARS-CoV-2 infections. Nat Med **2020**.
7. Chi X, Yan R, Zhang J, et al. A neutralizing human antibody binds to the N-terminal domain of the Spike protein of SARS-CoV-2. Science **2020**.
8. To KK, Tsang OT, Leung WS, et al. Temporal profiles of viral load in posterior oropharyngeal saliva samples and serum antibody responses during infection by SARS-CoV-2: an observational cohort study. Lancet Infect Dis **2020**; 20:565-74.
9. Liu A, Li Y, Peng J, Huang Y, Xu D. Antibody responses against SARS-CoV-2 in COVID-19 patients. J Med Virol **2020**.
10. Van Elslande J, Decru B, Jonckheere S, et al. Antibody response against SARS-CoV-2 spike protein and nucleoprotein evaluated by 4 automated immunoassays and 3 ELISAs. Clin Microbiol Infect **2020**.
11. Dogan M, Kozhaya L, Placek L, et al. SARS-CoV-2 specific antibody and neutralization assays reveal the wide range of the humoral immune response to virus. Commun Biol **2021**; 4:129.
12. Takahashi T, Ellingson MK, Wong P, et al. Sex differences in immune responses that underlie COVID-19 disease outcomes. Nature **2020**; 588:315-20.
13. Dittadi R, Afshar H, Carraro P. The early antibody response to SARS-Cov-2 infection. Clin Chem Lab Med **2020**.
14. Seow J, Graham C, Merrick B, et al. Longitudinal observation and decline of neutralizing antibody responses in the three months following SARS-CoV-2 infection in humans. Nat Microbiol **2020**; 5:1598-607.
15. Korte W, Buljan M, Rösslein M, et al. SARS-CoV-2 IgG and IgA antibody response is gender dependent; and IgG antibodies rapidly decline early on. J Infect **2020**.
16. Yin S, Tong X, Huang A, et al. Longitudinal anti-SARS-CoV-2 antibody profile and neutralization activity of a COVID-19 patient. J Infect **2020**.
17. Röltgen K, Wirz OF, Stevens BA, et al. SARS-CoV-2 Antibody Responses Correlate with Resolution of RNAemia But Are Short-Lived in Patients with Mild Illness. medRxiv **2020**.
18. Chang SC, Wang JT, Huang LM, et al. Longitudinal analysis of Severe Acute Respiratory Syndrome (SARS) coronavirus-specific antibody in SARS patients. Clin Diagn Lab Immunol **2005**; 12:1455-7.
19. Shi Y, Wan Z, Li L, et al. Antibody responses against SARS-coronavirus and its nucleocaspid in SARS patients. J Clin Virol **2004**; 31:66-8.
20. Liu L, Xie J, Sun J, et al. Longitudinal profiles of immunoglobulin G antibodies against severe acute respiratory syndrome coronavirus components and neutralizing activities in recovered patients. Scand J Infect Dis **2011**; 43:515-21.
21. Damoiseaux J, Dotan A, Fritzler MJ, et al. Autoantibodies and SARS-CoV2 infection: The spectrum from association to clinical implication: Report of the 15th Dresden Symposium on Autoantibodies. Autoimmun Rev **2022**; 21:103012.
22. Chang SE, Feng A, Meng W, et al. New-onset IgG autoantibodies in hospitalized patients with COVID-19. Nat Commun **2021**; 12:5417.

23. Anaya JM, Monsalve DM, Rojas M, et al. Latent rheumatic, thyroid and phospholipid autoimmunity in hospitalized patients with COVID-19. J Transl Autoimmun **2021**; 4:100091.
24. Xu C, Fan J, Luo Y, et al. Prevalence and Characteristics of Rheumatoid-Associated Autoantibodies in Patients with COVID-19. J Inflamm Res **2021**; 14:3123-8.
25. Nakamura M, Burastero SE, Notkins AL, Casal P. Human monoclonal rheumatoid factor-like antibodies from CD5 (Leu-1)+ B cells are polyreactive. J Immunol **1988**; 140:4180-6.
26. Son K, Jamil R, Chowdhury A, et al. Circulating anti-nuclear autoantibodies in COVID-19 survivors predict long COVID symptoms. Eur Respir J **2023**; 61.
27. Woodruff MC, Ramonell RP, Haddad NS, et al. Dysregulated naive B cells and de novo autoreactivity in severe COVID-19. Nature **2022**; 611:139-47.
28. Deane KD, O'Donnell CI, Hueber W, et al. The number of elevated cytokines and chemokines in preclinical seropositive rheumatoid arthritis predicts time to diagnosis in an age-dependent manner. Arthritis Rheum **2010**; 62:3161-72.
29. Mergaert AM, Zheng Z, Denny MF, et al. Rheumatoid Factor and Anti-Modified Protein Antibody Reactivities Converge on IgG Epitopes. Arthritis Rheumatol **2022**; 74:984-91.

Appendix A: Investigating the potential role of rheumatoid factors in enhancing virus neutralization

Maya F. Amjadi[1], Peter J. Halfmann[2], Yoshihiro Kawaoka[2], Miriam A. Shelef[1,3]

[1]Department of Medicine, University of Wisconsin-Madison, Madison, Wisconsin, United States of America.

[2]Department of Pathobiological Sciences, School of Veterinary Medicine, Influenza Research Institute, University of Wisconsin-Madison, Madison, Wisconsin, United States of America.

[3]William S. Middleton Memorial Veterans Hospital, Madison, Wisconsin, United States of America.

Contributions: I assisted in experimental design, selected samples, purified antibodies, performed ELISA experiments, coordinated project communications, wrote the chapter, and made the figures.

INTRODUCTION

The role of rheumatoid factors after infection is unknown. Some evidence suggests that rheumatoid factors may play an active role in clearance and resolution of inflammation through binding pathogens directly [1], activating complement [2, 3], and enhancing uptake by macrophages [4]. Given that rheumatoid factors are detected after SARS-CoV-2 infection [5, 6], they may play a role in the immune response to this pathogen. If true, defining the mechanism for rheumatoid factor aiding in the immune response would fill an existing gap in knowledge and may be harnessed as a future therapeutic in the treatment of viral infections.

One paper from 1971 published in *Science* reported that when rheumatoid factors were added to infectious Herpes Simplex Virus (HSV)-antibody complexes, there was increased neutralization by complement [2]. They suggested that the binding of IgM rheumatoid factor to the virus-antibody complex allowed for additional binding sites of complement (multivalency). Therefore, IgM rheumatoid factor could act as a large scaffold or docking site for complement. Whether rheumatoid factors post-COVID-19 could aid complement is unknown. Here we investigate whether rheumatoid factors elicited by SARS-CoV-2 infection enhance virus neutralization.

METHODS

Human Subjects

This study was conducted in accordance with the Declaration of Helsinki and was approved by the Institutional Review Board at the University of Wisconsin (UW). Samples and clinical data were obtained from the UW Rheumatoid Arthritis Biorepository [7] or the UW COVID-19 Convalescent Biorepository [8]. Healthy control serum and serum from rheumatoid arthritis subjects were collected prior to 2019. COVID-19 convalescent sera were collected three months

after symptom resolution from COVID-19 (initial polymerase chain reaction (PCR) positive COVID-19 test in spring/summer 2020).

Peptide Enzyme Linked Immunosorbent Assay (ELISA)

Peptide ELISAs were completed to screen naive and COVID-19 convalescent serum samples for antibodies that bound peptides IgG1-131, IgG1-238, or IgG1-293. Serum samples that did not bind these epitopes were considered for use in the neutralization assays, and samples that did contain these antibodies were considered for use in antibody purification. Peptide ELISAs were also used to quantify purified antibodies from COVID-19 convalescent serum that bound to IgG1-131, IgG1-293, IgG1-219J, mem-8, or spike-1253, using a standard curve as described below.

Costar 96-well high binding ELISA plates (Corning, Corning, NY) were coated with 5µg/ml streptavidin (Thermo Scientific Pierce, Waltham, MA) in phosphate buffered saline (PBS) (Corning) overnight at four degrees Celsius, washed twice with PBS, and coated with biotinylated antigens (1:500 0.5mM synthesized peptides: IgG1-131 KDTLMISRTPEVTCVV-K(biotin), IgG1-238 RDELTKNQVSLTCLVK-K(biotin), IgG1-293 LTVDKSRWQQGNVFSC-K(biotin), IgG1-219J (J indicates homocitrulline) ISJAJGQPREPQVYTLPPSRDEL-K(biotin), mem-8 ITVEELKKLLEQWNLV-K(biotin), or spike-1253 CCKFDEDDSEPVLKGV-K(biotin)) (Biomatik, Cambridge, Ontario, Canada), in PBS for one hour at room temperature, or uncoated wells received PBS alone. Plates were washed three times with wash buffer (PBS with 0.2% Tween 20), blocked with blocking solution (5% nonfat dehydrated milk in wash buffer) for at least two and a half hours at room temperature, and incubated with serum (diluted 1:100 in blocking solution) or purified antibodies (diluted 1:20 in blocking solution) overnight at four degrees Celsius. Plates were then washed four times with wash buffer and incubated for one

hour at room temperature with mouse anti-human IgG conjugated to horse radish peroxidase, goat anti-human IgM conjugated to horse radish peroxidase, or goat F(ab')2 anti-human kappa and goat F(ab')2 anti-human lambda conjugated to horse radish peroxidase (Southern Biotechnology, Birmingham, AL) diluted 1:5000 in blocking solution. Plates were washed four times with wash buffer, developed with tetramethylbenzidine substrate solution (Thermo Scientific Pierce), and reaction was stopped using 0.18M sulfuric acid. Endpoint absorbance (450-562nm) was read on a FilterMax F3 spectrophotometer (Molecular Devices, San Jose, CA) and absorbance values from uncoated wells and wells that received no serum were subtracted as nonspecific binding and background signal, respectively.

A standard curve was used for some ELISAs. After the above streptavidin and wash steps, wells were incubated with serially diluted biotinylated human IgM and human IgG (Novus Biologicals, Englewood, CO) in PBS for one hour at room temperature. Plates were washed, blocked, washed, incubated with detection antibody, developed, and absorbance was determined as above. Four parameter logistic curve was used on myassays.com to determine the concentration from absorbance values.

Depletion of light chain or IgM in Fc fragment

Streptavidin magnetic beads (Thermo Scientific Pierce) were washed three times with Tris Buffered Saline (TBS) (Fisher Bioreagent, Pittsburgh, PA) with 0.1% Tween (TBST) using magnet collection. Beads were resuspended in TBST and biotinylated goat F(ab')2 anti-human kappa, biotinylated goat F(ab')2 anti-human lambda or biotinylated goat F(abs')2 anti-human IgM (Southern Biotechnology) were added to beads. Beads were mixed for two hours at room temperature. Beads were collected with magnet, washed two times with TBST, and resuspended in TBS. Anti-kappa, anti-lambda, and anti-IgM-coated magnetic beads were added

to human Fc fragment (Millipore Sigma, Burlington, MA). Mixture was tumbled overnight at four degrees Celsius. Magnetic beads were collected with magnet to collect contaminating light chains and IgM. Fc was centrifuged at 20,000xg for five minutes to remove residual beads. Fc fragment was saved, stored at four degrees Celsius and used in ELISA.

Human Fc ELISA

Fc ELISAs were completed to screen naive and COVID-19 convalescent serum samples for antibodies that bound Fc. Serum samples that did not bind Fc were considered for use in the neutralization assays, and samples that did contain these antibodies were considered for use in antibody purification. Fc ELISAs were also used to quantify purified anti-IgG Fc antibodies from COVID-19 convalescent serum using a standard curve described above.

Costar 96-well high binding ELISA plates (Corning) were coated with 2.5μg/ml human Fc fragment (Millipore Sigma) in PBS. Plates were washed three times with wash buffer and blocked overnight with blocking solution at four degrees Celsius. Sera or purified antibodies were diluted 1:100 in blocking solution, added to Fc and PBS coated wells, and incubated overnight at four degrees Celsius. Plates were washed four times with wash buffer and goat F(ab')2 anti-human kappa and goat F(ab')2 anti-human lambda conjugated to horse radish peroxidase (Southern Biotechnology) at 1:5000 in blocking solution were added for one hour at room temperature. Plates were washed four times with wash buffer, developed using tetramethyl benzidine (Thermo Scientific Pierce), and reaction was stopped using 0.18M sulfuric acid. Endpoint absorbance was read as described above.

Affinity Chromatography

Streptavidin sepharose beads (BioVision, San Francisco, CA or Abcam, Waltham, MA) were washed three times with TBS (Fisher Bioreagent) and then incubated with biotinylated peptide (Biomatik) diluted 1:10 in TBS and tumbled at four degrees Celsius for two hours. Human sera from COVID-19 convalescent or rheumatoid arthritis subjects were diluted 1:5 in blocking solution. Peptide-labeled beads were resuspended in blocking solution, loaded onto a frit membrane in a spin column (G Biosciences, St. Louis, MO), and washed with blocking solution. A rubber stopper was added to column, diluted serum was added, and columns were capped for antibody incubation with the peptide labeled beads overnight at four degrees Celsius. Columns were washed twice with blocking solution to remove nonspecific antibodies and conditioned with conditioning buffer (Classic IP Kit, Thermo Scientific Pierce). Elution buffer (100mM glycine pH 2.6) was added, and antibodies bound by the beads were eluted off and collected in microfuge tubes with neutralizing buffer (Tris HCl pH 8.7). Columns were spun briefly on a tabletop Eppendorf 5430 centrifuge, and the elution step was repeated to elute antibodies. Concentration of purified antibodies was approximated by ELISA using the standard curve. Purified antibodies were concentrated using an Amicon® Ultra 0.5ml 30K Centrifugal Filtration device (Millipore Sigma) and resuspended at 15,000ng/ml for all antibodies, except anti-IgG1-293 antibodies were resuspended at 5,000ng/ml.

Purifying anti-IgG Fc antibodies

To purify anti-IgG Fc antibodies, the PureProteome™ NHS FlexiBind Magnetic Beads Kit was used (catalogue number LSKMAGN01, Millipore Sigma) and manufacturer's instructions were followed using centrifugation for concentration and buffer exchange and the general coupling protocol to incubate the ligand (Fc) with the magnetic beads. In the general immunoprecipitation protocol, COVID-19 convalescent serum was diluted 1:5 in blocking solution and 100µl of

diluted serum was added to 40µl of Fc coupled magnetic beads. Beads were incubated overnight at four degrees Celsius. Beads were washed three times with 500µl of blocking solution. Then antibodies were eluted off the Fc coupled beads using 100µl of elution buffer (100mM glycine pH 2.6). Beads were collected with a magnet, and the supernatant was transferred to a tube with 10µl of neutralizing buffer (1.5M Tris HCl pH 8.8) and stored at -80 degrees Celsius. The concentration of the anti-IgG Fc antibodies was approximated by ELISA, and antibodies were resuspended at 15,000ng/ml.

Focus reduction neutralization test (FRNT)

The FRNT has been previously described [9]. Briefly, serum and virus are co-incubated, and the mixture is inoculated onto plated cells, which are fixed, stained, and imaged to quantify infectivity. Three experimental designs investigated whether purified antibodies from COVID-19 convalescent samples enhanced SARS-CoV-2 neutralization. The neutralization assay was initially run with serum only (not purified antibodies) to determine a serum dilution (1:100) that reduced the foci number by 50-75%. Dilutions were in virus growth media (5% fetal bovine serum (FBS) in Dulbecco's Modified Eagle Medium (DMEM)).

In the first experiment, 55µl of the diluted serum (1:100) was mixed with 5µl purified antibody (75ng) and 60µl virus (~1000 focus-forming units). In the second experiment, 30µl of diluted serum (1:100) was mixed with 30µl purified antibody (450ng) and 60µl virus (~1000 focus-forming units) for all purified antibodies, except anti-IgG1-293, which was at a lower starting concentration so 30µl of anti-IgG1-293 antibodies was 150ng. In both experiments, the mixtures were incubated for one hour at 37 degrees Celsius. The serum-antibody-virus mixtures were inoculated onto Vero E6/TMPRSS2 cells in 96-well plates and incubated for one hour at 37 degrees Celsius. The mixtures were then removed, and methylcellulose solution was added to

each well. The cells were incubated for 16 hours at 37 degrees Celsius and then fixed with formalin. After the formalin was removed, the cells were immunostained with a mouse monoclonal antibody against SARS-CoV-1/2 nucleoprotein (clone 1C7C7 (Sigma-Aldrich, St. Louis, MO)), followed by a horseradish peroxidase-labeled goat anti-mouse immunoglobulin (SeraCare Life Sciences, Milford, MA). The infected cells were stained with TrueBlue Substrate (SeraCare Life Sciences) and then washed with distilled water. After cell drying, the focus numbers were quantified using an ImmunoSpot S6 Analyzer, ImmunoCapture software, and BioSpot software (Cellular Technology, Beachwood, OH).

In the third experiment, 3µl of diluted serum (diluted 1:15) was incubated with 60µl virus (~1000 focus-forming units) for two hours at 37 degrees Celsius. Then 30µl (450ng) or 50µl (750ng) purified antibody was added and incubated at 37 degrees Celsius for 15 minutes. Then 27µl or 7µl, respectively, of pooled naive sera were added as a source of complement and incubated for 15 minutes at 37 degrees Celsius. After these sequential additions and incubations, the mixture was inoculated onto Vero E6/TMPRSS2 cells, and the rest of the protocol was followed as described above.

RESULTS

In the first experiment, we investigated whether there was enhanced neutralization of SARS-CoV-2 when purified anti-IgG1-131 or anti-IgG Fc antibodies were added to convalescent serum. We determined the foci numbers when naive serum (with no neutralizing antibodies) had an irrelevant, influenza B monoclonal antibody added. This condition represented the negative control (100% infection) because no neutralization was expected from naive serum or an irrelevant monoclonal antibody. In contrast, foci numbers were a lot smaller when the irrelevant flu antibody was added to convalescent sera (140 average foci compared with 968, or only 14%

infection). This indicated that convalescent sera alone have neutralizing antibodies to inhibit 86% of infection (Figure 1). When we added anti-IgG1-131 antibody or anti-IgG Fc antibody to convalescent serum instead of the flu antibody, the inhibition of infection was similar (82% and 81%, respectively), but not improved (Figure 1). As a positive control, a SARS-CoV-2 antibody was added to convalescent serum and there were no foci detected, indicating that 100% inhibition of infection occurred (Figure 1). From this experiment we determined that the convalescent serum had high neutralizing antibodies to the extent that there was not much room to see an improvement in neutralization by the addition of purified antibodies. We did not see enhanced neutralization when our antibodies of interest (anti-IgG1-131 or anti-IgG Fc) were added compared with an irrelevant flu antibody, which suggests that either these rheumatoid factors do not enhance neutralization of SARS-CoV-2 or there were not enough purified antibodies to see their effects.

To investigate whether increasing the purified antibodies would reveal effects on virus neutralization, we increased the added antibodies to 450ng and decreased the volume of serum (so that there would be less neutralization from the convalescent serum and more of a range to see potential effects of the antibodies). By decreasing the volume of convalescent serum used, 60% inhibition (Figure 2) was achieved which was better than the 86% achieved in the previous experiment. Again, in the negative control (irrelevant influenza B antibody added to naive serum) no inhibition was expected and foci numbers were determined to represent 0% inhibition of infection (Figure 2). By comparison, the positive control (anti-SARS-CoV-2 monoclonal antibody added to naive serum) resulted in 99.5% inhibition (Figure 2). In the experimental groups, purified antibodies were added to convalescent serum to see whether they enhanced neutralization (measured as increasing the % inhibition of infection). The addition of anti-IgG1-131 antibodies purified from COVID-19 convalescent serum or anti-IgG1-219J antibodies from rheumatoid arthritis serum did not increase the % inhibition. However, when anti-IgG Fc

antibodies were added to convalescent serum, 67% inhibition of infection was achieved (Figure 2). This was an extremely modest increase, but it indicated that anti-IgG Fc antibodies might enhance neutralization if experimental conditions are appropriate. To try to determine if anti-IgG Fc antibodies enhanced neutralization, we wanted to see if this result was reproducible and whether increasing the amount of anti-IgG Fc antibodies would further increase neutralization.

Since we hypothesized that rheumatoid factors may enhance neutralization by complement, we considered whether there was enough complement present in the system for rheumatoid factors to amplify complements' effects. We had decreased the volume and diluted the convalescent serum used in the FRNT so that the neutralizing antibodies did not mask potential effects of added rheumatoid factors. However, this serum was also the source of complement. To increase complement without increasing neutralizing antibodies, we decided to add pooled naive sera to serve as a larger complement source. We also considered whether the order of reagents mattered. For example, we hypothesized that rheumatoid factors would bind virus-antibody complexes and serve as increased sites for complement binding. However, we had added the rheumatoid factors, virus, and convalescent serum all at once, so virus-antibody complexes likely had not yet formed, which may have hindered rheumatoid factor binding. Therefore, we designed a third experiment where these concerns were addressed. We sequentially added reagents with incubations to allow 1) virus-antibody complexes to form before rheumatoid factors were added, and 2) rheumatoid factors to bind the complexes before the complement source was introduced. We hypothesized that these changes would amplify rheumatoid factors' effects and result in increased % inhibition of infection.

In the third experiment, when the irrelevant influenza B antibody was added to naive serum, the foci numbers were determined to represent 100% infection and 0% inhibition (Figure 3). When the irrelevant influenza B antibody was added at 450ng or 750ng to convalescent serum, 56%

or 58% inhibition was achieved, respectively, which represents the contribution of the neutralizing antibodies in the diluted convalescent serum. When anti-IgG Fc antibodies were added at 450ng or 750ng, inhibition increased to 74% and 91%, respectively (Figure 3). This indicates that there may be increased inhibition of infection in the conditions when rheumatoid factor antibodies were added after the virus and convalescent serum had incubated alone, prior to rheumatoid factor addition and complement addition. In this first study, increasing the complement source with the addition of pooled naive sera may also have contributed to the results. Additionally, increasing the purified rheumatoid factors increased the inhibition further from 74% to 91%. These variables of allowing virus-antibody complexes to form before adding rheumatoid factors, increasing complement, and increasing purified rheumatoid factors, resulted in increased SARS-CoV-2 neutralization. These findings represent a sample size of one, and additional experiments are needed to determine whether the data are reproducible.

DISCUSSION

Rheumatoid factors can be polyreactive and are known to bind self and exogenous antigens [10]. Historically, two rheumatoid factor conformational epitopes, the Ga determinant and hinge of IgG were described [11, 12]. Additional rheumatoid factor linear epitopes in the IgG Fc region have been discovered more recently [13]. When IgG binds an antigen, a conformational change occurs, which reveals rheumatoid factor binding sites [14], thereby preventing rheumatoid factors from binding unbound IgG in circulation [15]. Thus, in our experiments, rheumatoid factors are likely binding to revealed IgG Fc sites when IgG forms immune complexes with SARS-CoV-2. An initial next step will be to repeat the third experiment with biological replicates in order to draw significant conclusions. Another possibility is that rheumatoid factors could bind to pathogens directly [1], especially given that rheumatoid factors post-COVID-19 were able to bind viral antigens including spike protein (Chapter 4). To investigate this, future studies are needed in which anti-IgG1-131 antibodies are added directly to the FRNT in the absence of

convalescent serum to see whether the antibodies can neutralize SARS-CoV-2 directly in the absence of anti-SARS-CoV-2 antibodies and neutralizing antibodies.

Complement in serum is unstable. Although the human serum that is processed for the biobank is frozen at -80 degrees Celsius, fluctuations of complement levels due to temperature changes and storage conditions could occur [16, 17]. Additionally, the biobank sera are precious and in limited supply. Other complement sources could be tried in these FRNT experiments. Guinea pig sera has been used as a complement source of choice for viral antigen-antibody systems [18, 19]. Therefore, future experiments may use guinea pig sera as a complement source.

Given the interesting results of the third experiment when the addition of increased anti-IgG Fc antibodies resulted in increased inhibition of infection, future studies will want to continue to investigate the role of anti-IgG Fc antibodies in virus neutralization. Knowing that anti-IgG1-131 antibodies bind viral antigens including spike protein (Chapter 4) makes them interesting to continue studying in the SARS-CoV-2 neutralization assays, despite the results from the second experiment that showed that they did not increase inhibition compared to an irrelevant influenza B antibody. Perhaps the modifications performed in the third experiment (adding purified antibodies after virus and convalescent serum have incubated and formed immune complexes, adding an additional source of complement after antibody incubation, and increasing the amount of antibody added) will enhance the effects of anti-IgG1-131 antibodies in the system. Alternatively, perhaps other experimental conditions are needed to see the effects of these antibodies such as an increased amount of antibody compared to the anti-IgG Fc antibodies or different incubations.

Anti-IgG1-293 antibodies may neutralize SARS-CoV-2, given the similar results in Figure 2 between anti-IgG Fc antibodies and anti-IgG1-293 antibodies. Anti-IgG1-293 antibodies were

also cross-reactive with the mem-8 peptide (Chapter 4), providing further evidence that these antibodies may bind SARS-CoV-2, which could be an early step leading to complement activation. In the second experiment, all the antibodies added were 450ng, except anti-IgG1-293, which was 150ng. Even at one-third the amount, these antibodies produced an effect that was similar to the anti-IgG Fc antibodies. Therefore, if the amount of anti-IgG1-293 antibodies was increased and if modifications were made similar to the third experiment (adding reagents during sequential incubations and adding a separate complement source), the SARS-CoV-2 neutralizing effects of anti-IgG1-293 may be more pronounced. However, there were fewer COVID-19 convalescent subjects who had detectable antibodies against IgG1-293 (Chapter 4), and subjects that did have anti-IgG1-293 antibodies had lower concentrations than the concentrations recovered for anti-IgG1-131. This reagent limitation may be a reason to focus on other rheumatoid factors.

Future experiments could investigate additional questions beyond the mechanism of rheumatoid factors enhancing virus neutralization. In the experiments presented here, the ancestral viral strain was used because the COVID-19 convalescent subjects were infected in the spring of 2020 before variants of concern were in circulation in the community. It would also be interesting to investigate whether rheumatoid factors were protective against other variants (such as Omicron). Variants of concern are difficult to contain and treat because they have higher infectivity and do not respond as well to treatments, due to mutations in key regions such as host receptor binding [20]. However, since rheumatoid factors may be primarily binding to virus-antibody complexes by revealed sites in the Fc region of IgG, viral mutations may not impede this interaction. If rheumatoid factors could still bind immune complexes and increase multivalency for complement binding and activation, they may be able to amplify signals to clear infection, even among emerging variants of concern. In that case, rheumatoid factors could potentially serve as a therapeutic antibody regardless of variant mutations. Expanding further on

this point, rheumatoid factors may generally be able to neutralize pathogens by binding pathogen-antibody immune complexes and allowing more complement fixation. If this is true, other respiratory viruses such as influenza could be used in neutralization assays to determine if rheumatoid factors could enhance influenza neutralization. This mechanism of rheumatoid factor enhancing neutralization of SARS-CoV-2 may not be coronavirus specific. The general pro-resolution characteristics of rheumatoid factors may be generalizable to other inflammatory states.

FIGURE LEGENDS

Figure 1. COVID-19 convalescent serum has high neutralizing antibodies regardless of additional antibodies added to neutralization assay. By focus reduction neutralization test (FRNT), % inhibition of SARS-CoV-2 infection was determined for naive serum with an irrelevant influenza (flu) B monoclonal antibody, or convalescent (conv.) serum with flu, anti-IgG1-131 (131), anti-IgG Fc (Fc), anti-mem-8 (m), or anti-SARS-CoV-2 (CoV-2) antibodies.

Figure 2. anti-IgG Fc antibodies may enhance neutralization. By focus reduction neutralization test (FRNT), % inhibition of SARS-CoV-2 infection was determined for naive serum with an irrelevant influenza (flu) B monoclonal antibody (negative control), or naive serum with a SARS-CoV-2 monoclonal antibody (positive control). Convalescent (conv.) serum with flu, anti-IgG1-131 (131), anti-IgG1-293 (293), anti-IgG1-219J (219J), anti-IgG Fc (Fc), anti-mem-8 (m), or anti-spike-1253 (s) antibodies was also assessed for % inhibition of SARS-CoV-2 infection.

Figure 3. In the presence of complement, anti-IgG Fc antibodies may enhance SARS-CoV-2 neutralization when added sequentially after virus-antibody complexes form. By focus reduction neutralization test (FRNT), % inhibition of SARS-CoV-2 infection was

determined for naive serum with an irrelevant influenza (flu) B monoclonal antibody (negative control), convalescent serum with flu (to represent neutralization from convalescent serum neutralizing antibodies), or convalescent serum with anti-IgG Fc (Fc) antibodies at two different amounts (450ng or 750ng). Pooled naive serum was added to all conditions after immune complex incubation with antibodies to serve as a complement source.

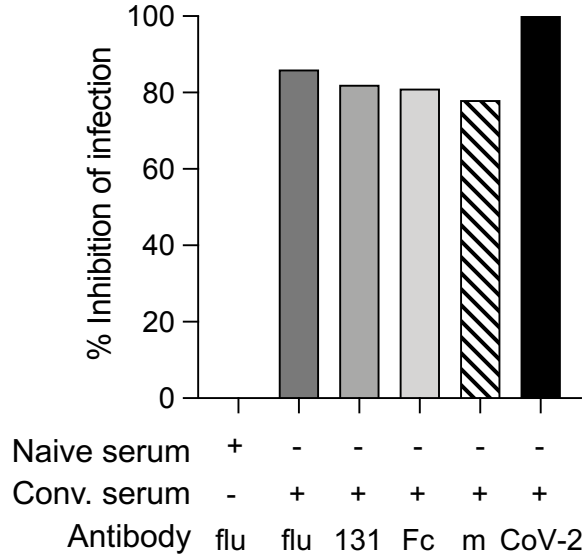

Figure 1. COVID-19 convalescent serum has high neutralizing antibodies regardless of additional antibodies added to neutralization assay. By focus reduction neutralization test (FRNT), % inhibition of SARS-CoV-2 infection was determined for naive serum with an irrelevant influenza (flu) B monoclonal antibody, or convalescent (conv.) serum with flu, anti-IgG1-131 (131), anti-IgG Fc (Fc), anti-mem-8 (m), or anti-SARS-CoV-2 (CoV-2) antibodies.

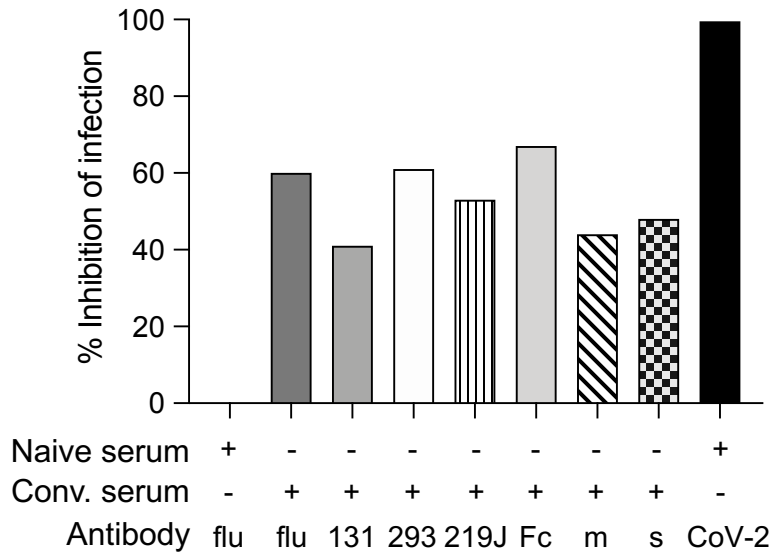

Figure 2. anti-IgG Fc antibodies may enhance neutralization. By focus reduction neutralization test (FRNT), % inhibition of SARS-CoV-2 infection was determined for naive serum with an irrelevant influenza (flu) B monoclonal antibody (negative control), or naive serum with a SARS-CoV-2 monoclonal antibody (positive control). Convalescent (conv.) serum with flu, anti-IgG1-131 (131), anti-IgG1-293 (293), anti-IgG1-219J (219J), anti-IgG Fc (Fc), anti-mem-8 (m), or anti-spike-1253 (s) antibodies was also assessed for % inhibition of SARS-CoV-2 infection.

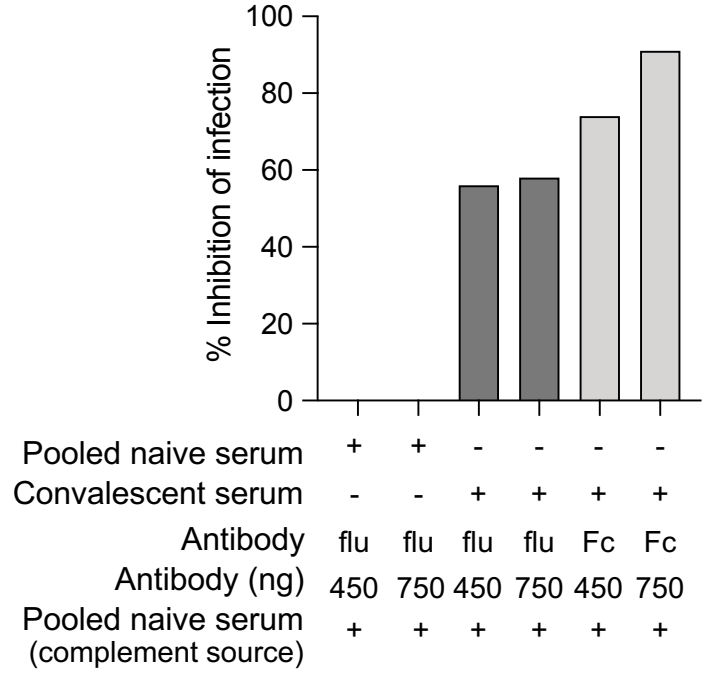

Figure 3. In the presence of complement, anti-IgG Fc antibodies may enhance SARS-CoV-2 neutralization when added sequentially after virus-antibody complexes form. By focus reduction neutralization test (FRNT), % inhibition of SARS-CoV-2 infection was determined for naive serum with an irrelevant influenza (flu) B monoclonal antibody (negative control), convalescent serum with flu (to represent neutralization from convalescent serum neutralizing antibodies), or convalescent serum with anti-IgG Fc (Fc) antibodies at two different amounts (450ng or 750ng). Pooled naive serum was added to all conditions after immune complex incubation with antibodies to serve as a complement source.

REFERENCES

1. Thé J, Ebersole JL. Rheumatoid factor from periodontitis patients cross-reacts with epitopes on oral bacteria. Oral Dis **1996**; 2:253-62.
2. Ashe WK, Daniels CA, Scott GS, Notkins AL. Interaction of rheumatoid factor with infectious herpes simplex virus-antibody complexes. Science **1971**; 172:176-7.
3. Tanimoto K, Cooper NR, Johnson JS, Vaughan JH. Complement fixation by rheumatoid factor. J Clin Invest **1975**; 55:437-45.
4. Van Snick JL, Van Roost E, Markowetz B, Cambiaso CL, Masson PL. Enhancement by IgM rheumatoid factor of in vitro ingestion by macrophages and in vivo clearance of aggregated IgG or antigen-antibody complexes. Eur J Immunol **1978**; 8:279-85.
5. Anaya JM, Monsalve DM, Rojas M, et al. Latent rheumatic, thyroid and phospholipid autoimmunity in hospitalized patients with COVID-19. J Transl Autoimmun **2021**; 4:100091.
6. Xu C, Fan J, Luo Y, et al. Prevalence and Characteristics of Rheumatoid-Associated Autoantibodies in Patients with COVID-19. J Inflamm Res **2021**; 14:3123-8.
7. Holmes CL, Peyton CG, Bier AM, et al. Reduced IgG titers against pertussis in rheumatoid arthritis: Evidence for a citrulline-biased immune response and medication effects. PLoS One **2019**; 14:e0217221.
8. Amjadi MF, O'Connell SE, Armbrust T, et al. Specific COVID-19 Symptoms Correlate with High Antibody Levels against SARS-CoV-2. Immunohorizons **2021**; 5:466-76.
9. Takashita E, Kinoshita N, Yamayoshi S, et al. Efficacy of Antibodies and Antiviral Drugs against Covid-19 Omicron Variant. N Engl J Med **2022**; 386:995-8.
10. Nakamura M, Burastero SE, Notkins AL, Casal P. Human monoclonal rheumatoid factor-like antibodies from CD5 (Leu-1)+ B cells are polyreactive. J Immunol **1988**; 140:4180-6.
11. Terness P, Kohl I, Hübener G, et al. The natural human IgG anti-F(ab')2 antibody recognizes a conformational IgG1 hinge epitope. J Immunol **1995**; 154:6446-52.
12. Artandi SE, Calame KL, Morrison SL, Bonagura VR. Monoclonal IgM rheumatoid factors bind IgG at a discontinuous epitope comprised of amino acid loops from heavy-chain constant-region domains 2 and 3. Proc Natl Acad Sci U S A **1992**; 89:94-8.
13. Mergaert AM, Zheng Z, Denny MF, et al. Rheumatoid Factor and Anti-Modified Protein Antibody Reactivities Converge on IgG Epitopes. Arthritis Rheumatol **2022**; 74:984-91.
14. Oda M, Kozono H, Morii H, Azuma T. Evidence of allosteric conformational changes in the antibody constant region upon antigen binding. Int Immunol **2003**; 15:417-26.
15. Maibom-Thomsen SL, Trier NH, Holm BE, et al. Immunoglobulin G structure and rheumatoid factor epitopes. PLoS One **2019**; 14:e0217624.
16. Mollnes TE, Garred P, Bergseth G. Effect of time, temperature and anticoagulants on in vitro complement activation: consequences for collection and preservation of samples to be examined for complement activation. Clin Exp Immunol **1988**; 73:484-8.
17. Yang S, McGookey M, Wang Y, Cataland SR, Wu HM. Effect of blood sampling, processing, and storage on the measurement of complement activation biomarkers. Am J Clin Pathol **2015**; 143:558-65.
18. Baumgarten A. Viral immunodiagnosis. Yale J Biol Med **1980**; 53:71-83.
19. Sethi J, Pei D, Hirshaut Y. Choice and specificity of complement in complement fixation assay. J Clin Microbiol **1981**; 13:888-90.
20. Chen J, Wang R, Gilby NB, Wei GW. Omicron Variant (B.1.1.529): Infectivity, Vaccine Breakthrough, and Antibody Resistance. J Chem Inf Model **2022**; 62:412-22.

Appendix B: Contributions to additional published works

The landscape of antibody binding in SARS-CoV-2 infection

Anna S. Heffron[1], Sean J. McIlwain[2,3], Maya F. Amjadi[4], David A. Baker[1], Saniya Khullar[2], Tammy Armbrust[5], Peter J. Halfmann[5], Yoshihiro Kawaoka[5], Ajay K. Sethi[6], Ann C. Palmenberg[7], Miriam A. Shelef [4,8], David H. O'Connor[1,9], Irene M. Ong[2,3,10]

[1]Department of Pathology and Laboratory Medicine, University of Wisconsin-Madison, Madison, WI, United States of America
[2]Department of Biostatistics and Medical Informatics, University of Wisconsin-Madison, Madison, WI, United States of America
[3]University of Wisconsin Carbone Comprehensive Cancer Center, University of Wisconsin-Madison, Madison, WI, United States of America
[4]Department of Medicine, University of Wisconsin-Madison, Madison, WI, United States of America
[5]Department of Pathobiological Sciences, School of Veterinary Medicine, Influenza Research Institute, University of Wisconsin-Madison, Madison, Wisconsin, United States of America
[6]Department of Population Health Sciences, University of Wisconsin-Madison, Madison, WI, United States of America
[7]Department of Biochemistry, Institute for Molecular Virology, University of Wisconsin–Madison, Madison, WI, United States of America
[8]William S. Middleton Memorial Veterans Hospital, Madison, WI, United States of America
[9]Wisconsin National Primate Research Center, University of Wisconsin-Madison, Madison, Wisconsin, United States of America
[10]Department of Obstetrics and Gynecology, University of Wisconsin-Madison, Madison, WI, United States of America

PLOS Biol. 2021 Jun 18;19(6):e3001265. doi: 10.1371/journal.pbio.3001265. PMID: 34143766; PMCID: PMC8245122.

Abstract:
The search for potential antibody-based diagnostics, vaccines, and therapeutics for pandemic severe acute respiratory syndrome coronavirus 2 (SARS-CoV-2) has focused almost exclusively on the spike (S) and nucleocapsid (N) proteins. Coronavirus membrane (M), ORF3a, and ORF8 proteins are humoral immunogens in other coronaviruses (CoVs) but remain largely uninvestigated for SARS-CoV-2. Here, we use ultradense peptide microarray mapping to show that SARS-CoV-2 infection induces robust antibody responses to epitopes throughout the SARS-CoV-2 proteome, particularly in M, in which 1 epitope achieved excellent diagnostic accuracy. We map 79 B cell epitopes throughout the SARS-CoV-2 proteome and demonstrate that antibodies that develop in response to SARS-CoV-2 infection bind homologous peptide sequences in the 6 other known human CoVs. We also confirm reactivity against 4 of our top-ranking epitopes by enzyme-linked immunosorbent assay (ELISA). Illness severity correlated with increased reactivity to 9 SARS-CoV-2 epitopes in S, M, N, and ORF3a in our population. Our results demonstrate previously unknown, highly reactive B cell epitopes throughout the full proteome of SARS-CoV-2 and other CoV proteins.

Contributions:
I processed human COVID-19 convalescent serum, abstracted clinical and demographic information from electronic medical records, selected human samples for the array, performed and analyzed ELISA experiments, made Figure 6, and assisted in manuscript writing and editing.

Rheumatoid Factor and Anti–Modified Protein Antibody Reactivities Converge on IgG Epitopes

Aisha M. Mergaert[1,3], Zihao Zheng [2,3], Michael F. Denny[3], Maya F. Amjadi[3], S. Janna Bashar[3], Michael A. Newton[2], Vivianne Malmström[4], Caroline Grönwall[4], Sara S. McCoy[3], Miriam A. Shelef[3,5]

[1]Department of Pathology and Laboratory Medicine, University of Wisconsin-Madison, Madison, USA
[2]Department of Statistics, University of Wisconsin-Madison, Madison, USA
[3]Department of Medicine, University of Wisconsin-Madison, Madison, USA
[4]Division of Rheumatology, Department of Medicine, Karolinska Institutet, Karolinska University Hospital, Stockholm, Sweden
[5]William S. Middleton Memorial Veterans Hospital, Madison, USA

Arthritis Rheumatol. 2022 Jun;74(6):984-991. doi: 10.1002/art.42064. Epub 2022 Apr 10. PMID: 35001558; PMCID: PMC9156533.

Abstract:
Objective: Rheumatoid arthritis (RA) patients often develop rheumatoid factors (RFs), antibodies that bind IgG Fc, and anti-modified protein antibodies (AMPAs), multireactive autoantibodies that commonly bind citrullinated, homocitrullinated, and acetylated antigens. Recently, antibodies that bind citrulline-containing IgG epitopes were discovered in RA, suggesting that additional undiscovered IgG epitopes could exist and that IgG could be a shared antigen for RFs and AMPAs. This study was undertaken to reveal new IgG epitopes in rheumatic disease and to determine if multireactive AMPAs bind IgG.
Methods: Using sera from patients with RA, systemic lupus erythematosus, Sjögren's disease (SjD), or spondyloarthropathy, IgG binding to native, citrulline-containing, and homocitrulline-containing linear epitopes of the IgG constant region was evaluated by peptide array, with highly bound epitopes further evaluated by enzyme-linked immunosorbent assay (ELISA). Binding of monoclonal AMPAs to IgG-derived peptides and IgG Fc was also evaluated by ELISA.
Results: Seropositive RA sera showed high IgG binding to multiple citrulline- and homocitrulline-containing IgG-derived peptides, whereas anti-SSA+ sera from SjD patients showed consistent binding to a single linear native epitope of IgG in the hinge region. Monoclonal AMPAs bound citrulline- and homocitrulline-containing IgG peptides and modified IgG Fc.
Conclusion: The repertoire of epitopes bound by AMPAs includes modified IgG epitopes, positioning IgG as a common antigen that connects the otherwise divergent reactivities of RFs and AMPAs.

Contributions: I performed and analyzed ELISA experiments, performed statistical analyses, and made Supplemental Tables 1-4. I assisted in manuscript writing and editing.

Bibliography

1. Birdsall HH, Casadevall A. Adaptive Immunity: Antibodies and Immunodeficiencies. Mandell, Douglas, and Bennett's Principles and Practice of Infectious Diseases. Ninth Edition ed: Elsevier, Inc., **2020**:35-50.
2. Janeway CAJ, Travers P, Walport M, Shlomchik MJ. The structure of a typical antibody molecule. Immunobiology: The Immune System in Health and Disease. 5th Edition ed. New York: Garland Science, **2001**.
3. Stanfield RL, Wilson IA. Antibody Structure. Microbiol Spectr **2014**; 2.
4. Antibodies. In: Flaherty DK, ed. Immunology for Pharmacy: Mosby, **2012**:70-8.
5. Garson JA, Quindlen EA, Kornblith PL. Complement fixation by IgM and IgG autoantibodies on cultured human glial cells. J Neurosurg **1981**; 55:19-26.
6. Bindon CI, Hale G, Brüggemann M, Waldmann H. Human monoclonal IgG isotypes differ in complement activating function at the level of C4 as well as C1q. J Exp Med **1988**; 168:127-42.
7. Vidarsson G, Dekkers G, Rispens T. IgG subclasses and allotypes: from structure to effector functions. Front Immunol **2014**; 5:520.
8. Allen HC, Sharma P. Histology, Plasma Cells. StatPearls. Treasure Island (FL): StatPearls Publishing, **2022**.
9. Janeway CJ, Travers P, Walport M, Shlomchik M. The rearrangement of antigen-receptor gene segments controls lymphocyte development. Immunobiology: The Immune System in Health and Disease. 5th Edition ed. New York: Garland Science, **2001**.
10. Nemazee D, Buerki K. Clonal deletion of autoreactive B lymphocytes in bone marrow chimeras. Proc Natl Acad Sci U S A **1989**; 86:8039-43.
11. Lee S, Ko Y, Kim TJ. Homeostasis and regulation of autoreactive B cells. Cell Mol Immunol **2020**; 17:561-9.
12. Cyster JG, Allen CDC. B Cell Responses: Cell Interaction Dynamics and Decisions. Cell **2019**; 177:524-40.
13. Allman DM, Ferguson SE, Lentz VM, Cancro MP. Peripheral B cell maturation. II. Heat-stable antigen(hi) splenic B cells are an immature developmental intermediate in the production of long-lived marrow-derived B cells. J Immunol **1993**; 151:4431-44.
14. Shinomiya N, Kuratsuji T, Yata J. The role of T cells in immunoglobulin class switching of specific antibody production system in vitro in humans. Cell Immunol **1989**; 118:239-49.
15. Kelsoe G. The germinal center: a crucible for lymphocyte selection. Semin Immunol **1996**; 8:179-84.
16. Kranich J, Krautler NJ. How Follicular Dendritic Cells Shape the B-Cell Antigenome. Front Immunol **2016**; 7:225.
17. LeBien TW, Tedder TF. B lymphocytes: how they develop and function. Blood **2008**; 112:1570-80.
18. Calame KL. Plasma cells: finding new light at the end of B cell development. Nat Immunol **2001**; 2:1103-8.
19. Slifka MK, Ahmed R. Long-lived plasma cells: a mechanism for maintaining persistent antibody production. Curr Opin Immunol **1998**; 10:252-8.
20. Brooks JF, Murphy PR, Barber JEM, Wells JW, Steptoe RJ. Peripheral Tolerance Checkpoints Imposed by Ubiquitous Antigen Expression Limit Antigen-Specific B Cell Responses under Strongly Immunogenic Conditions. J Immunol **2020**; 205:1239-47.
21. Sathe A, Cusick J. Biochemistry, Immunoglobulin M. StatPearls: StatPearls Publishing, **2021**.
22. Bandilla KK, McDuffie FC, Gleich GJ. Immunoglobulin classes of antibodies produced in the primary and secondary responses in man. Clin Exp Immunol **1969**; 5:627-41.
23. Palm AE, Henry C. Remembrance of Things Past: Long-Term B Cell Memory After Infection and Vaccination. Front Immunol **2019**; 10:1787.

24. Palma J, Tokarz-Deptuła B, Deptuła J, Deptuła W. Natural antibodies - facts known and unknown. Cent Eur J Immunol **2018**; 43:466-75.
25. Reyneveld GI, Savelkoul HFJ, Parmentier HK. Current Understanding of Natural Antibodies and Exploring the Possibilities of Modulation Using Veterinary Models. A Review. Front Immunol **2020**; 11:2139.
26. Sela-Culang I, Kunik V, Ofran Y. The structural basis of antibody-antigen recognition. Front Immunol **2013**; 4:302.
27. Benjamin DC, Perdue SS. Site-Directed Mutagenesis in Epitope Mapping. Methods **1996**; 9:508-15.
28. Dougan DA, Malby RL, Gruen LC, Kortt AA, Hudson PJ. Effects of substitutions in the binding surface of an antibody on antigen affinity. Protein Eng **1998**; 11:65-74.
29. Van Regenmortel MH. From absolute to exquisite specificity. Reflections on the fuzzy nature of species, specificity and antigenic sites. J Immunol Methods **1998**; 216:37-48.
30. Wedemayer GJ, Patten PA, Wang LH, Schultz PG, Stevens RC. Structural insights into the evolution of an antibody combining site. Science **1997**; 276:1665-9.
31. Alberts B, A J, Lewis J. The Generation of Antibody Diversity. Molecular Biology of the Cell. 4th Edition ed. New York: Garland Science, **2002**.
32. Sela M, Schechter B, Schechter I, Borek F. Antibodies to Sequential and Conformational Determinants. Vol. 32. Cold Spring Harbor Symposia on Quantitative Biology: Cold Spring Harbor Laboratory Press, **1967**:537-45.
33. Forsström B, Axnäs BB, Rockberg J, Danielsson H, Bohlin A, Uhlen M. Dissecting antibodies with regards to linear and conformational epitopes. PLoS One **2015**; 10:e0121673.
34. Gershoni JM, Roitburd-Berman A, Siman-Tov DD, Tarnovitski Freund N, Weiss Y. Epitope mapping: the first step in developing epitope-based vaccines. BioDrugs **2007**; 21:145-56.
35. Irving MB, Pan O, Scott JK. Random-peptide libraries and antigen-fragment libraries for epitope mapping and the development of vaccines and diagnostics. Curr Opin Chem Biol **2001**; 5:314-24.
36. Toride King M, Brooks CL. Epitope Mapping of Antibody-Antigen Interactions with X-Ray Crystallography. Methods Mol Biol **2018**; 1785:13-27.
37. Artandi SE, Calame KL, Morrison SL, Bonagura VR. Monoclonal IgM rheumatoid factors bind IgG at a discontinuous epitope comprised of amino acid loops from heavy-chain constant-region domains 2 and 3. Proc Natl Acad Sci U S A **1992**; 89:94-8.
38. Szymczak LC, Kuo HY, Mrksich M. Peptide Arrays: Development and Application. Anal Chem **2018**; 90:266-82.
39. Buus S, Rockberg J, Forsström B, Nilsson P, Uhlen M, Schafer-Nielsen C. High-resolution mapping of linear antibody epitopes using ultrahigh-density peptide microarrays. Mol Cell Proteomics **2012**; 11:1790-800.
40. Powell AM, Black MM. Epitope spreading: protection from pathogens, but propagation of autoimmunity? Clin Exp Dermatol **2001**; 26:427-33.
41. Sokolove J, Bromberg R, Deane KD, et al. Autoantibody epitope spreading in the pre-clinical phase predicts progression to rheumatoid arthritis. PLoS One **2012**; 7:e35296.
42. Kongpachith S, Lingampalli N, Ju CH, et al. Affinity Maturation of the Anti-Citrullinated Protein Antibody Paratope Drives Epitope Spreading and Polyreactivity in Rheumatoid Arthritis. Arthritis Rheumatol **2019**; 71:507-17.
43. Weiss SR. Forty years with coronaviruses. J Exp Med **2020**; 217.
44. Liu DX, Liang JQ, Fung TS. Human Coronavirus-229E, -OC43, -NL63, and -HKU1 (*Coronaviridae*): Encyclopedia of Virology, **2021**:428-40.
45. Zhu Z, Lian X, Su X, Wu W, Marraro GA, Zeng Y. From SARS and MERS to COVID-19: a brief summary and comparison of severe acute respiratory infections caused by three highly pathogenic human coronaviruses. Respir Res **2020**; 21:224.

46. WHO Director-General's opening remarks at the media briefing on COVID-19- 11 March 2020: World Health Organization, **2020**.
47. Lamba M, Mishra PR, Verma R, Bharti A, Punia V, Mittal S. The COVID-19 Clinical Spectrum and the Effect of Associated Comorbidities on Illness Severity in the North Indian Population: A Cross-Sectional Study. Cureus **2022**; 14:e28192.
48. Carrillo Hernandez-Rubio J, Sanchez-Carpintero Abad M, Yordi Leon A, et al. Outcomes of an intermediate respiratory care unit in the COVID-19 pandemic. PLoS One **2020**; 15:e0243968.
49. WHO Coronavirus Dashboard. January 23, 2023 ed. online, **2023**.
50. Satarker S, Nampoothiri M. Structural Proteins in Severe Acute Respiratory Syndrome Coronavirus-2. Arch Med Res **2020**; 51:482-91.
51. Singh D, Yi SV. On the origin and evolution of SARS-CoV-2. Exp Mol Med **2021**; 53:537-47.
52. Liu H, Wei P, Kappler JW, Marrack P, Zhang G. SARS-CoV-2 Variants of Concern and Variants of Interest Receptor Binding Domain Mutations and Virus Infectivity. Front Immunol **2022**; 13:825256.
53. SARS-CoV-2 Variant Classifications and Definitions. Centers for Disease Control and Prevention, **2022**.
54. Bálint G, Vörös-Horváth B, Széchenyi A. Omicron: increased transmissibility and decreased pathogenicity. Signal Transduct Target Ther **2022**; 7:151.
55. Mathieu E, Ritchie H, Rodés-Guirao L, et al. Coronavirus Pandemic (COVID-19). Coronavirus (COVID-19) Vaccinations: OurWorldInData.org, **2020**.
56. Park JW, Lagniton PNP, Liu Y, Xu RH. mRNA vaccines for COVID-19: what, why and how. Int J Biol Sci **2021**; 17:1446-60.
57. Zhang NN, Li XF, Deng YQ, et al. A Thermostable mRNA Vaccine against COVID-19. Cell **2020**; 182:1271-83.e16.
58. Mascellino MT, Di Timoteo F, De Angelis M, Oliva A. Overview of the Main Anti-SARS-CoV-2 Vaccines: Mechanism of Action, Efficacy and Safety. Infect Drug Resist **2021**; 14:3459-76.
59. Coronavirus (COVID-19) Update: FDA Limits Use of Janssen COVID-19 Vaccine to Certain Individuals: U.S. Food & Drug Administration, **2022**.
60. Sharifian-Dorche M, Bahmanyar M, Sharifian-Dorche A, Mohammadi P, Nomovi M, Mowla A. Vaccine-induced immune thrombotic thrombocytopenia and cerebral venous sinus thrombosis post COVID-19 vaccination; a systematic review. J Neurol Sci **2021**; 428:117607.
61. Heath PT, Galiza EP, Baxter DN, et al. Safety and Efficacy of NVX-CoV2373 Covid-19 Vaccine. N Engl J Med **2021**; 385:1172-83.
62. Stay Up to Date with COVID-19 Vaccines Including Boosters: Centers for Disease Control and Prevention, **2023**.
63. LeBlanc JJ, Gubbay JB, Li Y, et al. Real-time PCR-based SARS-CoV-2 detection in Canadian laboratories. J Clin Virol **2020**; 128:104433.
64. Sethuraman N, Jeremiah SS, Ryo A. Interpreting Diagnostic Tests for SARS-CoV-2. JAMA **2020**; 323:2249-51.
65. Nolan T, Hands RE, Bustin SA. Quantification of mRNA using real-time RT-PCR. Nat Protoc **2006**; 1:1559-82.
66. Gupta-Wright A, Macleod CK, Barrett J, et al. False-negative RT-PCR for COVID-19 and a diagnostic risk score: a retrospective cohort study among patients admitted to hospital. BMJ Open **2021**; 11:e047110.
67. Wölfel R, Corman VM, Guggemos W, et al. Virological assessment of hospitalized patients with COVID-2019. Nature **2020**; 581:465-9.
68. Fajardo Á, Perbolianachis P, Ferreiro I, Moreno P, Moratorio G. Molecular accuracy vs antigenic speed: SARS-CoV-2 testing strategies. Curr Opin Pharmacol **2022**; 62:152-8.

69. Jakobsen KK, Jensen JS, Todsen T, et al. Accuracy and cost description of rapid antigen test compared with reverse transcriptase-polymerase chain reaction for SARS-CoV-2 detection. Dan Med J **2021**; 68.
70. Yamayoshi S, Sakai-Tagawa Y, Koga M, et al. Comparison of Rapid Antigen Tests for COVID-19. Viruses **2020**; 12.
71. O'Farrell B. Evolution in Lateral Flow–Based Immunoassay Systems. Lateral Flow Immunoassay: Humana Press, **2008**:1-33.
72. Peto T, Team UC-LFO. COVID-19: Rapid antigen detection for SARS-CoV-2 by lateral flow assay: A national systematic evaluation of sensitivity and specificity for mass-testing. EClinicalMedicine **2021**; 36:100924.
73. Larremore DB, Wilder B, Lester E, et al. Test sensitivity is secondary to frequency and turnaround time for COVID-19 screening. Sci Adv **2021**; 7.
74. Love J, Wimmer MT, Toth DJA, et al. Comparison of antigen- and RT-PCR-based testing strategies for detection of SARS-CoV-2 in two high-exposure settings. PLoS One **2021**; 16:e0253407.
75. Ricks S, Kendall EA, Dowdy DW, Sacks JA, Schumacher SG, Arinaminpathy N. Quantifying the potential value of antigen-detection rapid diagnostic tests for COVID-19: a modelling analysis. BMC Med **2021**; 19:75.
76. Dimech W. The Standardization and Control of Serology and Nucleic Acid Testing for Infectious Diseases. Clin Microbiol Rev **2021**; 34:e0003521.
77. Liu C, Yu X, Gao C, et al. Characterization of antibody responses to SARS-CoV-2 in convalescent COVID-19 patients. J Med Virol **2021**; 93:2227-33.
78. Xiao K, Yang H, Liu B, et al. Antibodies Can Last for More Than 1 Year After SARS-CoV-2 Infection: A Follow-Up Study From Survivors of COVID-19. Front Med (Lausanne) **2021**; 8:684864.
79. Wiegand RE, Deng Y, Deng X, et al. Estimated SARS-CoV-2 antibody seroprevalence trends and relationship to reported case prevalence from a repeated, cross-sectional study in the 50 states and the District of Columbia, United States-October 25, 2020-February 26, 2022. Lancet Reg Health Am **2023**; 18:100403.
80. EUA Authorized Serology Test Performance. fda.gov, **2021**.
81. Macdonald PJ, Schaub JM, Ruan Q, Williams CL, Prostko JC, Tetin SY. Affinity of anti-spike antibodies to three major SARS-CoV-2 variants in recipients of three major vaccines. Commun Med (Lond) **2022**; 2:109.
82. Shrotri M, Fragaszy E, Nguyen V, et al. Spike-antibody responses to COVID-19 vaccination by demographic and clinical factors in a prospective community cohort study. Nat Commun **2022**; 13:5780.
83. Long QX, Tang XJ, Shi QL, et al. Clinical and immunological assessment of asymptomatic SARS-CoV-2 infections. Nat Med **2020**; 26:1200-4.
84. Long QX, Tang XJ, Shi QL, et al. Clinical and immunological assessment of asymptomatic SARS-CoV-2 infections. Nat Med **2020**.
85. Engvall E, Perlmann P. Enzyme-linked immunosorbent assay (ELISA). Quantitative assay of immunoglobulin G. Immunochemistry **1971**; 8:871-4.
86. Engvall E, Jonsson K, Perlmann P. Enzyme-linked immunosorbent assay. II. Quantitative assay of protein antigen, immunoglobulin G, by means of enzyme-labelled antigen and antibody-coated tubes. Biochim Biophys Acta **1971**; 251:427-34.
87. StatPearls, **2022**.
88. Vostrý M. Multiplex Immunoassays: Chips and Beads. EJIFCC **2010**; 20:162-5.
89. Morales-Núñez JJ, Muñoz-Valle JF, Torres-Hernández PC, Hernández-Bello J. Overview of Neutralizing Antibodies and Their Potential in COVID-19. Vaccines (Basel) **2021**; 9.
90. Khoury DS, Cromer D, Reynaldi A, et al. Neutralizing antibody levels are highly predictive of immune protection from symptomatic SARS-CoV-2 infection. Nat Med **2021**; 27:1205-11.

91. Perera RA, Mok CK, Tsang OT, et al. Serological assays for severe acute respiratory syndrome coronavirus 2 (SARS-CoV-2), March 2020. Euro Surveill **2020**; 25.
92. Okba NMA, Müller MA, Li W, et al. Severe Acute Respiratory Syndrome Coronavirus 2-Specific Antibody Responses in Coronavirus Disease Patients. Emerg Infect Dis **2020**; 26:1478-88.
93. Mendoza EJ, Manguiat K, Wood H, Drebot M. Two Detailed Plaque Assay Protocols for the Quantification of Infectious SARS-CoV-2. Curr Protoc Microbiol **2020**; 57:ecpmc105.
94. Vanderheiden A, Edara VV, Floyd K, et al. Development of a Rapid Focus Reduction Neutralization Test Assay for Measuring SARS-CoV-2 Neutralizing Antibodies. Curr Protoc Immunol **2020**; 131:e116.
95. Liu KT, Han YJ, Wu GH, Huang KA, Huang PN. Overview of Neutralization Assays and International Standard for Detecting SARS-CoV-2 Neutralizing Antibody. Viruses **2022**; 14.
96. Wang S, Sakhatskyy P, Chou TH, Lu S. Assays for the assessment of neutralizing antibody activities against Severe Acute Respiratory Syndrome (SARS) associated coronavirus (SCV). J Immunol Methods **2005**; 301:21-30.
97. Wouters E, Verbrugghe C, Devloo R, et al. A novel competition ELISA for the rapid quantification of SARS-CoV-2 neutralizing antibodies in convalescent plasma. Transfusion **2021**; 61:2981-90.
98. Walker SN, Chokkalingam N, Reuschel EL, et al. SARS-CoV-2 Assays To Detect Functional Antibody Responses That Block ACE2 Recognition in Vaccinated Animals and Infected Patients. J Clin Microbiol **2020**; 58.
99. Bergmann-Leitner ES, Mease RM, Duncan EH, Khan F, Waitumbi J, Angov E. Evaluation of immunoglobulin purification methods and their impact on quality and yield of antigen-specific antibodies. Malar J **2008**; 7:129.
100. Ayyar BV, Arora S, Murphy C, O'Kennedy R. Affinity chromatography as a tool for antibody purification. Methods **2012**; 56:116-29.
101. Arora S, Saxena V, Ayyar BV. Affinity chromatography: A versatile technique for antibody purification. Methods **2017**; 116:84-94.
102. Janeway CAJ, Travers P, Walport M, Shlomchik MJ. Autoimmune responses are directed against self antigens. Immunobiology: The Immune System in Health and Disease. 5th Edition ed. New York: Garland Science, **2001**.
103. Wardemann H, Yurasov S, Schaefer A, Young JW, Meffre E, Nussenzweig MC. Predominant autoantibody production by early human B cell precursors. Science **2003**; 301:1374-7.
104. Nemazee D. Mechanisms of central tolerance for B cells. Nat Rev Immunol **2017**; 17:281-94.
105. Cashman KS, Jenks SA, Woodruff MC, et al. Understanding and measuring human B-cell tolerance and its breakdown in autoimmune disease. Immunol Rev **2019**; 292:76-89.
106. Menard L, Saadoun D, Isnardi I, et al. The PTPN22 allele encoding an R620W variant interferes with the removal of developing autoreactive B cells in humans. J Clin Invest **2011**; 121:3635-44.
107. Khan MF, Wang G. Environmental Agents, Oxidative Stress and Autoimmunity. Curr Opin Toxicol **2018**; 7:22-7.
108. Bowen RA, Bertholf RL, Holmquist B. Maximizing the value of laboratory tests. Handbook of Diagnostic Endocrinology. 3rd Edition ed, **2021**.
109. Nicolò A, Amendt T, El Ayoubi O, et al. Rheumatoid factor IgM autoantibodies control IgG homeostasis. Front Immunol **2022**; 13:1016263.
110. Burbelo PD, Gordon SM, Waldman M, et al. Autoantibodies are present before the clinical diagnosis of systemic sclerosis. PLoS One **2019**; 14:e0214202.
111. Arbuckle MR, McClain MT, Rubertone MV, et al. Development of autoantibodies before the clinical onset of systemic lupus erythematosus. N Engl J Med **2003**; 349:1526-33.

112. Waaler E. On the occurrence of a factor in human serum activating the specific agglutintion of sheep blood corpuscles. 1939. APMIS **2007**; 115:422-38; discussion 39.
113. ROSE HM, RAGAN C. Differential agglutination of normal and sensitized sheep erythrocytes by sera of patients with rheumatoid arthritis. Proc Soc Exp Biol Med **1948**; 68:1-6.
114. PIKE RM, SULKIN SE, COGGESHALL HC. Serological reactions in rheumatoid arthritis; factors affecting the agglutination of sensitized sheep erythrocytes in rheumatid-arthritis serum. J Immunol **1949**; 63:441-6.
115. Aletaha D, Neogi T, Silman AJ, et al. 2010 Rheumatoid arthritis classification criteria: an American College of Rheumatology/European League Against Rheumatism collaborative initiative. Arthritis Rheum **2010**; 62:2569-81.
116. Witte T, Hartung K, Sachse C, et al. Rheumatoid factors in systemic lupus erythematosus: association with clinical and laboratory parameters. SLE study group. Rheumatol Int **2000**; 19:107-11.
117. Markusse HM, Otten HG, Vroom TM, Smeets TJ, Fokkens N, Breedveld FC. Rheumatoid factor isotypes in serum and salivary fluid of patients with primary Sjögren's syndrome. Clin Immunol Immunopathol **1993**; 66:26-32.
118. Philémon EA, Tume C, Okomo Assoumou MC, et al. A Cross Sectional Study of the Impact of Human Immunodeficiency Virus, Hepatitis B Virus and Hepatitis C Virus on Rheumatoid Factor Production. Arch Rheumatol **2018**; 33:402-7.
119. Lin KM, Chen WM, Tung SY, et al. Prevalence and predictive value of high-positive rheumatoid factor and anti-citrullinated protein antibody levels in nonarthritic patients with chronic hepatitis C infection. Int J Rheum Dis **2019**; 22:116-20.
120. Welch MJ, Fong S, Vaughan J, Carson D. Increased frequency of rheumatoid factor precursor B lymphocytes after immunization of normal adults with tetanus toxoid. Clin Exp Immunol **1983**; 51:299-304.
121. Ingegnoli F, Castelli R, Gualtierotti R. Rheumatoid factors: clinical applications. Dis Markers **2013**; 35:727-34.
122. Terness P, Kohl I, Hübener G, et al. The natural human IgG anti-F(ab')2 antibody recognizes a conformational IgG1 hinge epitope. J Immunol **1995**; 154:6446-52.
123. Maibom-Thomsen SL, Trier NH, Holm BE, et al. Immunoglobulin G structure and rheumatoid factor epitopes. PLoS One **2019**; 14:e0217624.
124. Zheng Z, Mergaert AM, Fahmy LM, et al. Disordered Antigens and Epitope Overlap Between Anti-Citrullinated Protein Antibodies and Rheumatoid Factor in Rheumatoid Arthritis. Arthritis Rheumatol **2020**; 72:262-72.
125. Mergaert AM, Zheng Z, Denny MF, et al. Rheumatoid Factor and Anti-Modified Protein Antibody Reactivities Converge on IgG Epitopes. Arthritis Rheumatol **2022**; 74:984-91.
126. Nakamura M, Burastero SE, Notkins AL, Casal P. Human monoclonal rheumatoid factor-like antibodies from CD5 (Leu-1)+ B cells are polyreactive. J Immunol **1988**; 140:4180-6.
127. Khandpur R, Carmona-Rivera C, Vivekanandan-Giri A, et al. NETs are a source of citrullinated autoantigens and stimulate inflammatory responses in rheumatoid arthritis. Sci Transl Med **2013**; 5:178ra40.
128. Pruijn GJ. Citrullination and carbamylation in the pathophysiology of rheumatoid arthritis. Front Immunol **2015**; 6:192.
129. van Delft MAM, Huizinga TWJ. An overview of autoantibodies in rheumatoid arthritis. J Autoimmun **2020**; 110:102392.
130. Vossenaar ER, Zendman AJ, van Venrooij WJ, Pruijn GJ. PAD, a growing family of citrullinating enzymes: genes, features and involvement in disease. Bioessays **2003**; 25:1106-18.
131. Trouw LA, Rispens T, Toes REM. Beyond citrullination: other post-translational protein modifications in rheumatoid arthritis. Nat Rev Rheumatol **2017**; 13:331-9.

132. Daha NA, Banda NK, Roos A, et al. Complement activation by (auto-) antibodies. Mol Immunol **2011**; 48:1656-65.
133. Trouw LA, Haisma EM, Levarht EW, et al. Anti-cyclic citrullinated peptide antibodies from rheumatoid arthritis patients activate complement via both the classical and alternative pathways. Arthritis Rheum **2009**; 60:1923-31.
134. Chang MH, Nigrovic PA. Antibody-dependent and -independent mechanisms of inflammatory arthritis. JCI Insight **2019**; 4.
135. Nishimura K, Sugiyama D, Kogata Y, et al. Meta-analysis: diagnostic accuracy of anti-cyclic citrullinated peptide antibody and rheumatoid factor for rheumatoid arthritis. Ann Intern Med **2007**; 146:797-808.
136. Steen J, Forsström B, Sahlström P, et al. Recognition of Amino Acid Motifs, Rather Than Specific Proteins, by Human Plasma Cell-Derived Monoclonal Antibodies to Posttranslationally Modified Proteins in Rheumatoid Arthritis. Arthritis Rheumatol **2019**; 71:196-209.
137. Nielsen SF, Bojesen SE, Schnohr P, Nordestgaard BG. Elevated rheumatoid factor and long term risk of rheumatoid arthritis: a prospective cohort study. BMJ **2012**; 345:e5244.
138. Rantapää-Dahlqvist S. What happens before the onset of rheumatoid arthritis? Curr Opin Rheumatol **2009**; 21:272-8.
139. Kelmenson LB, Wagner BD, McNair BK, et al. Timing of Elevations of Autoantibody Isotypes Prior to Diagnosis of Rheumatoid Arthritis. Arthritis Rheumatol **2020**; 72:251-61.
140. Greenblatt HK, Kim HA, Bettner LF, Deane KD. Preclinical rheumatoid arthritis and rheumatoid arthritis prevention. Curr Opin Rheumatol **2020**; 32:289-96.
141. Paul BJ, Kandy HI, Krishnan V. Pre-rheumatoid arthritis and its prevention. Eur J Rheumatol **2017**; 4:161-5.
142. Salma K, Nessrine A, Krystel E, et al. Rheumatoid Arthritis: Seropositivity versus Seronegativity; A Comparative Cross-sectional Study Arising from Moroccan Context. Curr Rheumatol Rev **2020**; 16:143-8.
143. Coffey CM, Crowson CS, Myasoedova E, Matteson EL, Davis JM. Evidence of Diagnostic and Treatment Delay in Seronegative Rheumatoid Arthritis: Missing the Window of Opportunity. Mayo Clin Proc **2019**; 94:2241-8.
144. Reed JH. Transforming mutations in the development of pathogenic B cell clones and autoantibodies. Immunol Rev **2022**; 307:101-15.
145. Newkirk MM. Rheumatoid factors: host resistance or autoimmunity? Clin Immunol **2002**; 104:1-13.
146. Shmerling RH, Delbanco TL. The rheumatoid factor: an analysis of clinical utility. Am J Med **1991**; 91:528-34.
147. Thé J, Ebersole JL. Rheumatoid factor from periodontitis patients cross-reacts with epitopes on oral bacteria. Oral Dis **1996**; 2:253-62.
148. Ashe WK, Daniels CA, Scott GS, Notkins AL. Interaction of rheumatoid factor with infectious herpes simplex virus-antibody complexes. Science **1971**; 172:176-7.
149. Chang SE, Feng A, Meng W, et al. New-onset IgG autoantibodies in hospitalized patients with COVID-19. Nat Commun **2021**; 12:5417.
150. Son K, Jamil R, Chowdhury A, et al. Circulating anti-nuclear autoantibodies in COVID-19 survivors predict long COVID symptoms. Eur Respir J **2023**; 61.
151. Xu C, Fan J, Luo Y, et al. Prevalence and Characteristics of Rheumatoid-Associated Autoantibodies in Patients with COVID-19. J Inflamm Res **2021**; 14:3123-8.
152. Anaya JM, Monsalve DM, Rojas M, et al. Latent rheumatic, thyroid and phospholipid autoimmunity in hospitalized patients with COVID-19. J Transl Autoimmun **2021**; 4:100091.
153. Woodruff MC, Ramonell RP, Haddad NS, et al. Dysregulated naive B cells and de novo autoreactivity in severe COVID-19. Nature **2022**; 611:139-47.
154. Novel Coronavirus (2019-nCoV) Situation Report. World Health Organization **2020**:5.

155. Fu L, Wang B, Yuan T, et al. Clinical characteristics of coronavirus disease 2019 (COVID-19) in China: A systematic review and meta-analysis. J Infect **2020**; 80:656-65.
156. worldometer. https://wwwworldometersinfo/coronavirus/.
157. Haleem A, Javaid M, Vaishya R. Effects of COVID-19 pandemic in daily life. Curr Med Res Pract **2020**; 10:78-9.
158. Chang SC, Wang JT, Huang LM, et al. Longitudinal analysis of Severe Acute Respiratory Syndrome (SARS) coronavirus-specific antibody in SARS patients. Clin Diagn Lab Immunol **2005**; 12:1455-7.
159. Shi Y, Wan Z, Li L, et al. Antibody responses against SARS-coronavirus and its nucleocaspid in SARS patients. J Clin Virol **2004**; 31:66-8.
160. Liu L, Xie J, Sun J, et al. Longitudinal profiles of immunoglobulin G antibodies against severe acute respiratory syndrome coronavirus components and neutralizing activities in recovered patients. Scand J Infect Dis **2011**; 43:515-21.
161. Dan JM, Mateus J, Kato Y, et al. Immunological memory to SARS-CoV-2 assessed for up to 8 months after infection. Science **2021**.
162. Wu J, Liang B, Chen C, et al. SARS-CoV-2 infection induces sustained humoral immune responses in convalescent patients following symptomatic COVID-19. medRxiv, **2020**.
163. Pradenas E, Trinité B, Urrea V, et al. Stable neutralizing antibody levels six months after mild and severe COVID-19 episode. bioRxiv, **2020**.
164. Rodda LB, Netland J, Shehata L, et al. Functional SARS-CoV-2-Specific Immune Memory Persists after Mild COVID-19. Cell **2021**; 184:169-83.e17.
165. Korte W, Buljan M, Rösslein M, et al. SARS-CoV-2 IgG and IgA antibody response is gender dependent; and IgG antibodies rapidly decline early on. J Infect **2020**.
166. Yin S, Tong X, Huang A, et al. Longitudinal anti-SARS-CoV-2 antibody profile and neutralization activity of a COVID-19 patient. J Infect **2020**.
167. Röltgen K, Wirz OF, Stevens BA, et al. SARS-CoV-2 Antibody Responses Correlate with Resolution of RNAemia But Are Short-Lived in Patients with Mild Illness. medRxiv **2020**.
168. Seow J, Graham C, Merrick B, et al. Longitudinal observation and decline of neutralizing antibody responses in the three months following SARS-CoV-2 infection in humans. Nat Microbiol **2020**; 5:1598-607.
169. Ibarrondo FJ, Fulcher JA, Goodman-Meza D, et al. Rapid Decay of Anti-SARS-CoV-2 Antibodies in Persons with Mild Covid-19. N Engl J Med **2020**.
170. Liu A, Li Y, Peng J, Huang Y, Xu D. Antibody responses against SARS-CoV-2 in COVID-19 patients. J Med Virol **2020**.
171. Girardin RC, Dupuis AP, Payne AF, et al. Temporal Analysis of Serial Donations Reveals Decrease in Neutralizing Capacity and Justifies Revised Qualifying Criteria for COVID-19 Convalescent Plasma. J Infect Dis **2021**.
172. Wajnberg A, Amanat F, Firpo A, et al. Robust neutralizing antibodies to SARS-CoV-2 infection persist for months. Science **2020**; 370:1227-30.
173. Bonifacius A, Tischer-Zimmermann S, Dragon AC, et al. COVID-19 immune signatures reveal stable antiviral T cell function despite declining humoral responses. Immunity **2021**; 54:340-54.e6.
174. Marklund E, Leach S, Axelsson H, et al. Serum-IgG responses to SARS-CoV-2 after mild and severe COVID-19 infection and analysis of IgG non-responders. PLoS One **2020**; 15:e0241104.
175. Klein SL, Pekosz A, Park HS, et al. Sex, age, and hospitalization drive antibody responses in a COVID-19 convalescent plasma donor population. J Clin Invest **2020**; 130:6141-50.
176. Salazar E, Kuchipudi SV, Christensen PA, et al. Convalescent plasma anti-SARS-CoV-2 spike protein ectodomain and receptor binding domain IgG correlate with virus neutralization. J Clin Invest **2020**.

177. Rijkers G, Murk JL, Wintermans B, et al. Differences in antibody kinetics and functionality between severe and mild SARS-CoV-2 infections. J Infect Dis **2020**.
178. Holmes CL, Peyton CG, Bier AM, et al. Reduced IgG titers against pertussis in rheumatoid arthritis: Evidence for a citrulline-biased immune response and medication effects. PLoS One **2019**; 14:e0217221.
179. Kind AJH, Buckingham WR. Making Neighborhood-Disadvantage Metrics Accessible - The Neighborhood Atlas. N Engl J Med **2018**; 378:2456-8.
180. Charlson ME, Pompei P, Ales KL, MacKenzie CR. A new method of classifying prognostic comorbidity in longitudinal studies: development and validation. J Chronic Dis **1987**; 40:373-83.
181. Alkhouli M, Nanjundappa A, Annie F, Bates MC, Bhatt DL. Sex Differences in Case Fatality Rate of COVID-19: Insights From a Multinational Registry. Mayo Clin Proc **2020**; 95:1613-20.
182. Zhou P, Yang XL, Wang XG, et al. A pneumonia outbreak associated with a new coronavirus of probable bat origin. Nature **2020**; 579:270-3.
183. Fonville JM, Wilks SH, James SL, et al. Antibody landscapes after influenza virus infection or vaccination. Science **2014**; 346:996-1000.
184. Wang P, Liu L, Nair MS, et al. SARS-CoV-2 neutralizing antibody responses are more robust in patients with severe disease. Emerg Microbes Infect **2020**; 9:2091-3.
185. Chen X, Pan Z, Yue S, et al. Disease severity dictates SARS-CoV-2-specific neutralizing antibody responses in COVID-19. Signal Transduct Target Ther **2020**; 5:180.
186. Wang Y, Zhang L, Sang L, et al. Kinetics of viral load and antibody response in relation to COVID-19 severity. J Clin Invest **2020**; 130:5235-44.
187. Mathew D, Giles JR, Baxter AE, et al. Deep immune profiling of COVID-19 patients reveals distinct immunotypes with therapeutic implications. Science **2020**; 369.
188. Hussain A, Mahawar K, Xia Z, Yang W, El-Hasani S. Obesity and mortality of COVID-19. Meta-analysis. Obes Res Clin Pract **2020**; 14:295-300.
189. Frasca D, Diaz A, Romero M, Blomberg BB. Ageing and obesity similarly impair antibody responses. Clin Exp Immunol **2017**; 187:64-70.
190. Kumakura S, Shibata H, Onoda K, Nishimura N, Matsuda C, Hirose M. Seroprevalence survey on measles, mumps, rubella and varicella antibodies in healthcare workers in Japan: sex, age, occupational-related differences and vaccine efficacy. Epidemiol Infect **2014**; 142:12-9.
191. Petersen LR, Sami S, Vuong N, et al. Lack of antibodies to SARS-CoV-2 in a large cohort of previously infected persons. Clin Infect Dis **2020**.
192. Wang F, Zheng S, Zheng C, Sun X. Attaching clinical significance to COVID-19-associated diarrhea. Life Sci **2020**; 260:118312.
193. Long QX, Liu BZ, Deng HJ, et al. Antibody responses to SARS-CoV-2 in patients with COVID-19. Nat Med **2020**; 26:845-8.
194. Gong F, Wei HX, Li Q, Liu L, Li B. Evaluation and Comparison of Serological Methods for COVID-19 Diagnosis. Front Mol Biosci **2021**; 8:682405.
195. Ripperger TJ, Uhrlaub JL, Watanabe M, et al. Orthogonal SARS-CoV-2 Serological Assays Enable Surveillance of Low-Prevalence Communities and Reveal Durable Humoral Immunity. Immunity **2020**; 53:925-33.e4.
196. Bolotin S, Tran V, Osman S, et al. SARS-CoV-2 Seroprevalence Survey Estimates Are Affected by Anti-Nucleocapsid Antibody Decline. J Infect Dis **2021**; 223:1334-8.
197. Gallais F, Gantner P, Bruel T, et al. Evolution of antibody responses up to 13 months after SARS-CoV-2 infection and risk of reinfection. EBioMedicine **2021**; 71:103561.
198. Wang Z, Muecksch F, Schaefer-Babajew D, et al. Naturally enhanced neutralizing breadth against SARS-CoV-2 one year after infection. Nature **2021**; 595:426-31.
199. Wang Z, Schmidt F, Weisblum Y, et al. mRNA vaccine-elicited antibodies to SARS-CoV-2 and circulating variants. Nature **2021**; 592:616-22.

200. Doria-Rose N, Suthar MS, Makowski M, et al. Antibody Persistence through 6 Months after the Second Dose of mRNA-1273 Vaccine for Covid-19. N Engl J Med **2021**; 384:2259-61.
201. Sadoff J, Gray G, Vandebosch A, et al. Safety and Efficacy of Single-Dose Ad26.COV2.S Vaccine against Covid-19. N Engl J Med **2021**; 384:2187-201.
202. Heffron AS, McIlwain SJ, Amjadi MF, et al. The landscape of antibody binding in SARS-CoV-2 infection. PLoS Biol **2021**; 19:e3001265.
203. Lopandić Z, Protić-Rosić I, Todorović A, et al. IgM and IgG Immunoreactivity of SARS-CoV-2 Recombinant M Protein. Int J Mol Sci **2021**; 22.
204. Jörrißen P, Schütz P, Weiand M, et al. Antibody Response to SARS-CoV-2 Membrane Protein in Patients of the Acute and Convalescent Phase of COVID-19. Front Immunol **2021**; 12:679841.
205. Amjadi MF, O'Connell SE, Armbrust T, et al. Specific COVID-19 Symptoms Correlate with High Antibody Levels against SARS-CoV-2. Immunohorizons **2021**; 5:466-76.
206. Noda K, Matsuda K, Yagishita S, et al. A novel highly quantitative and reproducible assay for the detection of anti-SARS-CoV-2 IgG and IgM antibodies. Sci Rep **2021**; 11:5198.
207. Newkirk MM, Mitchell S, Procino M, et al. Chronic smoke exposure induces rheumatoid factor and anti-heat shock protein 70 autoantibodies in susceptible mice and humans with lung disease. Eur J Immunol **2012**; 42:1051-61.
208. Salonen EM, Vaheri A, Suni J, Wager O. Rheumatoid factor in acute viral infections: interference with determination of IgM, IgG, and IgA antibodies in an enzyme immunoassay. J Infect Dis **1980**; 142:250-5.
209. Svec KH, Dingle JH. The Occurence of Rheumatoid Factor in Association with Antibody Response to Influenza A2(Asian) Virus. Arthritis Rheum **1965**; 8:524-9.
210. Maibom-Thomsen SL, Trier NH, Holm BE, et al. Immunoglobulin G structure and rheumatoid factor epitopes. PLoS One **2019**; 14:e0217624.
211. Burastero SE, Casali P, Wilder RL, Notkins AL. Monoreactive high affinity and polyreactive low affinity rheumatoid factors are produced by CD5+ B cells from patients with rheumatoid arthritis. J Exp Med **1988**; 168:1979-92.
212. Schroder AK, Gharavi AE, Steinitz M, Johansson PJ, Christensen P. Binding of monoclonal IgM rheumatoid factor to streptococci via the antibody combining site. Int Arch Allergy Appl Immunol **1987**; 83:88-91.
213. The J, Ebersole JL. Rheumatoid factor from periodontitis patients cross-reacts with epitopes on oral bacteria. Oral Dis **1996**; 2:253-62.
214. Joo YB, Lim YH, Kim KJ, Park KS, Park YJ. Respiratory viral infections and the risk of rheumatoid arthritis. Arthritis Res Ther **2019**; 21:199.
215. Arleevskaya MI, Albina S, Larionova RV, Gabdoulkhakova AG, Lemerle J, Renaudineau Y. Prevalence and Incidence of Upper Respiratory Tract Infection Events Are Elevated Prior to the Development of Rheumatoid Arthritis in First-Degree Relatives. Front Immunol **2018**; 9:2771.
216. Rojas M, Rodriguez Y, Acosta-Ampudia Y, et al. Autoimmunity is a hallmark of post-COVID syndrome. J Transl Med **2022**; 20:129.
217. Anaya JM, Monsalve DM, Rojas M, et al. Latent rheumatic, thyroid and phospholipid autoimmunity in hospitalized patients with COVID-19. J Transl Autoimmun **2021**; 4:100091.
218. Bailey TL, Johnson J, Grant CE, Noble WS. The MEME Suite. Nucleic Acids Res **2015**; 43:W39-49.
219. Hjelholt A, Christiansen G, Sørensen US, Birkelund S. IgG subclass profiles in normal human sera of antibodies specific to five kinds of microbial antigens. Pathog Dis **2013**; 67:206-13.
220. Steen J, Forsstrom B, Sahlstrom P, et al. Recognition of Amino Acid Motifs, Rather Than Specific Proteins, by Human Plasma Cell-Derived Monoclonal Antibodies to Posttranslationally Modified Proteins in Rheumatoid Arthritis. Arthritis Rheumatol **2019**; 71:196-209.

221. Peterson C, Malone CC, Williams RC, Jr. Rheumatoid-factor-reactive sites on CH3 established by overlapping 7-mer peptide epitope analysis. Mol Immunol **1995**; 32:57-75.
222. Williams RC, Jr., Malone CC. Rheumatoid-factor-reactive sites on CH2 established by analysis of overlapping peptides of primary sequence. Scand J Immunol **1994**; 40:443-56.
223. Williams RC, Jr., Malone CC, Kolaskar AS, Kulkarni-Kale U. Antigenic determinants reacting with rheumatoid factor: epitopes with different primary sequences share similar conformation. Mol Immunol **1997**; 34:543-56.
224. Gaynor B, Putterman C, Valadon P, Spatz L, Scharff MD, Diamond B. Peptide inhibition of glomerular deposition of an anti-DNA antibody. Proc Natl Acad Sci U S A **1997**; 94:1955-60.
225. DeGiorgio LA, Konstantinov KN, Lee SC, Hardin JA, Volpe BT, Diamond B. A subset of lupus anti-DNA antibodies cross-reacts with the NR2 glutamate receptor in systemic lupus erythematosus. Nat Med **2001**; 7:1189-93.
226. Cusick MF, Libbey JE, Fujinami RS. Molecular mimicry as a mechanism of autoimmune disease. Clin Rev Allergy Immunol **2012**; 42:102-11.
227. Fujinami RS, Oldstone MB. Amino acid homology between the encephalitogenic site of myelin basic protein and virus: mechanism for autoimmunity. Science **1985**; 230:1043-5.
228. Liao B, Chen Z, Zheng P, et al. Detection of Anti-SARS-CoV-2-S2 IgG Is More Sensitive Than Anti-RBD IgG in Identifying Asymptomatic COVID-19 Patients. Front Immunol **2021**; 12:724763.
229. Haynes BF, Fleming J, St Clair EW, et al. Cardiolipin polyspecific autoreactivity in two broadly neutralizing HIV-1 antibodies. Science **2005**; 308:1906-8.
230. Guthmiller JJ, Lan LY, Fernandez-Quintero ML, et al. Polyreactive Broadly Neutralizing B cells Are Selected to Provide Defense against Pandemic Threat Influenza Viruses. Immunity **2020**; 53:1230-44 e5.
231. Jones DD, DeIulio GA, Winslow GM. Antigen-driven induction of polyreactive IgM during intracellular bacterial infection. J Immunol **2012**; 189:1440-7.
232. Lang AK, Macht LM, Kirwan JR, Wraith DC, Elson CJ. Ability of T cells from patients with rheumatoid arthritis to respond to immunoglobulin G. Immunology **1999**; 98:116-22.
233. Bikoff EK. Tolerance for self IG at the level of the Ly1+ T cell. J Exp Med **1983**; 158:1868-80.
234. Sahlstrom P, Hansson M, Steen J, et al. Different hierarchies of anti-modified protein autoantibody reactivities in rheumatoid arthritis. Arthritis Rheumatol **2020**.
235. Yurasov S, Wardemann H, Hammersen J, et al. Defective B cell tolerance checkpoints in systemic lupus erythematosus. J Exp Med **2005**; 201:703-11.
236. Glauzy S, Sng J, Bannock JM, et al. Defective Early B Cell Tolerance Checkpoints in Sjogren's Syndrome Patients. Arthritis Rheumatol **2017**; 69:2203-8.
237. Pascolini S, Vannini A, Deleonardi G, et al. COVID-19 and Immunological Dysregulation: Can Autoantibodies be Useful? Clin Transl Sci **2021**; 14:502-8.
238. Muratori P, Lenzi M, Muratori L, Granito A. Antinuclear antibodies in COVID 19. Clin Transl Sci **2021**; 14:1627-8.
239. Agnello V, Arbetter A, Ibanez de Kasep G, Powell R, Tan EM, Joslin F. Evidence for a subset of rheumatoid factors that cross-react with DNA-histone and have a distinct cross-idiotype. J Exp Med **1980**; 151:1514-27.
240. Leadbetter EA, Rifkin IR, Hohlbaum AM, Beaudette BC, Shlomchik MJ, Marshak-Rothstein A. Chromatin-IgG complexes activate B cells by dual engagement of IgM and Toll-like receptors. Nature **2002**; 416:603-7.
241. Van Snick JL, Van Roost E, Markowetz B, Cambiaso CL, Masson PL. Enhancement by IgM rheumatoid factor of in vitro ingestion by macrophages and in vivo clearance of aggregated IgG or antigen-antibody complexes. Eur J Immunol **1978**; 8:279-85.

242. Nielen MM, van Schaardenburg D, Reesink HW, et al. Specific autoantibodies precede the symptoms of rheumatoid arthritis: a study of serial measurements in blood donors. Arthritis Rheum **2004**; 50:380-6.
243. Fechtner S, Berens H, Bemis E, et al. Antibody Responses to Epstein-Barr Virus in the Preclinical Period of Rheumatoid Arthritis Suggest the Presence of Increased Viral Reactivation Cycles. Arthritis Rheumatol **2022**; 74:597-603.
244. Lebedin M, Garcia CV, Spatt L, et al. Discriminating promiscuous from target-specific autoantibodies in COVID-19. Eur J Immunol **2023**:e2250210.
245. Shelef MA. New Relationships for Old Autoantibodies in Rheumatoid Arthritis. Arthritis Rheumatol **2019**; 71:1396-9.
246. Acosta-Ampudia Y, Monsalve DM, Rojas M, et al. Persistent Autoimmune Activation and Proinflammatory State in Post-COVID Syndrome. J Infect Dis **2022**.
247. Tamariz L, Bast E, Abad M, Klimas N, Caralis P, Palacio A. Post COVID-19 joint pain: Preliminary report of the relationship with antinuclear antibodies and inflammation. J Med Virol **2022**; 94:3479-81.
248. Wang H, Li X, Li T, et al. The genetic sequence, origin, and diagnosis of SARS-CoV-2. Eur J Clin Microbiol Infect Dis **2020**; 39:1629-35.
249. Adam D. When will COVID stop being a global emergency? Nature **2023**; 614:201-2.
250. COVID Data Tracker Weekly Review: Centers for Disease Control and Prevention, **2023**.
251. Ma H, Zeng W, He H, et al. Serum IgA, IgM, and IgG responses in COVID-19. Cell Mol Immunol **2020**; 17:773-5.
252. Chi X, Yan R, Zhang J, et al. A neutralizing human antibody binds to the N-terminal domain of the Spike protein of SARS-CoV-2. Science **2020**.
253. To KK, Tsang OT, Leung WS, et al. Temporal profiles of viral load in posterior oropharyngeal saliva samples and serum antibody responses during infection by SARS-CoV-2: an observational cohort study. Lancet Infect Dis **2020**; 20:565-74.
254. Van Elslande J, Decru B, Jonckheere S, et al. Antibody response against SARS-CoV-2 spike protein and nucleoprotein evaluated by 4 automated immunoassays and 3 ELISAs. Clin Microbiol Infect **2020**.
255. Dogan M, Kozhaya L, Placek L, et al. SARS-CoV-2 specific antibody and neutralization assays reveal the wide range of the humoral immune response to virus. Commun Biol **2021**; 4:129.
256. Takahashi T, Ellingson MK, Wong P, et al. Sex differences in immune responses that underlie COVID-19 disease outcomes. Nature **2020**; 588:315-20.
257. Dittadi R, Afshar H, Carraro P. The early antibody response to SARS-Cov-2 infection. Clin Chem Lab Med **2020**.
258. Damoiseaux J, Dotan A, Fritzler MJ, et al. Autoantibodies and SARS-CoV2 infection: The spectrum from association to clinical implication: Report of the 15th Dresden Symposium on Autoantibodies. Autoimmun Rev **2022**; 21:103012.
259. Deane KD, O'Donnell CI, Hueber W, et al. The number of elevated cytokines and chemokines in preclinical seropositive rheumatoid arthritis predicts time to diagnosis in an age-dependent manner. Arthritis Rheum **2010**; 62:3161-72.
260. Tanimoto K, Cooper NR, Johnson JS, Vaughan JH. Complement fixation by rheumatoid factor. J Clin Invest **1975**; 55:437-45.
261. Takashita E, Kinoshita N, Yamayoshi S, et al. Efficacy of Antibodies and Antiviral Drugs against Covid-19 Omicron Variant. N Engl J Med **2022**; 386:995-8.
262. Oda M, Kozono H, Morii H, Azuma T. Evidence of allosteric conformational changes in the antibody constant region upon antigen binding. Int Immunol **2003**; 15:417-26.
263. Mollnes TE, Garred P, Bergseth G. Effect of time, temperature and anticoagulants on in vitro complement activation: consequences for collection and preservation of samples to be examined for complement activation. Clin Exp Immunol **1988**; 73:484-8.

264. Yang S, McGookey M, Wang Y, Cataland SR, Wu HM. Effect of blood sampling, processing, and storage on the measurement of complement activation biomarkers. Am J Clin Pathol **2015**; 143:558-65.
265. Baumgarten A. Viral immunodiagnosis. Yale J Biol Med **1980**; 53:71-83.
266. Sethi J, Pei D, Hirshaut Y. Choice and specificity of complement in complement fixation assay. J Clin Microbiol **1981**; 13:888-90.
267. Chen J, Wang R, Gilby NB, Wei GW. Omicron Variant (B.1.1.529): Infectivity, Vaccine Breakthrough, and Antibody Resistance. J Chem Inf Model **2022**; 62:412-22.